الجمهورية الجزائرية الديمقراطية الشعبية
Democratic and Popular Republicof Algeria
وزارة التعليم العالي و البحث العلمي
Ministry of Higher Education and Scientific Research

جامعة محمد خيضر - بسكرة
كلية العلوم و التكنولوجيا
قسم الهندسة الكهربائية
المرجع : .....

Mohamed Khider Uuniversity–Biskra
Faculty of Science and Technology
Department of Electrical Engineering
Réf:……

Thesis presented for obtaining the **LMD Doctorate degree**

Specialty: Automatic

Option: Automatic and systems

Modeling and Robust Control of Flying Robots Using Intelligent Approaches

Modélisation et commande robuste des robots volants en utilisant des approches intelligentes

Presented by:

Lemya Guettal

Publicly discussed in: **19/03/2023**

In front of the jury composed of :

Abderrazek Debilou	**Professor**	**President**	**University of Biskra**
Abdelmalik Ouamane	**Professor**	**Supervisor**	**University of Biskra**
Hatem Ghodbane	**Professor**	**Examiner**	**University of Biskra**
Djamel Saigaa	**Professor**	**Examiner**	**University of M'sila**

Modeling and Robust Control of Flying Robots Using Intelligent Approaches

Acknowledgment

*I must express my greatest thanks to **Abdelmalik Ouamane** the thesis director for supporting me and encouragement (in every sense of the word) as well as giving me a good mindset for research and overcoming all obstacles but also for constantly ensuring his assistance, pushing me to continue in difficult times. For this he has all my gratitude, Thank you Pr.Abdelmalik OUAMANE.*

*A thesis is not only the culmination of the work of the doctoral student; it is also a burden for the jury. This short acknowledgment page is dedicated to them. I would like to thank all those who have helped me to develop this work. First of all, I would like to thank all the members of my jury for their presence and their participation in this thesis. My first thanks to Pr. **Abderrazek Debilou**, Professor at the University of Biskra, who have honored us me by chairing the examination committee.*

*All my gratitude to Pr. **Djamel Saigaa** Professor at the University of M'sila, have come from afar just for the pleasure of participating in this day and accept the responsibility of being examiner of this work, I'm very honored by his presence and for having judged without hesitation this work as well for his valuable advice.*

*A big gratefulness to Pr. **Hatem Ghodbane**, professor at the electrical engineering department of the University of Biskra who finds my deep gratitude for his advice and for having accepted to judge this work and for his support for all PhD students as the Head of the Faculty.*

*Finally, I should express my gratitude and deep appreciation to Dr**. Glida Hossam Eddine** for his help*

Dedication

In the name of Allah. Praise is to you as befits the glory of your face and the greatness of your might. I would like to dedicate this thesis to my family, especially my father, ***Abbes Guettal****, who passed away too early, and who always pushed and motivated me in my studies. May God, the Almighty, have him in his holy mercy .I would like to express my gratitude to my husband* ***Pr. Riadh Ajgou****, whose support has been the backbone of my development. Likewise, special gratefulness to* ***my mather*** *who have always supported and encouraged me.* ***My sisters, my brothers.*** *Finally, I would like to dedicate this work to my kids* ***Sari****,* ***Younes*** *and* ***Liliane****, who have made me stronger, better and more fulfilled than I could have ever imagined.*

Abstract

This thesis aims to modeling and robust controlling of a flying robot of quadrotor type. Where we focused in this thesis on quadrotor unmanned Aerial Vehicle (QUAV). Intelligent nonlinear controllers and intelligent fractional-order nonlinear controllers are designed to control. The QUAV system is considered as MIMO large-scale system that can be divided on six interconnected single-input–single-output (SISO) subsystems, which define one DOF, i.e., three-angle subsystems with three position subsystems. In addition, nonlinear models is considered and assumed to suffer from the incidence of parameter uncertainty. Every parameters such as mass, inertia of the system are assumed completely unknown and change over time without prior information. Next, basing on nonlinear, Fractional-Order nonlinear and the intelligent adaptive approximate techniques a control law is established for all subsystems. The stability is performed by Lyapunov method and getting the desired output with respect to the desired input. The modeling and control is done using MATLAB/Simulink. At the end, the simulation tests are performed to that, the designed controller is able to maintain best performance of the QUAV even in the presence of unknown dynamics, parametric uncertainties and external disturbance.

Keywords: Quadrotor, UAV, nonlinear control ,fractional-order calculus, adaptive intelligent approaches, lyapunov method.

Abstract

ملخص

تهدف هذه الأطروحة إلى النمذجة والتحكم القوي في روبوت طائر من النوع الرباعي . حيث ركزنا في هذه الأطروحة على مركبة جوية بدون طيار رباعية المحركات (QUAV). تم تصميم أجهزة التحكم الذكية غير الخطية وأجهزة التحكم الذكية غير الخطية ذات الترتيب الجزئي للتحكم .يعتبر نظام QUAV بمثابة نظام MIMO واسع النطاق يمكن تقسيمه على ستة أنظمة فرعية مترابطة ذات مدخل واحد ومخرج واحد (SISO)، والتي تحدد DOF واحدًا ، أي أنظمة فرعية ثلاثية الزوايا مع ثلاثة أنظمة فرعية للمواضع .بالإضافة إلى ذلك ، يتم أخذ النموذج غير الخطي في الاعتبار ويعتبر يعاني من وجود عدم اليقين في المعلمة .تعتبر جميع المعلمات ، مثل الكتلة والقصور الذاتي للنظام ، غير معروفة تمامًا وتتغير بمرور الوقت دون أي معلومات مسبقة .بعد ذلك ، استنادًا إلى تقنيات غير الخطية ، غير الخطية ذات الترتيب الجزئي ، وتقنيات المقارب الذكي التكيفي ، يتم وضع قانون تحكم لجميع الأنظمة الفرعية .يتم تنفيذ الاستقرار بواسطة طريقة Lyapunov والحصول على الإخراج المطلوب فيما يتعلق بالمدخلات المطلوبة .النمذجة والتحكم يتم باستخدام MATLAB / Simulinkفي النهاية ، يتم إجراء اختبارات المحاكاة لذلك ، تكون وحدة التحكم المصممة قادرة على الحفاظ على أفضل أداء لـ QUAV حتى في وجود ديناميكيات غير معروفة ، وشكوك معلمية واضطراب خارجي.

الكلمات المفتاح رباعية المحرك ، الطائرات بدون طيار ، التحكم غير الخطي ، الأساليب الذكية التكيفية ، حساب التفاضل والتكامل الجزئي ، طريقةLyapunov .

Abstract

Résumé

Cette thèse a pour objectif la modélisation et le contrôle robuste d'un robot volant de type quadrotor. Où nous nous sommes concentrés dans cette thèse sur le véhicule aérien sans pilote quadrotor (QUAV). Les contrôleurs non linéaires intelligents et les contrôleurs non linéaires intelligents d'ordre fractionnaire sont conçus pour contrôler. Le système QUAV est considéré comme un système MIMO à grande échelle qui peut être divisé en six sous-systèmes interconnectés à entrée unique et sortie unique (SISO), qui définissent un DOF, c'est-à-dire des sous-systèmes à trois angles avec des sous-systèmes à trois positions. De plus, un modèle non linéaire est pris en compte et considéré comme souffrant de la présence d'incertitude sur les paramètres. Tous les paramètres, tels que la masse, l'inertie du système, sont considérés comme totalement inconnus et variant dans le temps sans aucune information préalable. Ensuite, en se basant sur les techniques non linéaires, non linéaires d'ordre fractionnaire et les approximateurs adaptatifs intelligents, une loi de commande est établie pour tous les sous-systèmes. La stabilité est effectuée par la méthode Lyapunov et l'obtention de la sortie souhaitée par rapport à l'entrée souhaitée. La modélisation et le contrôle se font sous MATLAB/Simulink. À la fin, les tests de simulation sont effectués pour que le contrôleur conçu soit capable de maintenir les meilleures performances du QUAV même en présence de dynamique inconnue, d'incertitudes paramétriques et de perturbations externes.

Mots clés: Quadrotor, UAV, contrôle non linéaire, calcul d'ordre fractionnaire, approches intelligentes adaptatives, méthode Lyapunov.

Following Research Papers Related to this Work

JOURNALS

1. **Guettal, Lemya** *et al.* Robust Tracking Control for Quadrotor with Unknown Nonlinear Dynamics Using Adaptive Neural Network Based Fractional-Order Backstepping Control. *Journal of the Franklin Institute*, 359, (14), 2022. P. 7337-7364 2022. https://doi.org/10.1016/j.jfranklin.2022.07.043.
2. **Guettal Lemya** *et al*, Intelligent adaptive fractional-order backstepping control for uncertain non-linear quadrotor, Advances in Differential Equations and Control Processes 28 (2022), 99-117. http://dx.doi.org/10.17654/0974324322026.

CONFERENCES

1. **Guettal Lemya** *et al.* Neural Network-based Adaptive Backstepping Controller for UAV Quadrotor system. In : *2020 1st International Conference on Communications, Control Systems and Signal Processing (CCSSP)*. IEEE, 2020. p. 388-393. **DOI:** 10.1109/CCSSP49278.2020.9151813.
2. **Guettal Lemya** *et al*. Adaptive Fuzzy-Neural Network based Decentralized Backstepping Controller for Attitude Control of Quadrotor Helicopter. In : *2020 1st International Conference on Communications, Control Systems and Signal Processing (CCSSP)*. IEEE, 2020. p. 394-399. **DOI:** 10.1109/CCSSP49278.2020.9151463.
3. **Guettal Lemya** *et al.* Adaptive Fuzzy-Chebyshev Network-based Continuous Sliding Mode Controller for Quadrotor Unmanned Aerial Vehicle. In : *2020 1st International Conference on Communications, Control Systems and Signal Processing (CCSSP)*. IEEE, 2020. p. 382-387. **DOI:** 10.1109/CCSSP49278.2020.9151733.

Table of Contents

Table of Contents

Table of Contents

List of Figures

List of Figures

List of Figures

List of Tables

List of Symbols and Acronyms

$e_{i,1}(t)$	Trajectory tracking error.
J	Quadrotor's diagonal inertia Matrix.
I_x, I_y and I_z	Moments of inertia.
l	Quadrotor arm length (m).
J_r	Inertia of the quadrotor (kg.m2).
m	Mass of the quadrotor (kg).
Ω_r	Rotors' relative speed.
ρ	Air density A blade area.
C_T, C_D	Aerodynamic coefficients.
r	Radius of blade.
g	Gravitational acceleration ($\frac{9.81m}{s^2}$) .
$\mathcal{U}_i$	Input vector.
u_{swi}	Robust switching control term.
u_{eqi}	Equivalent control term.
V	Lyapunov function.
F_B	Non gravitational forces acting.
LQR	Linear-Quadratic Regulator.
PID	Proportional–Integral–Derivative.
6DOF	Six Degrees of Freedom.
SISO	Single-Input Single-Output.
MIMO	Multi-Input–Multi-Output.
RL, Ca	Riemann-Liouville, Caputo.
SMC	Sliding Mode Control.

List of Symbols and Acronyms

UAV	Unmanned Aerial Vehicle.
QUAV	Quadrotor Unmanned Aerial Vehicle.
NNs	Artificial Neural Networks.
FCN	Fuzzy-Chebyshev Network.
FNN	Adaptive Fuzzy Neural Network.
FLS	Fuzzy Logic System.
SOSMC	Second Order Sliding Mode.
BC	Backstepping Control.
FO	Fractional Order.
TS	Takaji-Seguino
RBFNN	Radial Basis Function Neural Network.
AFNN-DBC	Adaptive Fuzzy-Neural Network Based Decentralized Backstepping Controller.
FOBC	Fractional-Order Backstepping Controller.
NNFOBC	Neural Network-Based Fractional-Order Backstepping Controller.
IO	Integer order.
x and y	Variables characterizing the quadrotor location in space.
z	Quadrotor altitude.
ϕ	The angle around the x axis named Roll angle which.
θ	The angle around the y-axis named Pitch angle which represents.
ψ	Yaw angle it denotes angle around the z-axis.
q , r	FO derivative and integral order.

General Introduction

This thesis aims to model and develop robust control of flying robots where we have focused on quadrotor is a flying robot it belongs to the multirotors family. This thesis aims to propose and design various adaptive robust nonlinear control techniques for of a quadrotor unmanned aerial vehicles (QUAVs) type flying robot against external disturbances, system uncertainties and unknown dynamics. Despite various works, this challenge has not yet been sufficiently studied and resolved due to the complexity of offering significant precision flight path tracking on the existence of these disturbances. This work developed robust control approaches to reach sufficient set-point tracking of diverse complex of QUAV trajectories. Noting that despite the complexity of QUAV trajectories, we succeeded in proposing robust control techniques to achieve sufficient tracking of the setpoint with smoother control action. Using sliding mode control (SMC) hypothesis, backstepping approach, fractional-order calculus, artificial neural networks (NNs) and/or fuzzy logic system as universal approximators to solve the control problem of nonlinear uncertain systems and adaptive laws, are offered for the QUAV system control.

1. Motivation and problems

The central motivations of this thesis are specified as follows:

1. Developing a control approaches for QUAV to satisfy specific requirements (precision, minimum energy consumption……) produce more challenge. In addition, designing a flight controllers for these multi-rotor drones gives three significant challenges: (i) the vehicle dynamics are multi-input, multi-output (MIMO) and highly nonlinear coupled; (ii) the QUAV dynamics include diverse sources of uncertainties, as well as parametric uncertainties, unmodeled uncertainties, and external disturbances. So, this thesis suggests robust QUAV control schemes over the mentioned perturbations.
2. Design a second order sliding mode (SOSMC), backstepping controllers (BC) based on adaptive neural networks and/or fuzzy. The main objective is control of QUAV

system against uncertainties and disturbances. The neural networks and/or fuzzy logic with adaptive parameters is exploited to approximate the unkown nonlinear functions and improve the robustness against parametric uncertainties and external disturbances.

3. The development of robust nonlinear controls by using the fractional-order calculs, the path tracking of the QUAV is performed and enhanced robustness can be achieved over parametric uncertainties and perturbations. These control techniques are very significant once the QUAV is concerned by unknown complex disturbances throughout flights. The control using fractional-order controllers could lead to a good performance than integer controllers. Consequently, it is essential to investigate these control designs. The control performance as well as the transient and stable states of the tracking errors must be improved against disturbances for the QUAV. The study considers robust nonlinear controllers as well as fractional calculs of these actions where the performance can be enhanced against disturbances effects.

2. Main contributions

We can outline the essential contributions obtained in this thesis as follows:

- At first, studied the attitude control problem for a quadrotor system in the presence of unknown dynamics, parametric uncertainties and external disturbances. The designed controller for quadrotor system is divided firstly into three controllers: yaw angle controller, pitch angle controller, and roll angle controller. Second, the control law of each controller is approximated indirectly by using a combination of approximation function of the fuzzy system and the neural network. Then, based on the Lyapunov stability theorem, the proposed controller scheme can guarantee the stability of the closed loop system and achieve a good tracking performance. Finally, simulation results are presented to demonstrate the effectiveness of the proposed structure. The contributions are various and significant as, the problems of singularity and the need of a robust additional term in BC methodology are avoided. In addition, the prior knowledge of uncertainty limits is not necessary and ideal dynamics of the mathematical system are not needed.

- Secondly, study the attitude control problem of quadrotor system in the presence of unknown dynamics, parametric uncertainties, and external perturbations. Here, the model quadrotor is considered as large-scale system which is divided into three subsystems. Thus, the control of multiple-input multiple-output(MIMO) system is achieved through decentralized control of three single-input single-output (SISO)subsystems. Firstly, the adaptive Fuzzy-Chebyshev network (FCN) is used to approximate unknown dynamic function for each subsystem. Then, second order sliding mode (SOSMC) control is applied to deal with the approximation error and , parameters uncertainties and external disturbances and eliminating the chattering effect. Finally, simulation results are presented to demonstrate the effectiveness of the proposed controller. The main contribution is to demonstrate that prior knowledge of the limits of uncertainties is not necessary and the perfect mathematical system dynamics is not required.
- Thirdly, a new tracking control approach named NNFOBC based fractional order (FO) control technique, backstepping controller and neural networks for QUAV is proposed. The NNFOBC will lead to a strong robustness and high tracking accuracy. The FO backstepping controller is employed to decrease uncertainties and disturbances effect. The adaptive RBFNN approximator of unknown dynamics and a local robust control term are incorporated to ensure a robust tracking convergence of the closed-loop quadrotor. an efficient fractional-order virtual stabilizing function was designed, such that the proposed NNFOBC rule includes more FO differential and integral terms of the tracking error. By the augmented degrees of freedom for the control parameters and proper choice of fractional orders, the designed NNFOBC be able to successfully improve the control performance of the classical BC.

3. Structure of the thesis

In this thesis, the QUAV dynamics model, the second order continuous sliding mode control(SOSMC), backstepping controller (BC), the adaptive neural network, the adaptive Fuzzy-Chebyshev network (FCN) ,fractional-order backstepping controller (FOBC), external disturbances, parametric uncertainties, the unknown dynamic functions, will be study and investigated . The relations between chapters are illustrated in figure1.

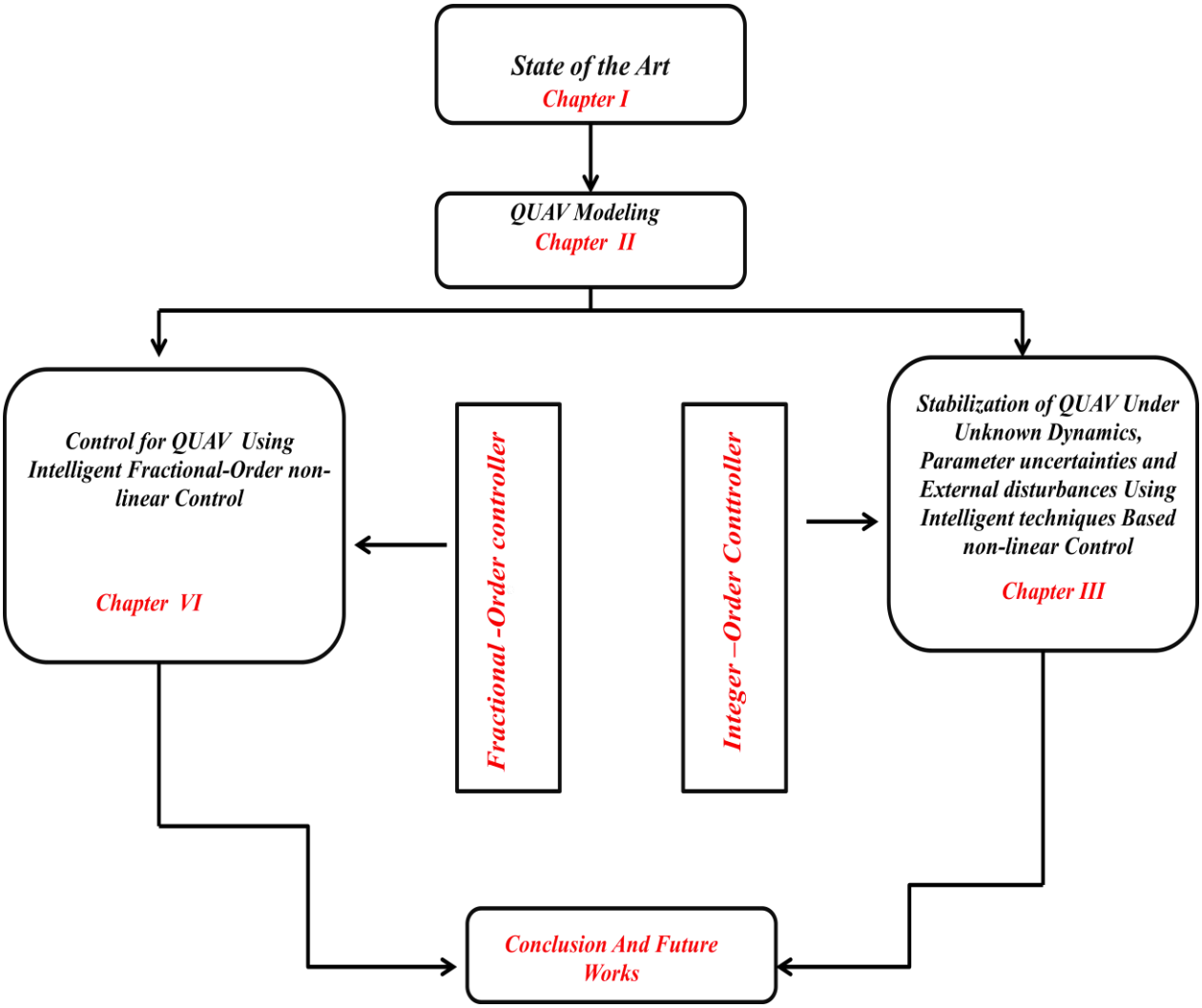

Figure 1. Block diagram of this thesis.

Chapter I

State of the Art

Chapter I : State of the Art

I.1 Introduction

In current years, we found a very growth with rapidity in the development of autonomous unmanned aircraft equipped with autonomous control devices named unmanned aerial vehicles (UAV). Hence, the use of such vehicles is extensively wide. It can be divided depending to their applications for military or civilian field. Thus we have a amazing growth of UAVs especially for military fiels. UAV give main advantages while operated for in surveillances, reconnaissance and inspections in difficult and challenging conditions. In reality, UAVs are better suitable to boring, unclean or complex as well as dangerous missions than manned aircraft to keep pilots alive. Low risk of loss and greater confidence in operation success are two important parameters for the continued growth of the employ of unmanned aircraft system. In addition, numerous other technological and economic elements have supported the improvement and use of UAVs. This chapter will talk about a short introduction in relation to Unmanned Aerial Vehicles (UAVs) on terms of their histories, types and utilization and the complexity of UAVs system that lead to a complexity in control. In the literature there are various types of UAVs however in the thesis we have focused on Quadrotor Unmanned Aerial Vehicles (QUAV), hence we discuss their concept, system control and architecture.

I.2 Unmanned aerial vehicles (UAV)

The description of drones varies across literature. In our case, UAVs are small unmanned aircraft. They can whichever be remote-controlled by a person or stand alone; UAVs to be controlled by an on-board computer which could be pre-programmed to achieve a definite task or a wide range of tasks. Whilst, in further literatures, UAV could refers to powered or unpowered, tethered or untethered aerial [1]. Our adopted description which taken in this work supports the same as the American Institute of Aeronautic and Astronautic [1]: an aircraft that is developed or modified to not take an individual aviator and that is functioned throughout electronic input initiated by the flight controller or by an autonomous flight command control system that does not require the intervention from the flight controller. Although, UAV were mostly employed in armed purpose except lately they used in civilian field too [2].

I.2.1 Histories of UAVs

UAV was initially produced by Lawrence and Sperry in the United States of America 1916 as it shown in Figure I.1. They call it the Aviation Torpedo and capable to hover it for about 30

miles. Furthermore, the use of gyroscope by Lawrence and Sperry is to balance the body of UAVs [2].

Figure I.1: (UAV) Lawrence and Sperry [2].

I.2.1.1 Military history

A The United States showed great interest in developing UAV for use in the First World War and two schemes were financed. The initial was by Elmer Sperry to design the "Flying Bomb" UAVs and the next development is the "Kettering Bug" done by General Motors. Both projects were blocked with the cancellation of all funds due to failure. Owing of the absence of the mandatory technical advances in the field of supervision system and engine [3]. The purpose of UAV in progress hugely by years of 1950 until 1960, the Unites states of America used them throughout the Vietnam conflict to reduce the victims in pilots against enemy lands. Following the efficiency of UAVs, the uninvited states and other countries determined to spend further to make slighter and not expensive UAV, they utilized tiny engine similar to those used in motorcycles to obtain UAVs light small. Furthermore, cameras were used on the UAVs for transmitting images to operators in the land. But in 1991, the United states employed UAV usually in the conflict with Iraq, where the popular well-known model was the Predator illustrated in Figure I.2 . UAVs were strongly adopted in various clashes and conflict in the 1990's and the years of 2000 by USA. Unmanned aerial vehicles were widely utilized various with more development especially among the war of Iraq in 2003 [4].

Figure I.2: (UAV) Predator Military [2]

I.2.1.2 Civil History

Using drones were not just limited to military employ; in 1969, The National Aeronautics and Space Administration proposed the worry to control an airplane in automatic, the first tests were the PA-30 program. The plan was booming, except the mission requires a person on board to take control of the plane in case something leads to mistake. An additional investigate plan go behind the achievement of the PA-30 plan such as: the Drones for Aerodynamic and Structural Testing (DAST) and Highly Maneuverable Aircraft Technology (HiMAT) program [5]. After that time, in the years of 1990, The National Aeronautics and Space Administration joined with manufacturing corporations to advance a nine-year study projects named the Environmental Research Aircraft and Sensor Technology research (ERAST), where they have designed a variety of representation of drones capable of flying at altitudes of until 30 km and supporting the flights until 6 months. Follow-on UAVs models incorporated: Pathfinder, Helios, Atlus and Perseus B. The proposed drones approved multiple sensors to perform environmental dimensions; the on-board sensors comprises cameras, a digital scanning interferometers (DASI) and an active detections, vision and prevention (DSA) systems [5].

I.2.2 Applications of UAVs

Otherwise, UAVs can be employed in various fields such as civilian or commercial application that are too tedious, very polluted, or excessively unsafe for manned airplane. These employments comprise, but are not restricted to:

Earth Sciences remarks using unmanned aerial vehicles could be exploited side-to-side with that gained from satellite. As missions comprise [5]:

(a) Measure of deformations in the crust of the Earth which might be indications to natural disaster similar to earthquake, landslide or volcanos [5].

(b) Measurement of Cloud and Aerosol [5].

(c) Tropospheric pollutions with air qualities measurement to decide pollutions sources and how plume of contamination to be moved from place to a new places [5, 6].

(d) Ice sheet size and surface deformations for study overall warming [5].

(e) Measurement of the accelerations of Gravity, because the accelerations of Gravity is different close to Earth, UAV to be utilized perfectly measure gravitational accelerations at numerous spaces to describe accurate inputs [5].

(f) River discharges to be calculated from the water of flowing in a river with various positions. This will assist in general and local water stability investigations [5].

Searches and save drones advanced with camera to be employed to look for persons following disasters such as earthquake and hurricane or survivors due to shipwrecks and airplane crash [6, 7].

Wild fire removal drones prepared by infrared sensor to be forwarded to hover above forest down to discover any fires and make the suitable reaction by transmitting information to the responsible by indicating the precise area of the fire earlier than it extends [5–7].

Law enforcement drones to be employed as a cost-effective replacement for manned police helicopter [7].

Border surveillance: drones to be exploited to guard borders searching for intruder, illegitimate immigrant and arms trafficking [2, 5, 7].

Research: drones are too adopted by researchers carried out at laboratories to prove a theory. Moreover, drones prepared with suitable sensors to be utilized by environmental research institution to monitor different environmental phenomena as well as pollutions in major states [7].

Applications in manufacturing: drones employed in different manufacturing purpose such as pipeline inspections or surveillances and nuclear plant monitoring [6, 7].

Agriculture development, in addition, drones to be adopted agriculture field such as crops spraying [2, 6, 7].

I.2.3 Drones classification (UAVs)

It is easy to discover, there are various methods to categorize UAVs, either depending to their actions, their aerodynamics configurations, their sizes, and their payload, or according to

their capability of autonomies [8]. UAV can be classified depending to their highest altitude and survival as illustrated in figure I.3:

(a)

(b)

(c) (d)

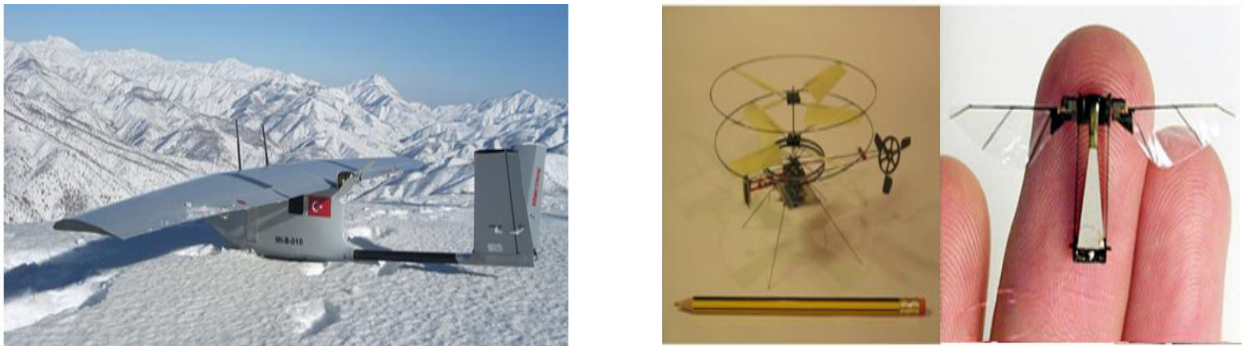

(e) (f)

Figure I.3 : Classification of UAVs: (a) UAVs HALE, (b) UAVs MALE, (c) UAVs TUAV, (d) Short Range UAVs,(e) Mini UAVs, (f) Micro UAVs [8,9].

– High-Altitude Long Endurance (HALE): this kind of UAV able to hover more than 15.000 m with an autonomous of about 24 hours. The main use of this type is the large surveillance missions.

– Medium-Altitude Long-Endurance (MALE): this kind of UAV able to hover between 5.000 and 15.000 m altitude with an autonomous of 24 hours. These UAV are suitable for surveillance missions.

– Tactical Unmanned Air Vehicle (TUAV): this kind of UAV are minor and maneuver with simple systems than the mentioned types that are described above: HALE and MALE. They be able to hover in an altitude in the range of 100 to 300 km.

–UAVs with small Range: the kind are mostly utilized in civil purposes as well as pipe line inspections, harvest spraying, traffic check, home securities in the range of 100 km.

– Mini UAV (MUAV): with a weigh of 20 kg with hovering of 30 km.

– Micro UAV (MAV): their greatest wingspan is about 150 mm. They are largely adopted in indoors, where they must hover gradually and continue flying.

Furthermore, the aerodynamics configurations play a significant role in the next classification:

– Fixed-wing UAVs: this group necessitates a landing strip to fly and land. They can hover lengthy with elevated-velocity cruising. They are largely adopted in scientific filed as well as climatic investigations and environment monitoring.

– Rotary Wing UAVs: this type of drones can fly, land vertically and hovering with large maneuverability. As shown in Figure I.4, this kind of UAVs is categorized by:

(a) Monorotors: these types of drones cauterized by the central rotor at the summit and an additional rotor at the rear for stability, as in the quadrotor configurations.

(b) Coaxial: they have two rotors turning in reverse directions installed on the same tree.

(c) Quadrotor: these kinds of drones have four rotors positioned in a cross.

(d) Multirotor: drones mounted by six or eight rotors. These kind of drones are nimble and hover even with in case of engine stoppage, because of the numerous rotors that are mounted with the redundancy.

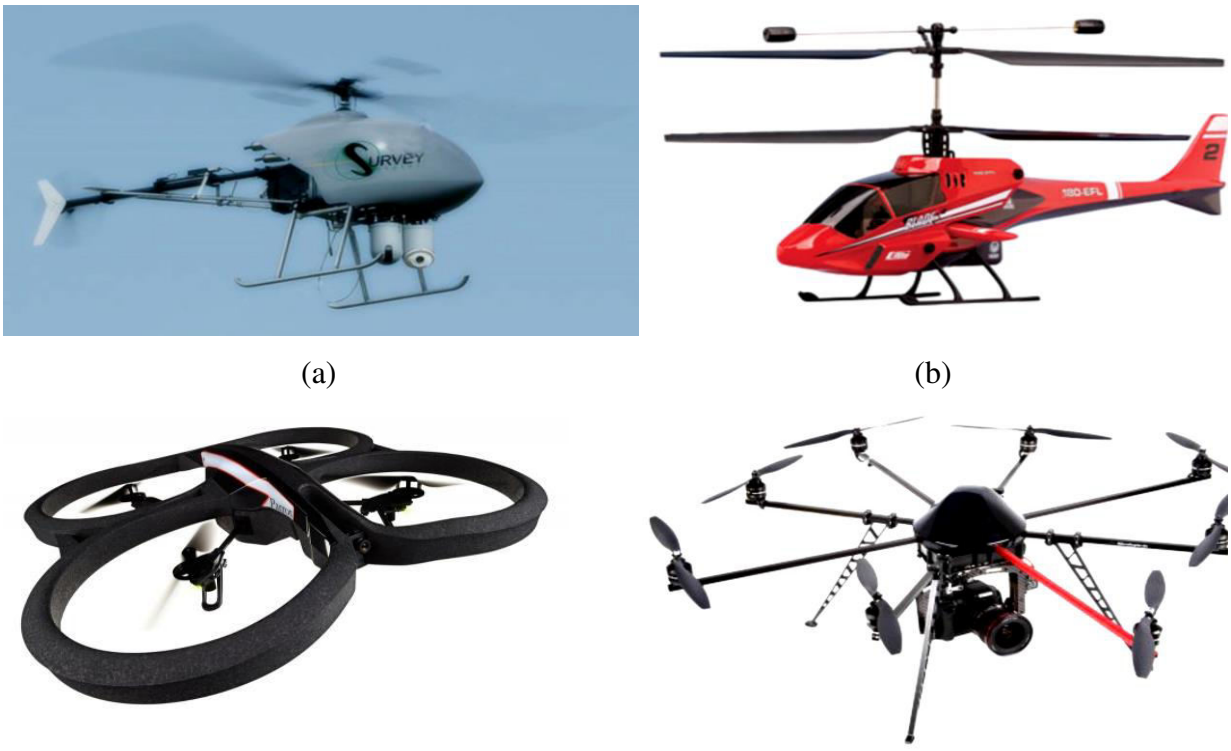

(a) (b)

(c) (d)

Figure I.4: (a) Monorotor drone, (b) Coaxial rotary-wing drone, (c) Quadrotor drone, (d) Multirotor drone [8,1].

I.3 Quadrotors

A quadrotor consisting of four rotors, each attached to one end of a cross-shaped composition shown in figure I.5. Each rotor consists of a propeller attached to an independently powered DC motor. Propellers 1 and 3 spin the same while propellers 2 and 4 spin in the opposite direction, balancing the entire system torque and eliminating gyroscopic and aerodynamic torque in hover aviation [10, 11].

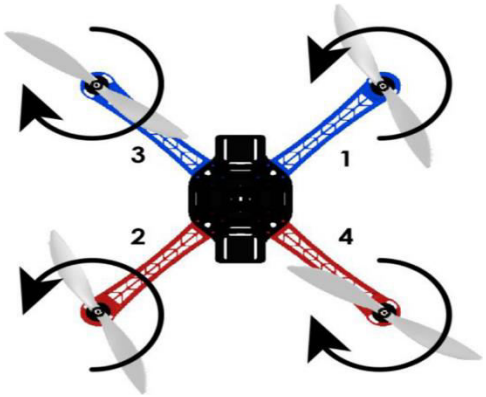

Figure I.5 Quadrotor configuration[11].

To produce perpendicular upwards movement, the velocity of the four propellers is augmented collectively while the velocity is reduced to produce perpendicular downwards action. To generate roll rotation coupled with movement along the y-axis, the velocities of the second and fourth helices are changed while for pitch rotation coupled with movement along the x-axis, the velocities of the first and third propellers that need to be tainted. Additionally, there is a difficulty with quadcopter configurations, which is that to generate yaw rotation, there must be a difference in the reverse torque generated by each pair of propellers. For example, for positive yaw rotation, the velocities of both clockwise rotating rotors require amplification while the velocities of both counterclockwise rotating rotors require reduction [11, 12]. Figure I.6 illustrates how various movements can be generated; note that a thicker arrow means a large propeller speed.

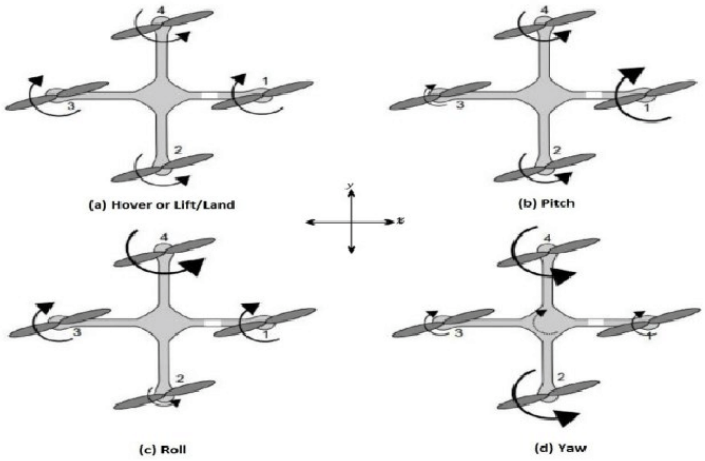

Figure I.6 Different movements of quadrotor UAV [13].

I.3.1 Quadrotors advantages and drawbacks

A number of advantages of the quadrotor over helicopters is that the rotor mechanics are basic as it is linked to four fixed-pitch rotors different from the variable-pitch rotor that characterizes the helicopter, which facilitates mechanization and maintenance . In addition, due to the symmetry of the configuration, the gyroscopic effects are diminished by a simple control. Stability flight can be more stable in quadrotor than in helicopters due to the appearance of four propellers providing four thrust forces displaced at a fixed distance from the center of gravity rather than a single mid-mounted propeller as in the construction of helicopters [10]. Other advantages are perpendicular flight and landing capabilities, improved maneuverability, and less dimension due to the non-existence of a tail [14], these capabilities keep quadcopters

practical in surveying small areas and l building review [15]. Additionally, quadcopters contain higher payload capacities due to the existence of four motors thus providing superior thrust [10]. In the other side, quadrotors use a huge power owing to the existence of four propellers [15]. In addition, they contain a big dimension and heavier than a number of their counterpart again to the fact that there is four distinct propellers [15, 16].

Whereas advances in technologies and the ability to build miniature sensors and controllers by the Micro-Electo-Mechanical Systems (MEMS) technologies, so that we obtain several advance in the UAVs areas. In the literature we find various works focusing on the quadrotor owing to its significant advantages such as that quadrotors are easy to be manufactured, assembled, compactness and maneuverability compared to others. A number of literatures studying just on advancing control algorithms that will be used in simulation. In this we explore several control methods that usually adopted in the most work.

I.4 Quadrotors control approaches

In the literature we found numerous control approaches which can be adopted to control a quadrotor differentiating from the traditional linear Proportional-Integral-Derivative (PID) or Proportional Derivative (PD) controller until the further complex nonlinear designs such as backstepping and sliding-mode controllers. It is noticed that we can classify the flight control into five major groups that are: linear control approaches, non-linear control approaches, adaptive approaches, Robust approaches and artificial intelligence techniques. It is concluded that the mainly familiar control approach that are adopted are the PID and PD controller.

I.4.1 Linear Control approaches

This control technique represents the mainly universal and the usual flight control systems, classically used PID, Linear Quadratic (LQ) or H∞ algorithms. It is important to note that in the late 1960s, a large-scale helicopter achieved autonomous waypoint navigation by a conventional linear control method [17].In [11], the authors proposed the use of PID and LQ control methods to be adopted with micro quadrotor in indoor area, the result that these types of controllers provided a remarkable aptitude to make the quadrotor more stable in terms of its attitude around its fly location over little disturbances. Otherwise, in [14] a traditional PID is utilized to control the quadrotor situation and orientation and it was capable to stabilize in a little velocity wind environment. In [18], the authors employs a self tuning PID controller by taking into account an adaptive pole position to control the attitude and heading of a quadrotor.

Simulations illustrated that the developed controller behave good in the case of online tuning of parameters. In [19], the authors used H∞ controller to maintain stabilization of the rotational angles simultaneously with a Model Predictive Controller (MPC) to follow the preferred situation. The wind and model uncertainties effects were taken into account with the simulated model and it demonstrated robustness with a zero steady-state error. H∞ is a robust linear controller; robust controllers are those that take into account parametric uncertainty and unmodeled dynamics. In the literature, H∞ it is utilized for controlling of complete-scaled helicopters [17].

I.4.2 Nonlinear Control approaches

Since QUAV dynamics is a nonlinear character, the development of nonlinear control methods for use as flight controllers is necessary. In the literature there are different nonlinear control approaches used with quadrotors as well as: feedback linearization, backstepping and sliding-mode.

A) **Backstepping and Sliding-mode:** Backstepping defined as a recursive control technique that can be applied to both linear and nonlinear systems [17]. From the literature, we found that the most current work used this kind of controllers. In [15] the authors developed the use of backstepping and sliding-mode nonlinear control techniques to control the quadrotor, where it is concluded the effectiveness of such controller against the existence of disturbances. In addition the authors in [20], have developed controllers that can maintain stabilization of the quadrotor in an outdoors conditions, the assessment of the integral sliding-mode controller was performed by a comparison with an a reinforcement learning controller. It is concluded that both controllers were able to stabilize the quadcopter outdoors with improved performance over traditional control methods [20]. From [21], the authors used a backstepping controller with the use of Lyapunov stability theory to follow preferred values for QUAV position and orientation. The authors decomposed the model of QUAV into three subsystems: underactuated, fully-actuated and propeller subsystems. The developed technique was efficient to stabilize the system without disturbances. Otherwise, in [22], a technique is proposed by merging a backstepping controller with an adaptive controller to surmount the model uncertainties and external disturbances problems. The evaluation of the developed adaptive integral backstepping algorithm leads to conclude that the system is capable to decrease the overshoot and response time

and get rid of steady state error. Furthermore, in [23] a backstepping controller is adopted to control the QUAV position and attitude, where the investigation leads to conclude the efficiency despite the presence of a noisy conditions [23]. Furthermore in [24], the authors combination of a backstepping controller with an adaptive algorithm to control QUAV attitude. Wherever, a robust adaptive function is utilized to approximate the external disturbances and errors in system modeling. Simulation results illustrated the accomplishment of the developed controller by surmounting uncertainties and disturbances. Besides in [25], the authors suggested the use of a chattering free sliding mode controller for the QUAV altitude control. The developed technique demonstrated a remarkable performance by simulation results and also in a real environment with disturbances and in noisy environment.

B) **Feedback Linearization:** feedback linearization defined as a control method which adopted nonlinear transformation between nonlinear states of system variables into linear states. Linear algorithms can then be used to stabilize the linear transformed system which will then be oppositely transformed back into the original state variables. Dans ce contexte, les auteurs de [10, 26] ont proposé un contrôleur capable de contrôler un QUAV dans de nombreuses expériences de vol stationnaire en considérant les théories du concept de linéarisation par rétroaction [10].

I.4.3 Adaptive control techniques

The quadrotors have various parameters which can be parametric uncertainties such as mass variance, inertia and aerodynamic coefficients, in which case the usage of adaptive approximation methods is necessary. In [26], an adaptive integral backstepping approach has been developed to deal through external perturbations. The referential adaptive control approach is widely used to adaptive control [27].

I.4.4 Robust methods

Although quadcopters are obedient to uncertainty and external disturbances such as wind. Thus, the quadcopter system requires powerful robust control features to cope with these effects. By the use of different powerful approaches. For example, in [28] an efficient terminal sliding mode control was developed to achieve finite time convergence and guarantee

asymptotic convergence of the sliding mode, besides this developed approach suffered from interruption in the switching signal generating in chattering occurrence.

I.4.5 Intelligence control methods

Numerous works have studied the integration of artificial intelligence approaches with process control to improve performance by the use of data reached throughout the flight procedure. These methods assume non-parametric effects and non-modelled effects, that becomes superior to adaptive approach, and numerous methods related to these approaches can be approved, the most well-known are fuzzy approach, neural network and learning control approach.

I.4.5.1 Neural networks with radial basis functions (RBF)

Radial basis function networks are relatively recent classes of adaptive neural networks (ANN). they comprise of an input, a hidden layer and an output layer. The general input/ output structure of an RBF network is shown in Figure I.7, where $x_i = [x_{1,i} \quad x_{2,i}]^T$ represent the reference vector, $\Pi = \hat{\mathcal{F}}_i, \hat{\mathcal{G}}_i$ the output vector [29].

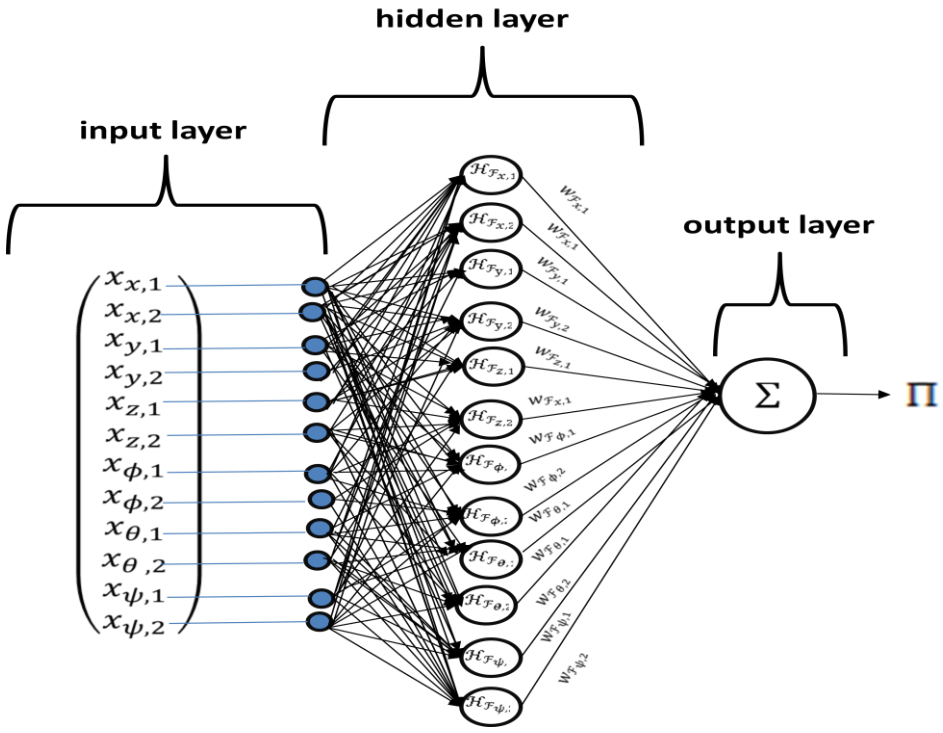

Figure I.7 The input/output structure of an radial basis function neural network (RBFNN).

I.4.5.2 Universal approximation theorem

The work of proved the possibility to approach continuous functions by neural networks. The networks considered are of the network type with a layer of hidden neurons with a nonlinear activation function, and with linear output neurons [29].

I.5 Stable neural adaptive control

In this control strategy, neural networks are introduced, taking advantage of their universal approximation property, to develop adaptive control systems according to two approaches. In the first approach, [29], called indirect adaptive, whose algorithm scheme is given in Figure I.8, generally two neural networks to be utilized to approximate the nonlinearities of the nonlinear system to be controlled. A control law is then deduced from these approximations by following the input-output linearization technique. This approach suffers from the singularity problem in the case where the control gain approximation is zero. Precautionary measures must then be taken to remedy this problem. Generally, projection algorithm is used in adaptation laws to force them to stay in admissible sets, while other algorithms use variable structure additive control law to avoid singularity problem [29].

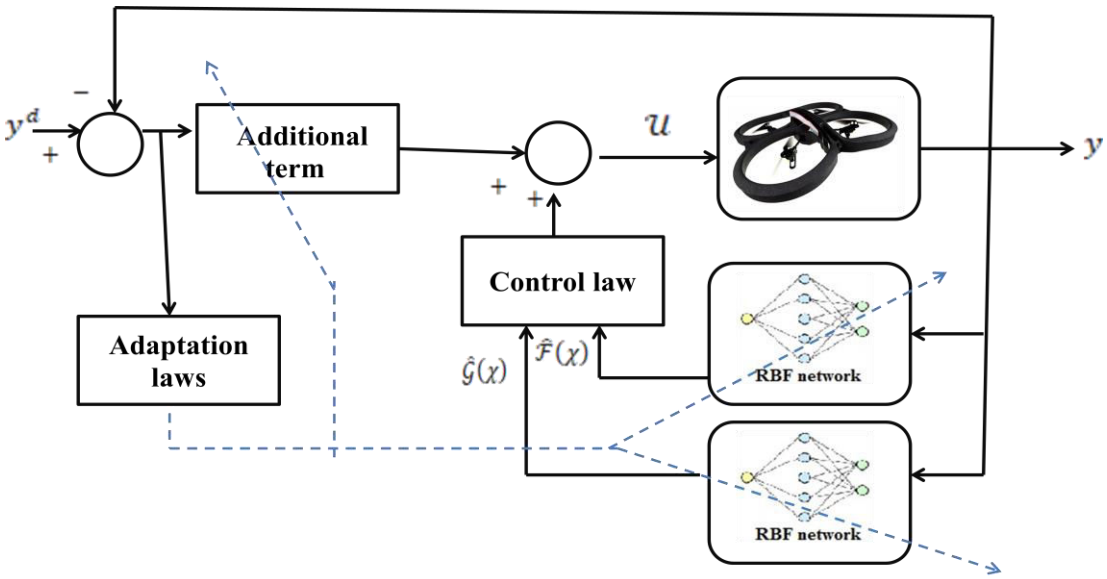

Figure I.8 Indirect neural adaptive control.

In the second approach for example in [29], called direct adaptive, a single neural network is used to directly approach an ideal control law under certain constraints on the control gain and/or on its derivative. The approximate control law is always Given by the input-output linearization technique whose diagram is given in Figure I.9.

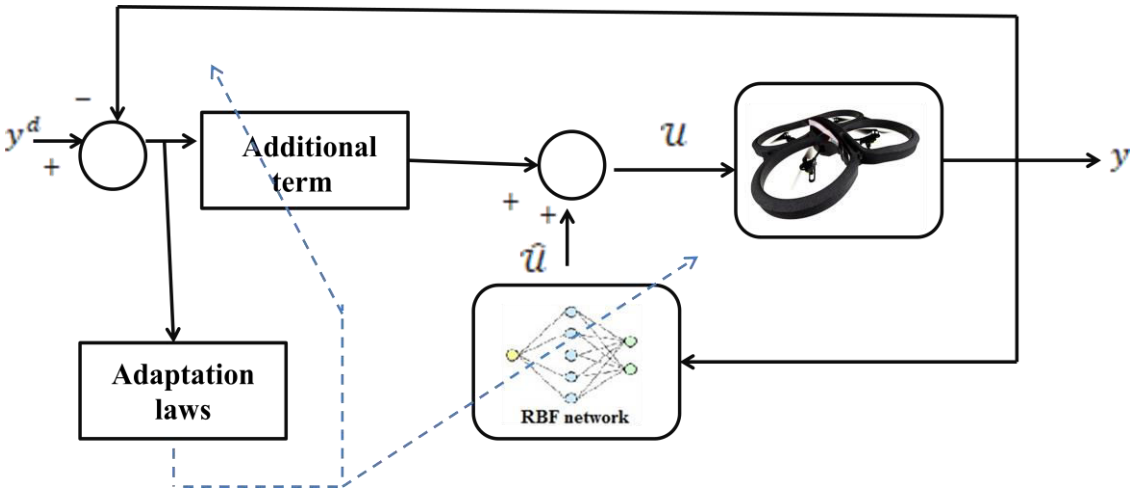

Figure I.9 Direct neural adaptive control.

In the two approaches cited in various studies, the direct Lyapunov method is used to analyze the control system stability. Based on this method, a Lyapunov function is constructed from the tracking error and its derivatives as well as the adaptation error of the weights of the neural networks. Consequently, the network adaptation laws are directly drawn from this analysis to fulfill Lyapunov's stability conditions.

I.6 Control techniques using fractional-order control

Fractional-order (FO) control approaches wre acknowledged as an efficient instrument to get better constitution to design control scheme for nonlinear system, in present years. The mentioned controllers will be very useful in different difficult systems [30].

I.7 Conclusion

In this chapter, we have discussed quadrotor in terms on, their control and their applications, which has allowed to note that in the field of mini drones, in particular quadrotor, there has been an interest growing by either researchers or engineers. What is with the evolutions of the instruments of control, communication and sensors. However, quadrotor involve challenges in due to the characteristics of their dynamic system; unstable, coupled, non-linear, complex, sensitive, and under-actuated. Since, the main factor to study any UAV is to offer proper mathematical models to plan and assess the control system to retain UAV stability thus, the next chapter is devoted to provide a QUAV modeling.

Chapter II

QUAV Modeling

II.1 Introduction

The quadrotor UAV (QUAV) type is perhaps the mostly general type for civilian purposes, as it does not require complex remote control skills to work with. This reputation, needs more investigations, to perceive the mathematical modeling, design, and analysis where quadrotor control methods are model based, it is essential to realize an accurate dynamical model. Since, the main objective is to achieve an appropriate mathematical model to develop and assess the control system in order to preserve the stability. This chapter expresses a mathematical modeling process of a quadrotor to be used in this work. It is significant to note, the most common modeling technique is based on Newton-Euler equations. which will be recalled hereafter.

II.2 QUAV concepts

A quadrotor is a flying robot with four rotors fixed uniformly over its center as it is shown in figure II.1. The displacement the QUAV is the consequences according to the rise or the reduce of the rotational rapidity of all the rotors. Two motors installed on the identical arm turn around in a dissimilar direction from the two other motors installed on the second arm, that withdraws the aerodynamic effect and gyro moments in the floating [31, 32]. Prior to deriving the QUAV model, it is essential to explicate the mechanism of the quadrotor.

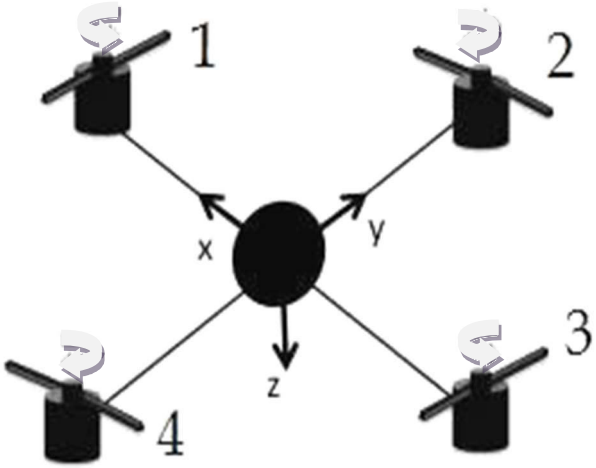

Figure II.1: Motion of QUAV [33].

QUAV represented by 6 Degree of Freedom, thus we have 6 variables ($x, y, z, \phi, \theta$and ψ) which are considered to describe the orientation in space ϕ, θ and ψ are also identified as Euler's angles as depicted in Figure II.2. More details of every variable are expressed as [33]:

- x and y: are used to characterize the QUAV location in space.
- z: represents the QUAV altitude.
- ϕ: represents the Roll angle which describes angle around the x-axis.
- θ : named Pitch angle that expresses the angle around the y-axis.
- ψ: named Yaw angle which expresses the angle around the z-axis.

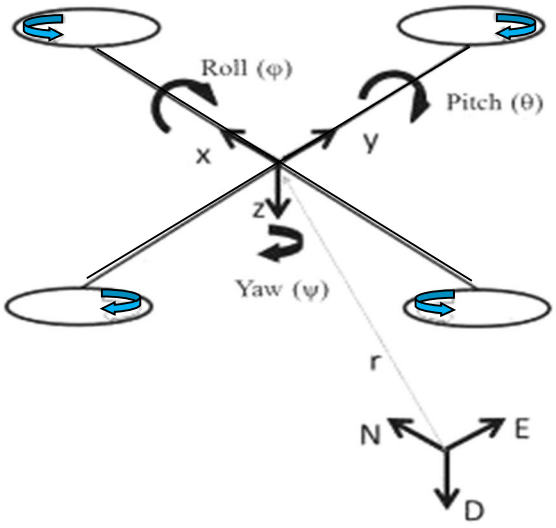

Figure II.2: Euler angles representation [33]

Even though the fact that the QUAV has 6 degrees of freedom, it is furnished presently by four propellers, as a result, it is not practical to attain the preferred set-point for every DOF, yet at most extreme four. In opposition, considering the structure, it is extremely easy to pick the four best controllable factors and that are Z, Roll, Pitch and Yaw.

II.3 System modeling

It is noticed that in this work, Newton-Euler formalism to be utilized to get the QUAV dynamics. Below are all assumptions that are adopted for the design [31]:

a) The Structure considered rigid and symmetrical

b) The propellers are rigid

c) Thrust and drag are relative to the square of propellers.

II.3.1 Dynamics modeling

The QUAV movement to be composed of two subsystems; rotational subsystem (roll, pitch and yaw) with translational subsystem (altitude and x and y position).

The rotational subsystem is entirely actuated as the translational subsystem is under actuated [34]

II.3.1.1 Rotational equations of motion

Rotational equations of motion are derived at the body frame according to the Newton-Euler method in general formulae described by:

$$\mathrm{J}\dot{\omega} + \omega \times \mathrm{J}\omega + \mathrm{M}_G = \mathrm{M}_B \qquad \text{(II.1)}$$

Where:

J ： diagonal inertia Matrix of QUAV

ω： angular body rates.

M_G ：Gyroscopic moments produced by inertia of rotors.

M_B: moments affecting the QUAV of the body frame.

The first two terms $\mathrm{J}\dot{\omega}$ and$\omega \times \mathrm{J}\omega$, in equation (II.1) correspond to the rate of change of angular momentum in the body's coordinate system. M_G specifies the gyroscopic moment correponding to rotor inertia J_r.

The Gyroscopic moments are determined to be $\omega \times [0 \quad 0 \quad \mathrm{J}_r\Omega_r]^T$, therefore the rotational equation of the QUAV movement to be represented by [34],

$$\mathrm{J}\dot{\omega} + \omega \times \mathrm{J}\omega + \omega \times [0 \quad 0 \quad \mathrm{J}_r\Omega_r]^T = \mathrm{M}_B \qquad \text{(II.2)}$$

Wherever:

J_r : inertia of rotors.

Ω_r : relative speed of rotors: $\Omega_r = -\Omega_1 + \Omega_2 - \Omega_3 + \Omega_4$.

The reason for deriving the motion-rotational equations in the body coordinate system instead of the inertial coordinate system is to obtain a time-independent inertial matrix.

Inertia matrix

The quadrotor inertia matrix is a diagonal matrix and due to the symmetry of the quadrotor the off-diagonal elements representing the inertia results are zero.

$$\mathrm{J} = \begin{bmatrix} I_x & 0 & 0 \\ 0 & I_y & 0 \\ 0 & 0 & I_z \end{bmatrix} \tag{II.3}$$

I_x, I_y with I_z represent moments inertia of area around the principle axes of the frame of body.

Moment of gyroscopic

The moment of the gyroscopic witch characterize the rotor represents the physical outcome in which gyroscopic torques or moments try to bring into line the spin axis of the rotor alongside the inertial z-axis [35].

Moments acting on the quadrotor ($\mathbf{M_B}$)

It is noticed that the last term of equation (II.2) needs defining two physical effects that are the forces of aerodynamic with moments created by the rotor. Under the effect of rotation, it is produced a force named aerodynamic or the lift force furthermore, there is a produced moment named the aerodynamic moment. Equations (II.4) and (II.5) illustrate the aerodynamic force F_i with a moment M_i which generated through the ith rotor [34].

$$F_i = \frac{1\rho A C_T}{2} r^2 \Omega_i \tag{II.4}$$

$$M_i = \frac{1\rho A C_D}{2} r^2 \Omega_i \tag{II.5}$$

Where

ρ : air density of the blade area.

C_T, C_D : represent the coefficient of the aerodynamic

r : blade radius .

Ω_i : velocity of the angular that describes the rotor i .

Noticeably, the force of the aerodynamic and moments related to the propeller geometry and the density of the air. In view of the fact that for quadrotor, the altitude maximum is

generally considered limited, therefore the density of the air can be adopted as constant, Equations (II.4) and (II.5) can be simplified to [34].

$$F_i = k_f \Omega_i^2 \tag{II.6}$$

$$M_i = k_M \Omega_i^2 \tag{II.7}$$

k_f with k_M represent the aerodynamic force with moment constants correspondingly and Ω_i defines the angular velocity that characterizes the rotor i. The moment constants and the force of aerodynamic can be obtained experimentally for every propeller type. Through determining moments and the forces that are produced by the propellers, it is easy to investigate the moments M_B take action on the QUAV. Figure II.3 illustrates the forces and moments affecting the QUAV system. Every rotor leads to an upwards thrust force F_i and produces a moment M_i with way opposite to the direction of rotation of the related rotor i. Beginning with moments around the body frame's x-axis, by the use of the right-hand rule in relationship with the axes of the frame of body, F_2 multiplied by the moment arm l produces a negative moment around the y-axis, whereas in the same way, F_4 produces a positive moment. Therefore the whole moment around the x-y-z-axis can be given as:

$$M_B = \begin{bmatrix} lk_f(-\Omega_2^2 + \Omega_4^2) \\ lk_f(\Omega_1^2 - \Omega_2^2) \\ lk_f(\Omega_1^2 - \Omega_2^2) \end{bmatrix} \tag{II.8}$$

l : represents the moment arm representing the space between each rotor's axis of Rotation about the origin of the body frame. This should coincide with the center of the QUAV.

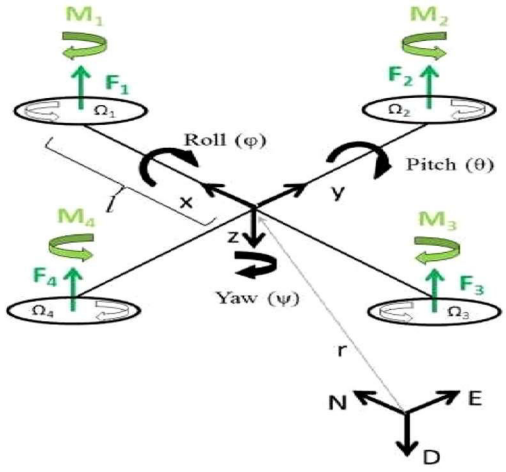

Figure II.3: Moments and forces affecting QUAV [33].

II.3.1.2 Translational equations of motion

The QUAV translational equations of motion use Newton's second law and are derived in the Earth's inertial frame of reference [34]:

$$m\ddot{r} = \begin{bmatrix} 0 \\ 0 \\ mg \end{bmatrix} + RF_B \tag{II.9}$$

$r = [x, y, z]^T$: characterizes the distance of the QUAV from the inertial frame.

m : the mass of QUAV.

g : acceleration of gravity $g = 9.81m/s^2$.

F_B :Forces of non-gravitational that affect the QUAV in the chassis.

II.4 Model of the state space

Formulating the mathematical model obtained for QUAV by a state-space model formulates the control problem very simply.

II.4.1 State vector X

Expressing the state vector of the QUAV by:

$$\chi = [x_1, x_2, x_3, x_4, x_5, x_6, x_7, x_8, x_9, x_{10}, x_{11}, x_{12}]^T \tag{II.10}$$

That is mapped to the DOF of the QUAV by:

$$\chi = \left[x, \dot{x}, y, \dot{y}, z, \dot{z}, \phi, \dot{\phi}, \theta, \dot{\theta}, \psi, \dot{\psi}\right]^T \tag{II.11}$$

The vector of state determines the QUAV position in space with its angular and linear speeds.

II.4.2 Control input vector $\mathcal{U}_i$

A control input vector $\mathcal{U}_i$, consists of four inputs; $\mathcal{U}_{z,}$ through $\mathcal{U}_\psi$ to be expressed by:

$$\mathcal{U}_i = [\mathcal{U}_{z,}\mathcal{U}_\phi, \mathcal{U}_\theta, \mathcal{U}_\psi] \tag{II.12}$$

Where :

$$\begin{aligned} \mathcal{U}_z &= k_f(\Omega_2^2 + \Omega_2^2 + \Omega_2^2 + \Omega_4^2) \\ \mathcal{U}_\phi &= k_f(-\Omega_2^2 + \Omega_4^2) \\ \mathcal{U}_\theta &= (\Omega_1^2 - \Omega_3^2) \\ \mathcal{U}_\psi &= k_M(\Omega_1^2 - \Omega_2^2 + \Omega_3^2 - \Omega_4^2) \end{aligned} \tag{II.13}$$

Equation (II.13) to be given in a matrix as follows:

$$\begin{bmatrix} \mathcal{U}_z \\ \mathcal{U}_\phi \\ \mathcal{U}_\theta \\ \mathcal{U}_\psi \end{bmatrix} = \begin{bmatrix} k_f & k_f & k_f & k_f \\ 0 & -k_f & 0 & k_f \\ -k_f & 0 & k_f & 0 \\ k_M & -k_M & k_M & -k_M \end{bmatrix} \begin{bmatrix} \Omega_1^2 \\ \Omega_2^2 \\ \Omega_3^2 \\ \Omega_4^2 \end{bmatrix} \tag{II.14}$$

$\mathcal{U}_z$ denotes the outgoing upward force of the four rotors which is the main cause of the QUAV altitude and its rate of change (z, $\dot{z}$). $\mathcal{U}_\phi$ represents the difference in force between rotors two and four that is accountable for the roll rotation with its rate of change (ϕ, $\dot{\phi}$). $\mathcal{U}_\theta$ otherwise denotes the variation in thrust between rotors one and three therefore producing the pitch rotation with its rate of change (θ, $\dot{\theta}$). Lastly $\mathcal{U}_\psi$ represent the difference in torque among the two clockwise rotating rotors with the two counterclockwise rotating rotors producing the yaw rotation with ultimately its rate of change (ψ, $\dot{\psi}$). This option of the control vector $\mathcal{U}_i$ decouples the rotational system, wherever $\mathcal{U}_z$will cause the preferred altitude of the QUAV, $\mathcal{U}_\phi$ produces the preferred roll angle, the preferred pitch angle to be produced by $\mathcal{U}_\theta$ while $\mathcal{U}_\psi$ will produce the preferred heading.

When calculating the rotor rapidity from the control input, we need an inverse relationship between the control input and the rotor speed. This is obtained by inverting the matrix in Eq. (II.14) as follows:

$$\begin{bmatrix} \Omega_1^2 \\ \Omega_2^2 \\ \Omega_3^2 \\ \Omega_4^2 \end{bmatrix} = \begin{bmatrix} \frac{1}{4k_f} & 0 & \frac{1}{2k_f} & \frac{1}{4k_M} \\ 0 & -\frac{1}{2k_f} & 0 & -\frac{1}{4k_M} \\ \frac{1}{4k_f} & 0 & -\frac{1}{2k_f} & \frac{1}{4k_M} \\ \frac{1}{4k_f} & \frac{1}{2k_f} & 0 & -\frac{1}{4k_M} \end{bmatrix} \begin{bmatrix} \mathcal{U}_z \\ \mathcal{U}_\phi \\ \mathcal{U}_\theta \\ \mathcal{U}_\psi \end{bmatrix} \tag{II.15}$$

If we take the square root of that, the control inputs leads to conclude rotors speeds as:

$$\Omega_1 = \sqrt{\frac{1}{4k_f}\mathcal{U}_z + \frac{1}{2k_f}\mathcal{U}_\theta + \frac{1}{4k_M}\mathcal{U}_\psi}$$

$$\Omega_2 = \sqrt{\left|\frac{1}{4k_f}\mathcal{U}_z - \frac{1}{2k_f}\mathcal{U}_\phi - \frac{1}{4k_M}\right|\mathcal{U}_\psi} \qquad \text{(II.16)}$$

$$\Omega_3 = \sqrt{\left|\frac{1}{4k_f}\mathcal{U}_z - \frac{1}{2k_f}\mathcal{U}_\theta + \frac{1}{4k_M}\right|\mathcal{U}_\psi}$$

$$\Omega_4 = \sqrt{\frac{1}{4k_f}\mathcal{U}_z + \frac{1}{2k_f}\mathcal{U}_\phi - \frac{1}{4k_M}\mathcal{U}_\psi}$$

II.4.3 Motion rotational equation

If we substitute the equation (II.13) in equation (II.8), we obtain the whole moments that affecting the QUAV as:

$$M_B = \begin{bmatrix} l\mathcal{U}_\phi \\ l\mathcal{U}_\theta \\ \mathcal{U}_\psi \end{bmatrix} \qquad \text{(II.17)}$$

Substituting (II.17) into the rotational equation of motion (II.2) and expanding terms related to their previous definition from Chapter II, we can derive the relation by:

$$\begin{bmatrix} I_x & 0 & 0 \\ 0 & I_y & 0 \\ 0 & 0 & I_z \end{bmatrix}\begin{bmatrix} \ddot{\phi} \\ \ddot{\theta} \\ \ddot{\psi} \end{bmatrix} + \begin{bmatrix} \dot{\phi} \\ \dot{\theta} \\ \dot{\psi} \end{bmatrix} \times \begin{bmatrix} I_x & 0 & 0 \\ 0 & I_y & 0 \\ 0 & 0 & I_z \end{bmatrix}\begin{bmatrix} \dot{\phi} \\ \dot{\theta} \\ \dot{\psi} \end{bmatrix} + \begin{bmatrix} \dot{\phi} \\ \dot{\theta} \\ \dot{\psi} \end{bmatrix} \times \begin{bmatrix} 0 \\ 0 \\ \mathrm{J}_r\Omega_r \end{bmatrix} = \begin{bmatrix} l\mathcal{U}_\phi \\ l\mathcal{U}_\theta \\ \mathcal{U}_\psi \end{bmatrix} \qquad \text{(II.18)}$$

Expanding that, leads to

$$\begin{bmatrix} I_x\ddot{\phi} \\ I_y\ddot{\theta} \\ I_z\ddot{\psi} \end{bmatrix} + (-1) \times \begin{bmatrix} \dot{\phi} \\ \dot{\theta} \\ \dot{\psi} \end{bmatrix}\begin{bmatrix} I_x & 0 & 0 \\ 0 & I_y & 0 \\ 0 & 0 & I_z \end{bmatrix}\begin{bmatrix} \dot{\phi} \\ \dot{\theta} \\ \dot{\psi} \end{bmatrix} + \begin{bmatrix} \dot{\theta}\mathrm{J}_r\Omega_r \\ -\dot{\phi}\mathrm{J}_r\Omega_r \\ 0 \end{bmatrix} = \begin{bmatrix} l\mathcal{U}_\phi \\ l\mathcal{U}_\theta \\ \mathcal{U}_\psi \end{bmatrix} \qquad \text{(II.19)}$$

Expressing again the equation II.19 to obtain the angular accelerations regarding to further variables

$$\ddot{\phi} = I_x{}^{-1}\left(l\mathcal{U}_\phi + I_y - I_z\dot{\theta}\dot{\psi} - I_r\,\Omega_r\,\dot{\theta}\right)$$
$$\ddot{\theta} = I_y{}^{-1}\left(l\mathcal{U}_\theta + I_z - I_x\dot{\phi}\dot{\psi} - I_r\,\Omega_r\dot{\phi}\right) \quad \text{(II.20)}$$
$$\ddot{\psi} = I_z{}^{-1}\left(l\mathcal{U}_\psi + I_x - I_y\,\dot{\psi}\dot{\phi}\right)$$

Choosing of the control reference vector $\mathcal{U}_i$, we can realize that the rotational subsystem will be totally-actuated, which is just related to the rotational state variables $x_7 \to x_{12}$ corresponding to $\phi, \dot{\phi}, \theta, \dot{\theta}, \psi, \dot{\psi}$ respectively.

II.4.4 Motion of translational equation

The forces of no gravitational that affecting the QUAV to be expressed by:

$$F_B = \begin{bmatrix} 0 \\ 0 \\ k_f(\Omega_1^2 - \Omega_2^2 + \Omega_3^2 - \Omega_4^2) \end{bmatrix} \quad \text{(II.21)}$$

Substituting equation (II.13) into equation (II.21), the equation for the total moment affecting QUAV is:

$$F_B = \begin{bmatrix} 0 \\ 0 \\ -\mathcal{U}_z \end{bmatrix} \quad \text{(II.22)}$$

Inserting this into the translational equation (II.9) and expanding the terms yields the state space:

$$m\begin{bmatrix} \ddot{x} \\ \ddot{y} \\ \ddot{z} \end{bmatrix} = \begin{bmatrix} 0 \\ 0 \\ mg \end{bmatrix} + \begin{bmatrix} c\theta c\psi & c\psi s\phi s\theta - s\psi c\phi & c\psi c\phi s\theta + s\psi s\phi \\ c\theta s\psi & s\psi s\phi s\theta + c\psi c\phi & s\psi c\phi s\theta - c\psi s\phi \\ -s\theta & c\theta s\phi & c\theta c\phi \end{bmatrix}\begin{bmatrix} 0 \\ 0 \\ -\mathcal{U}_z \end{bmatrix} \quad \text{(II.23)}$$

Rewriting equation (II.18) to obtain the accelerations in depending on the other variables, the expression below is obtained:

$$\ddot{x} = m^{-1}\left(\mathcal{U}_z(c\psi s\theta c\phi + s\psi s\phi)\right)$$
$$\ddot{y} = m^{-1}(\mathcal{U}_z(c\psi s\theta s\phi - c\psi s\phi)) \quad \text{(II.24)}$$
$$\ddot{z} = m^{-1}\mathcal{U}_z(c\theta s\phi) - g + m^{-1}$$

II.4.5 Representation of the state space

Generally, the dynamic equations (II.20) and (II.24) are a second-order underactuated nonlinear system that can be rewritten as:

$$\dot{\chi} = \mathcal{F}_i(\chi) + \mathcal{G}_i(\chi)\mathcal{U}_i \tag{II.25}$$

Where : $\mathcal{F}_i(\chi)$ and $\mathcal{G}_i(\chi)$ are unknown smooth nonlinear functions of the ith subsystem, respectively.

$$\begin{cases} \mathcal{F}_x(\chi) = 0 \quad , & \mathcal{G}_x(\chi) = 1/m \\ \mathcal{F}_y(\chi) = 0 \quad , & \mathcal{G}_y(\chi) = 1/m \\ \mathcal{F}_z(\chi) = -g, & \mathcal{G}_z(\chi) = cx_{\phi,1}cx_{\theta,1}/m \\ \mathcal{F}_\phi(\chi) = (I_y - I_z)/I_x x_{\theta,2}x_{\psi,2} - I_r\,\Omega_r/I_x x_{\theta,2}\,, & \mathcal{G}_\phi(\chi) = l/I_x \\ \mathcal{F}_\theta(\chi) = (I_z - I_x)/I_y x_{\phi,2}x_{\psi,2} + I_r\,\Omega_r/I_y x_{\phi,2}\,, & \mathcal{G}_\theta(\chi) = l/I_y \\ \mathcal{F}_\psi(\chi) = (I_x - I_y)/I_z x_{\theta,2}x_{\phi,2} + I_r\,\Omega_r/I_y x_{\phi,2,} & \mathcal{G}_\psi(\chi) = 1/I_z \end{cases} \tag{II.26}$$

Based on Eq.(10), we reformulate the state space of the system model by:

$$\begin{cases} \dot{x}_{i,1} = x_{i,2} \\ \dot{x}_{i,2} = \mathcal{F}_i(\chi) + \mathcal{G}_i(\chi)\mathcal{U}_i \\ y_i = x_{i,1}, i \in \{x, y, z, \phi, \theta, \psi\} \end{cases} \tag{II.27}$$

$x_i \in [x_{i,1}, x_{i,2}]$ is the vector of the local state of every subsystem where, $y_i = x_{i,1}$ and $x_{i,2}$, its derivative. From equation (II.20), (II.24), the system has six outputs including the position outputs (x, y, z) and the orientation outputs (ϕ, θ, ψ) with only four independent inputs. Thus, it is not easy to control the six subsystems individually. To defeat this problem, two virtual control inputs μ_x and μ_y to be generated to drive the Cartesian position subsystems x and y, respectively [36]. From equation (II.20), (II.24)and (II.26) μ_x and μ_y are chosen as:

$$\begin{bmatrix} \mu_x \\ \mu_y \end{bmatrix} = \begin{bmatrix} \mu_z(c\phi s\theta c\psi + s\psi s\phi) \\ \mu_z(c\phi s\theta c\psi - s\psi s\phi) \end{bmatrix} \tag{II.28}$$

The control inputs (μ_x, μ_y) update the desired values of roll ϕ^d and pitch θ^d angles. Therefore, (ϕ^d, θ^d) angles are obtained as solutions of the system described by equation. (II.28) and can be gvien by:

$$\begin{bmatrix} \phi^d \\ \theta^d \end{bmatrix} = \begin{bmatrix} arcsin(\mu_x s\psi - \mu_y c\psi) \\ arcsin(\frac{\mathcal{U}_x c\psi + \mathcal{U}_y s\psi}{c\theta^d}) \end{bmatrix} \tag{II.29}$$

II.5 Conclusion

In this chapter, we have discussed the dynamic modeling of multi-rotors. Where a 6 degrees of freedom rigid body model were advanced by the Newton-Euler theories. After that, the forces that characterize the most important moments that affecting the QUAV were considered. The oncoming results described by equations are nonlinear and for that reason the direct application of such parameters to synthesizing of control with estimation algorithms remain complex. To surmount this dilemma, many simplifications have been made to design reasonably simple control laws for applications. In general, QUAV systems are represented as state-space to show control and wind effects. In the next chapters that are related to the main contributions of this thesis we use the developed representation of the state space with the control laws.

Chapter III

Stabilization of QUAV Under Unknown Dynamics, Parameter uncertainties and External disturbances Using intelligent techniques Based non-linear control

III.1 Introduction

The control of quadrotor is difficult because of the highly coupled nonlinear dynamics, unstable and multi-variable nature, under-actuation characteristic, as well as presence of unknown dynamics, parameter uncertainties and external disturbances. So far, many efforts have been made for altitude and attitude control of the quadrotor. Some strategies ranging from classical to advanced and intelligent techniques have been proposed in the literature [37-39]**.** Among the most advance non-linear feedback control techniques applied recently to the quadrotor to overwhelm the undesirable effects of uncertainties and disturbances those that combine, the adaptive control (AC), the backstepping control (BC) and sliding mode control (SMC) [39-42]. From the literature survey, these methods provide a good transient performance, easy tuning and implementation, and strong robustness against system uncertainties and external disturbances. However, the BC needs the knowledge of the precise mathematical model and the physical parameters of quadrotor model, which decreases the control performance in the case of uncertainties and disturbances. Also, the SMC has the inherent problem of the undesired large control chattering phenomenon, caused by the large switching gain of the discontinuous switching control term. To tackle these disadvantages, many researchers have used artificial neural networks (NN) and / or fuzzy logic system (FLS) to approximate universal systems to solve the problem of controlling uncertain nonlinear systems, such as quadrotor.

In this chapter, two plans of nonlinear control schemes to propose and study for a quadrotor system. Backstepping controller based on an adaptive fuzzy neural network(FNN) .Also, an adaptive fuzzy-chebyshev network-based continuous sliding mode controller is developed are proposed for the quadrotor under uncertainties , external disturbance and the unknown dynamics.

III.2 Adaptive fuzzy-neural network based decentralized backstepping controller

This section (1) studies and design a backstepping controller based on an adaptive fuzzy neural network (FNN). The FNN with adaptive parameters is exploited to approximate the nonlinear functions and improve the robustness against parametric uncertainties and external disturbances. FNN is included in classical backstepping control (BC) to solve the unknown dynamics problem. Otherwise, a robust control term is added

to improve performance in tracking a reference signal when parametric uncertainties and disturbances exist. The stability of the quadrotor attitude control system is proven by the Lyapunov method.

In this section(1) is to a combination of the nonlinear approximation function of the fuzzy system and the neural network with backstepping controller was done to design a robust adaptive control scheme. The main of this section are diverse and important as, the problems of singularity and the need of a robust additional term in BC methodology are avoided. In addition, the prior knowledge of uncertainty limits is not necessary and ideal dynamics of the mathematical system are not needed

Mathematical model and problem statement

In section (1), the quadrotor model can be specified in the state-space form shown below.

$$\dot{\chi} = F(\chi) + G_i U_i \tag{III.1}$$

where χ denotes the global state variable, $F_i(\chi)$ and G_i are the nonlinear functions matrix and input gains, written as follows:

$$\chi = [x_{1\phi},\ x_{2\phi}, x_{1\theta}, x_{2\theta}, x_{1\psi}, x_{2\psi}]^T$$
$$= [\phi, \dot{\phi}, \theta, \dot{\theta}, \psi, \dot{\psi}]^T$$

$$F(x) = \begin{pmatrix} x_{2,\varphi} \\ a_\varphi x_{2,\theta} x_{2,\psi} - \dfrac{J_r \Omega_r}{I_x} x_{2,\theta} \\ x_{2,\theta} \\ a_\theta x_{2,\varphi} x_{2,\psi} + \dfrac{J_r \Omega_r}{I_y} x_{2,\varphi} \\ x_{2,\psi} \\ a_\psi x_{2,\varphi} x_{2,\theta} \end{pmatrix} \tag{III.2}$$

$$G = \begin{pmatrix} \frac{l}{I_{xx}} & 0 & 0 \\ 0 & 0 & 0 \\ 0 & \frac{l}{I_{yy}} & 0 \\ 0 & 0 & 0 \\ 0 & 0 & \frac{1}{I_{zz}} \end{pmatrix} \quad \text{(III.3)}$$

From (III.1) to (III.3), the quadrotor model can be considered as a complex large-scale system, which is composed of three Single-Input Single-Output (SISO) interconnected nonlinear subsystems. Let us redefine the variables for simplicity as $x_i = [x_{1,i} \quad x_{2,i}]^T$ for $i \in \{\phi, \theta, \psi\}$. Then, the model of quadrotor can be described by a generalized state equation as follows:

$$\begin{aligned} \dot{x}_{1,i} &= x_{2,i} \\ \dot{x}_{2,i} &= \mathcal{F}_i(\chi) + \mathcal{G}_i u_i + \ p_i, i \in \{\phi, \theta, \psi\} \\ y_i &= x_{1,i} \end{aligned} \quad \text{(III.4)}$$

In which $\mathcal{F}_i(x)$ and $\mathcal{G}_i$ are the nonlinear dynamic and input control functions of the i th subsystem, respectively and p_i represents the total uncertainty, the external disturbances and the interactions with other subsystems, with:

$$\begin{aligned} &\mathcal{F}_\phi(x) = (I_y - I_z)x_{2\theta}x_{2\psi}/I_x - J_r\Omega_d x_{2\theta}/I_x \\ &\mathcal{F}_\theta(x) = (I_z - I_x)x_{2\phi}x_{2\psi}/I_y - J_r\Omega_d x_{2\phi}/I_y \\ &\mathcal{F}_\psi(x) = (I_x - I_y)x_{2\phi}x_{2\theta}/I_z, \\ &\mathcal{G}_\phi(x) = l/I_x, \mathcal{G}_\theta(x) = l/I_y, \mathcal{G}_\psi(x) = 1/I_z \end{aligned} \quad \text{(III.5)}$$

For quadrotor system (III.4), the objective of the AFNN-DBC is to force the system output y_i, to follow successfully a given bounded reference signal y_i^d in the presence of uncertainties such as parametric variations and external disturbances. In order to achieve this control objective, the following assumptions are made:

Assumption.*1*: *The desired quadrotor path, y_i^d and its time derivatives, $\dot{y}_i^d$, $\ddot{y}_i^d$ are assumed to be well known, smooth and bounded. Besides, all the closed-loop system states are assessable and accessible. There is a problem encountered by the users of the*

backstepping method in the trajectory tracking. As see in [43,44]*, this assumption is habitually adopted*.

Assumption.2: *The $p_i(t)$ term represents the disturbances that are included in the QUAV model for characterizing impacts of unmodeled dynamics, parameters uncertainties and wind effort where, exist unknown positive constants $\mathcal{L}_i^*$ that satisfy the inequality:*

$$|p_i(t)| \leq \mathcal{L}_i^* \tag{III.6}$$

Assumption 3*: The roll, the pitch and the yaw angles (ϕ, θ, ψ) are enclosed as: Roll angle by $-\pi/2 < \phi < \pi/2$, pitch angle by $-\pi/2 < \theta < \pi/2$ and yaw angle by $-\pi < \psi < \pi$*

III.2.1 Classical backstepping controller

In this subsection, we will apply the classical BC design methodology. This designed BC obliged ensuring the attitude control, stability and desired position tracking. The control system method is separated on three steps one for every subsystem

Step 1. We define the tracking error variables for the reference signals y_i^d as:

$$\begin{aligned} \mathrm{e}_{i,1} &= y_i^d - y_i \\ \mathrm{e}_{i,1} &= y_i^d - x_{i,1} \end{aligned} \tag{III.7}$$

Their first derivative is expressed by:

$$\dot{\mathrm{e}}_{i,1} = \dot{y}_i^d - \dot{x}_{i,1} = \dot{y}_i^d - x_{i,2} \tag{III.8}$$

To confirm the stability and the convergence of the first tracking errors we use the Lyapunov function candidate as $\mathcal{V}_{i,1} = \frac{1}{2}\mathrm{e}_{i,1}^2$ [45]:

$$\mathcal{V}_1 = \sum_{i=\{\phi,\theta,\psi\}} \mathcal{V}_{i,1} = \frac{1}{2}\sum_{i=\{\phi,\theta,\psi\}} \mathrm{e}_{i,1}^2 \tag{III.9}$$

The time derivative of $\mathcal{V}_1$ and substituting equation.(III.7) we found:

$$\dot{\mathcal{V}}_1 = \sum_{i=\{\phi,\theta,\psi\}} \mathrm{e}_{i,1}\dot{\mathrm{e}}_{i,1}$$

$$= \sum_{i=\{\phi,\theta,\psi\}} \mathrm{e}_{i,1}(\dot{y}_i^d - x_{i,2}) \quad \text{(III.10)}$$

To stabilize the errors dynamic equation (III.7), we construct the virtual control law $\mathcal{Q}_i$ as $x_{2,i}$ which can be defined as:

$$\mathcal{Q}_i = \dot{y}_i^d + \mathcal{C}_i\mathrm{e}_{i,1} \quad \text{(III.11)}$$

$\mathcal{C}_i > 0$ is a design parameter selected by the user through the simulation experiments. Substituting the virtual control by its chosen value, the time derivative of $\dot{\mathcal{V}}_1$equation(III.10) can be expressed again by:

$$\dot{\mathcal{V}}_1 = -\sum_{i=\{\phi,\theta,\psi\}} \mathcal{C}_i\mathrm{e}_{i,1}^2 \leq 0 \quad \text{(III.12)}$$

Thus, $\mathcal{V}_1$is semi-define negative, $\mathrm{e}_{1,i}$ is stable and converges to zero.

Step2. We describe the second local tracking error of *i* th subsystem:

$$\mathrm{e}_{i,2} = \dot{y}_i - \mathcal{Q}_i = x_{i,2} - \mathcal{Q}_i \,, i \in \{\phi,\theta,\psi\} \quad \text{(III.13)}$$

Differentiating $\mathrm{e}_{i,2}$ and using equation.(III.1), we achieve:

$$\dot{\mathrm{e}}_{i,2} = \ddot{y}_i - \dot{\mathcal{Q}}_i = \mathcal{F}_i(\chi) + \mathcal{G}_i\mathcal{U}_i + p_i(t) - \ddot{y}_i^d - \mathcal{C}_i\dot{\mathrm{e}}_{i,1} \,, i \in \{\phi,\theta,\psi\} \quad \text{(III.14)}$$

Then, choose the augmented Lyapunov function candidate $\mathcal{V}_{\mathcal{B}c} = \mathcal{V}_1 + \frac{1}{2}\sum_{i=\{\phi,\theta,\psi\}} \mathrm{e}_{i,2}^2$ for the stability analysis of position/attitude:

$$\mathcal{V}_{\mathcal{B}c} = \frac{1}{2}\sum_{i=\{\phi,\theta,\psi\}} \mathrm{e}_{i,1}^2 + \mathrm{e}_{i,2}^2 \quad \text{(III.15)}$$

Then, the time derivative of $\mathcal{V}_{\mathcal{B}c}$ can be given by:

$$\dot{\mathcal{V}}_{\mathcal{B}c} = \frac{1}{2}\sum_{i=\{\phi,\theta,\psi\}} \dot{\mathrm{e}}_{i,1}^2 + \dot{\mathrm{e}}_{i,2}^2 = \sum_{i=\{\phi,\theta,\psi\}} \dot{\mathrm{e}}_{i,1}\mathrm{e}_{i,1} + \dot{\mathrm{e}}_{i,2}\mathrm{e}_{i,2} \quad \text{(III.16)}$$

$$\dot{\mathcal{V}}_{\mathcal{B}c} = \sum_{i=\{\phi,\theta,\psi\}} (\dot{y}_i^d - x_{i,2})\mathrm{e}_{i,1} + (\ddot{y}_i - \dot{\mathcal{Q}}_i)\mathrm{e}_{i,2} \quad \text{(III.17)}$$

$$\dot{\mathcal{V}}_{\mathcal{B}c} = \sum_{i=\{\phi,\theta,\psi\}} -\mathcal{C}_i\mathrm{e}_{i,1}^2 + \sum_{i=\{\phi,\theta,\psi\}} -\mathrm{e}_{i,1}\mathrm{e}_{i,2} + (\mathcal{F}_i(\chi) + \mathcal{G}_i\mathcal{U}_i + p_i(t) - \quad \text{(III.18)}$$

$\ddot{y}_i^d - \mathcal{C}_i \dot{e}_{i,1}) e_{i,2}$

Step 3. We assume that $\mathcal{F}_i(\chi)$ and $\mathcal{G}_i$ are known and $p_i(t) = 0$. The BC law can be gotten by the feedback linearization methodology by:

$$\mathcal{U}_{Bc,i} = \mathcal{G}_i^{-1}\left(-\mathcal{F}_i(\chi) - \check{\mathcal{C}}_i e_{i,2} + e_{i,1} + \mathcal{C}_i \dot{e}_{i,1} + \ddot{y}_i^d\right) \quad \text{(III.19)}$$

$\check{\mathcal{C}}_i > 0$ is a new design parameter. Subsisting (III.19)in (III.18),we obtain:

$$\dot{\mathcal{V}}_{Bc} = \sum\nolimits_{i=\{\phi,\theta,\psi\}} -\mathcal{C}_i e_{i,1}^2 - \check{\mathcal{C}}_i e_{i,2}^2 \leq 0 \quad \text{(III.20)}$$

Since $\dot{\mathcal{V}}_{Bc}$ is semi-negative definite, the BC controlled system stability will be ensured. As gotten in equation (III.20), the control parameters $\mathcal{C}_i$ and $\check{\mathcal{C}}_i$ describe the dynamic behavior of the quadrotor tracking responses [46–47].

III.2.2 Fuzzy-neural network approximator

In this section (1) we propose an adaptive fuzzy-neural network in order to address the problem of the classical BC law outlined in the previous section. This can be done by eliminating its dependence model functions and parameters, i.e. $\mathcal{F}_i(x)$ and $\mathcal{G}_i$(see (III.19). The combination of the fuzzy and neural networks with the continuous BC leads to the development of the proposed AFNN-DBC methodology. The main advantage of this method is that the robust behaviour of the quadrotor attitude is guaranteed. In the developed control design procedure, the used hybrid network is a parallel network topology composed of the radial basis function neural network (RBFNN) and the Takaji-Seguino (TS) fuzzy logic system (FLS). This approach allows to combine the power of the approximation capability of RBFNN and the robustness of FLS to deal with the erreur approximation and disturbances. Following from [48], for local continuous function $h_i(Z_i)$ defined in compact set Θ_i, the FNN is applied according to the following equation:

$$\hat{h}_i(Z_i) = \widehat{W}_i^T \Phi_i(Z_i) \quad \text{(III.21)}$$

$$= \widehat{W}_{i,F}^T \Phi_{i,\mathcal{F}}(Z_i) + \widehat{W}_{i,N}^T \Phi_{i,N}(Z_i) \quad \text{(III.22)}$$

where $Z_i = \left[x^T, y_{i,d}, \dot{y}_{i,d}, \ddot{y}_{i,d}\right]^T$ and $\widehat{W}_i = \left[\widehat{W}_{i,\mathcal{F}}^T, \widehat{W}_{i,N}^T\right]^T$ denote the estimate vector of network parameters which includes the fuzzy weight vector $\widehat{W}_{i,\mathcal{F}} = \left[\widehat{w}_{i,\mathcal{F}}^1, \dots, \widehat{w}_{i,\mathcal{F}}^l\right]^T$ and the neural weight vector $\widehat{W}_{i,N} = \left[\widehat{w}_{i,N}^1, \dots, \widehat{w}_{i,N}^r\right]^T$ for l and r are the number of fuzzy rules and

the RBFNN nodes, respectively. $\Phi_i(Z_i) = \left[\Phi_{i,\mathcal{F}}^T, \Phi_{i,N}^T\right]^T$ represents the basis function vector that as contains the fuzzy basis functions $\Phi_{i,\mathcal{F}}(Z_i) = [\vartheta_{i,\mathcal{F}}^1(Z_i), \dots, \vartheta_{i,\mathcal{F}}^l(Z_i)]^T$ and the RBFNN activate functions $\Phi_{i,N}(Z_i) = [\xi_{i,N}^1(Z_i), \dots, \xi_{i,N}^r(Z_i)]^T$ designed according to [43,49]. The FLS is constructed using a singleton fuzzifier, product inference engine and centroid defuzzifier leads to calculate $\vartheta_{i,\mathcal{F}}^j(Z_i)$ as:

$$\vartheta_{i,\mathcal{F}}^j(Z_i) = \frac{\prod_{\eta=1}^{9} \mu_{\breve{\mathcal{A}}_{i,\eta}^j}(z_{i,\eta})}{\sum_{j=1}^{l} \prod_{\eta=1}^{9} \mu_{\breve{\mathcal{A}}_{i,\eta}^j}(z_{i,\eta})}, j = 1, \dots, l \tag{III.23}$$

where $\mu_{\breve{\mathcal{A}}_{i,\eta}^j}(z_{i,\eta})$ are membership functions of the linguistic variables $z_{i,\eta} \in \{x^T, y_{i,d}, \dot{y}_{i,d}, \ddot{y}_{i,d}\}$ having the fuzzy sets $\breve{\mathcal{A}}_{i,\eta}^j$. The RBFNN activate functions are selected generally as the Gaussian-like function: for $i \in \{\phi, \theta, \psi\}$

$$\xi_{i,N}^j(Z_i) = exp\left(-\frac{\|Z_i - \upsilon_{i,j}\|^2}{2\varrho_{i,j}^2}\right), j = 1, \dots, r \tag{III.24}$$

with $\upsilon_{i,j} \in \{\upsilon_{i,1}, \dots, \upsilon_{i,r}\}$ and $\varrho_{i,j}$ are the center of the receptive domain, the width of the Gaussian functions, respectively. By universal approximate theorem [43], there exist optimal approximation parameters W_i which are defined for the functions $h_i(Z)$ by:

$$W_i = \text{argmin}\left[\sup_{Z_i \in \Theta_i} \left|h_i(Z_i) - \hat{h}_i(Z_i|\widehat{W}_i)\right|\right] \tag{III.25}$$

knowing that these nonlinear functions $h_i(Z_i)$ can be expressed as:

$$h_i(Z_i) = W_i^T \Phi_i(Z_i) + \delta_i(Z_i) \tag{III.26}$$

where $\delta_i(Z_i)$ are the minimum approximation errors that satisfy the following assumption.

Assumption 4. Based on the universal approximation ability, the approximation errors $\delta_i(Z_i)$ are assumed to be small and bounded:

$$|\delta_i(Z_i)| \leq \varepsilon_i, Z_i \in \Theta_i \tag{III.27}$$

where ε_i are postive constants. For the development of our controller, it should be mentioned that the lemma 4 in [50] can be extended to the used FNN. For that, let $X_i =$

$[x_i^T, y_{i,d}, \dot{y}_{i,d}, \ddot{y}_{i,d}]$ be the augmented local state vector which the following inequality holds:

$$\|\Phi_i(Z_i)\|^2 \leq \|\Phi_i(X_i)\|^2 \tag{III.28}$$

On the basis of the above approximations, the control of the attitude quadrotor system is carried out via a decentralized scheme, where the local adaptive control law is obtained by backstepping technique and Lyapunov method to stabilize the attitude quadrotor and to cope with parameters uncertainties, external disturbances and approximation errors. The proposed adaptive control signal is defined as [50]:

$$u_i = -\lambda_{2,i} e_{2,i} - \frac{1}{2\tau_i^2} e_{2,i} \hat{\pi}_i \Phi_i^T(X_i)\Phi_i(X_i) \tag{III.29}$$

with $\hat{\pi}_i$ are the adaptation parameters governed by the following law:

$$\dot{\hat{\pi}}_i = \frac{\gamma_i}{2\tau_i^2} e_{2,i}^2 \Phi_i^T(X_i)\Phi_i(X_i) - \gamma_i \sigma_i \hat{\pi}_i \tag{III.30}$$

where $\lambda_{2,i} > 0$,$\tau_i > 0$, $\alpha_i > 0$and $\sigma_i > 0$ are positive designing constants.

Theorem. Consider the altitude model (III.4) of quadrotor system which meets the assumptions (1) into (4), the proposed AFNN-DBC law (III.29), associated with the virtual controller (III.11) and the updating law (III.30) for $i \in \{\phi, \theta, \psi\}$ ensures the attitude stability of quadrotor, the tracking errors $e_{1,i}$and $e_{2,i}$ converge to a small neighborhood of the origin and all the signals of the closed-loop system are bounded.

III.2.3 Stability analysis

In this section, we consider the next improved Lyapunov's candidate function:

$$V_3 = V_2 + \sum_{i\in\{\phi,\theta,\psi\}} \frac{\mathcal{G}_i}{2\gamma_i} \tilde{\pi}_i^2 \tag{III.31}$$

$$\dot{V}_3 = \dot{V}_2 - \sum_{i\in\{\phi,\theta,\psi\}} \frac{1}{\gamma_i} \tilde{\pi}_i \dot{\hat{\pi}}_i \tag{III.32}$$

Substituting (III.18) into (III.32), results in:

$$\dot{V}_3 = \sum_{i\in\{\phi,\theta,\psi\}} -\lambda_{1,i}e_{1,i}^2 + e_{2,i}\left(\mathcal{F}_i(x) + \mathcal{G}_i u_i + p_{i_i} - \ddot{y}_{i,d} - e_{1,i} - \lambda_{1,i}\dot{e}_{1,i}\right) - \sum_{i\in\{\phi,\theta,\psi\}} \frac{\mathcal{G}_i}{\gamma_i}\tilde{\pi}_i\dot{\hat{\pi}}_\iota \quad \text{(III.33)}$$

$$= \sum_{i\in\{\phi,\theta,\psi\}} -\lambda_{1,i}e_{1,i}^2 + e_{2,i}(h_i(Z_i) + \mathcal{G}_i u_i + p_i) - \frac{1}{2}e_{2,i}^2 - \sum_{i\in\{\phi,\theta,\psi\}} \frac{\mathcal{G}_i}{\gamma_i}\tilde{\pi}_i\dot{\hat{\pi}}_\iota$$

Where $h_i(Z_i) = \mathcal{F}_i(x) - e_{1,i} - \lambda_{1,i}\dot{e}_{1,i} - \ddot{y}_{i,d} + (1/2)e_{2,i}$and $Z_i = \left[x, y_{i,d}, \dot{y}_{i,d}, \ddot{y}_{i,d}\right]^T$. According to (31), it is known that

$$h_i(Z_i) = W_i^T\Phi_i(Z_i) + \delta_i(Z_i),\ \|\delta_i(Z_i)\| \le \varepsilon_i \quad \text{(III.34)}$$

By using the Young's inequality, we can get:

$$\begin{aligned} e_{2,i}(\hbar_i(Z_i) + p_i) &= e_{2,i}(W_i^T\Phi_i(Z_i) + \delta_i(Z_i) + p_i) \\ &\le |e_{2,i}|(\|W_i\|\|\Phi_i(Z_i)\| + \varepsilon_i + \mathcal{L}_i^*) \\ &\le |e_{2,i}|(\|W_i\|\|\Phi_i(X_i)\| + \varepsilon_i + \mathcal{L}_i^*) \\ &\le \frac{1}{2\tau_i^2}e_{2,i}^2\mathcal{G}_i\pi_i\Phi_i^T(X_i)\Phi_i(X_i) + \frac{\tau_i^2}{2} + \frac{e_{2,i}^2}{2} + \frac{\varepsilon_i^2}{2} + \frac{\mathcal{L}_i^{*2}}{2} \end{aligned} \quad \text{(III.35)}$$

where $\pi_i = (\|W_i\|^2/\mathcal{G}_i)$are unknown constants to be estimated, and $\tau_i > 0$ are design constants. Thereafter, using the result (III.33) in (III.35) gives

$$\dot{V}_3 \le \sum_{i\in\{\phi,\theta,\psi\}} -\lambda_{1,i}e_{1,i}^2 + e_{2,i}\left(\frac{1}{2\tau_i^2}e_{2,i}\mathcal{G}_i\pi_i\Phi_i^T(X_i)\Phi_i(X_i) + \mathcal{G}_i u_i\right) + \frac{\tau_i^2}{2} + \frac{\varepsilon_i^2}{2} + \frac{\mathcal{L}_i^{*2}}{2} - \sum_{i\in\{\phi,\theta,\psi\}} \frac{\mathcal{G}_i}{\gamma_i}\tilde{\pi}_i\dot{\hat{\pi}}_\iota \quad \text{(III.36)}$$

Introducing (III.29) and (III.30) into (III.36) and then after some mathematical manipulation yield:

$$\dot{V}_3 \le -\sum_{i\in\{\phi,\theta,\psi\}} \left(\lambda_{1,i}e_{1,i}^2 + \lambda_{2,i}e_{2,i}^2\right) + \sum_{i\in\{\phi,\theta,\psi\}} \left(\frac{\tau_i^2}{2} + \frac{\varepsilon_i^2}{2} + \frac{\mathcal{L}_i^{*2}}{2}\right) - \sum_{i\in\{\phi,\theta,\psi\}} \frac{\mathcal{G}_i}{\gamma_i}\sigma_i\tilde{\pi}_i\hat{\pi}_i \quad \text{(III.37)}$$

Considering the expression of $\tilde{\pi}_i$, it follows that:

$$\tilde{\pi}_i\hat{\pi}_i \leq \frac{\pi_i^2}{2} - \frac{\tilde{\pi}_i^2}{2} \tag{III.38}$$

Substituting (III.38) into (III.37) gives:

$$\dot{V}_3 \leq -\sum_{i\in\{\phi,\theta,\psi\}} \lambda_{1,i}e_{1,i}^2 + \lambda_{2,i}e_{2,i}^2 - \sum_{i\in\{\phi,\theta,\psi\}} \frac{\mathcal{G}_i\sigma_i\tilde{\pi}_i}{\gamma_i 2} + \sum_{i\in\{\phi,\theta,\psi\}} \left(\frac{\mathcal{G}_i\sigma_i\pi_i^2}{\gamma_i} + \frac{\tau_i^2}{2} + \frac{\varepsilon_i^2}{2} + \frac{\mathcal{L}_i^{*2}}{2}\right) \tag{III.39}$$

We define $c_i = min\{2\lambda_{1,i}, 2\lambda_{2,i}, \mathcal{G}_i\sigma_i/\gamma_i\}$ and $\rho_i = \left(\mathcal{G}_i\sigma_i\pi_i^2/\alpha_i + \tau_i^2 + \varepsilon_i^2 + \mathcal{L}_i^{*2}\right)/2$, results in:

$$\dot{V}_3 \leq -\mathrm{c}V_3 + \rho \tag{III.40}$$

where c=$\sum_{i\in\{\phi,\theta,\psi\}} c_i$and ρ =$\sum_{i\in\{\phi,\theta,\psi\}} \rho_i$. Integrating (III.40) over $[0, t]$, one can obtain:

$$0 \leq V_3(t) \leq V_3(0)\mathrm{e}^{-ct} + \frac{\rho}{\mathrm{c}} \tag{III.41}$$

From (III.41), it can be shown that the signals $x_i, \hat{\pi}_i$ and u_i for $i\epsilon\{\phi,\theta,\psi\}$ are bounded. Furthermore, the tracking errors $e_i = \left[e_{1,i}, e_{2,i}\right]$ satisfy that $\| e_i\| \leq \sqrt{2(V_3(0)\mathrm{e}^{-ct} + \rho/\mathrm{c})}$ where their values can be reduced as close to zero as possible by choosing appropriately the design parameters $\lambda_{1,i}$, $\lambda_{2,i}$,τ_i, $\gamma_i$and σ_i. Especially, we have $\| e_i\| \to \sqrt{2\rho/\mathrm{c}}$ for $t \to \infty$.

III.2.4 Simulation Results

In this section (1), several simulations will be given to illustrate the efficiency of the proposed method (AFNN-DBC) for the attitude dynamic model of the quadrotor. The proposed control scheme is tested for two different reference signals (Two cases), in which the external disturbance forces of about 6(*N)* and the parameter uncertainties $\Delta I_{xx} = 0.3I_{xx}$, $\Delta I_{yy} = 0.3I_{yy}$and $\Delta I_{zz} = 0.3I_{zz}$ are applied at $20 < t < 40$ sec. The reference signals employed in case 1 are selected as $y_{\varphi,d} = 1\mathrm{rad}, y_{\theta,d} = 1rad$ and $y_{\psi,d} = 1\mathrm{rad}$, and a square wave reference signals for all subsystems in case 2, as shown in figures(III.1) and (III.3). The physical parameters of quadrotor system are selected as

given in Tables III.1 [39]. The design parameters of the proposed controller are selected as $\lambda_{1,\phi} = 1, \quad \lambda_{1,\theta} = 0.9, \quad \lambda_{1,\psi} = 0.6, \quad \lambda_{2,\phi} = 0.3, \quad \lambda_{2,\theta} = 0.6, \quad \lambda_{2,\psi} = 0.5, \gamma_\phi = \gamma_\theta = \gamma_{\psi=} 1,\ \tau_\phi = \tau_\theta = \tau_\psi = 0.0017, \sigma_\phi = \sigma_\theta = \sigma_\psi = 1.$

The hybrid control networks of the three attitude subsystems are composed of identical RBFNNs and FLS's. The input variables of the hybrid networks are chosen as $X_i = [x_i^T, y_{i,d}, \dot{y}_{i,d}, \ddot{y}_{i,d}]^T$ for $i \epsilon \{\phi, \theta, \psi\}$. The used RBFNN include three hidden layers with five Gaussian membership functions definded as (III.24) having centers υ_j selected linearly spaced in $[-3\ ,3]$ and standard deviations ϱ_j chosen equal to 0.03. For both test cases, the FLS controller is constructed of twenty five fuzzy rules when the membership functions of each component $\chi_{i,\eta}$ of X_i are defined as:

$$\mu_{\breve{\mathcal{A}}_{hj}^1}(\chi_{i,\eta}) = \frac{1}{(1 + \exp(3pi/2(\chi_{i,\eta} + 2pi/3)))}$$
$$\mu_{\breve{\mathcal{A}}_{i,j}^2}(\chi_{i,\eta}) = \exp\left\{-\left(\frac{\chi_{i,\eta} + pi/6}{pi/3}\right)^2\right\}$$
$$\mu_{\breve{\mathcal{A}}_{hj}^3}(\chi_{i,\eta}) = \exp\left\{-\left(\frac{\chi_{i,\eta}}{pi/3}\right)^2\right\}$$
$$\mu_{\breve{\mathcal{A}}_{hj}^4}(\chi_{i,\eta}) = \exp\left\{-\left(\frac{\chi_{i,\eta} - pi/6}{pi/3}\right)^2\right\}$$
$$\mu_{\breve{\mathcal{A}}_{hj}^5}(\chi_{i,\eta}) = \frac{1}{(1 + \exp(-3pi/2(\chi_{i,\eta} - 2pi/3)))}$$

The closed-loop attitude controller performance in test cases 1 an 2 are presented in figure (III.1) and (III.3), respectively. The corresponding control efforts required to achieve desired results are shown in figure (III.2) and and figure (III.4)It is clear that the quadrotor is closely following reference trajectory in regulation and tracking tests even in the presence of parameter uncertainties and external disturbance. Thus, the proposed controller is robust and reveals good match in comparison with the classical BC.

Table III.1 Prameters of the Quadrotor

Parameters	Value
m	0.65 [kg]
g	$9.81[m/s2]$
I_x	7.5×10^{-3}[kg.m^2]
I_y	7.5×10^{-3}[kg.m^2]
I_z	1.3×10^{-2}[kg.m^2]
J_r	6.5×10^{-5}[kg.m^2]
l	0.23[m]
b	3.1×10^{-5}[N.s^2]
d	7.5×10^{-7}[N.m.s^2]

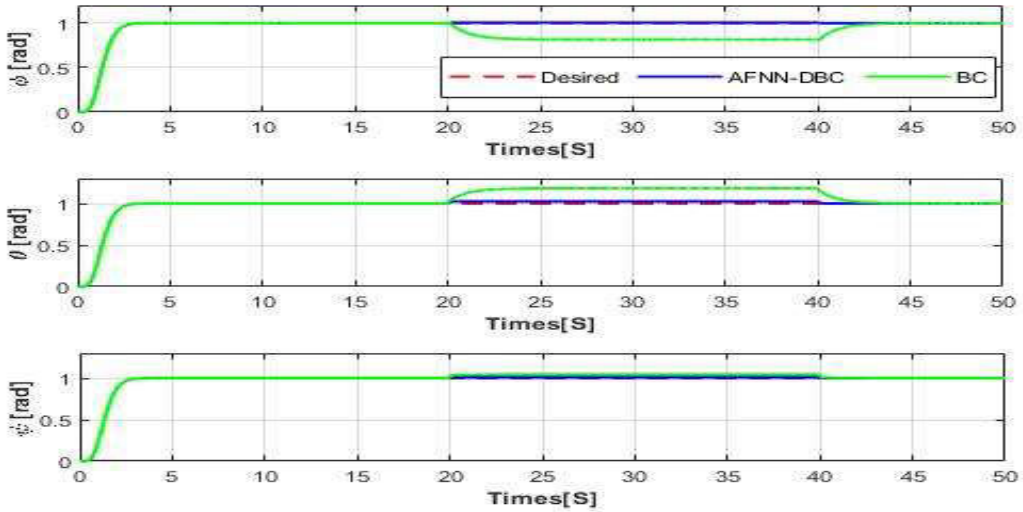

Figure III.1. Attitude responses of quadrotor, roll angle (ϕ), pitch angle (θ) and yaw angle (ψ), (case1).

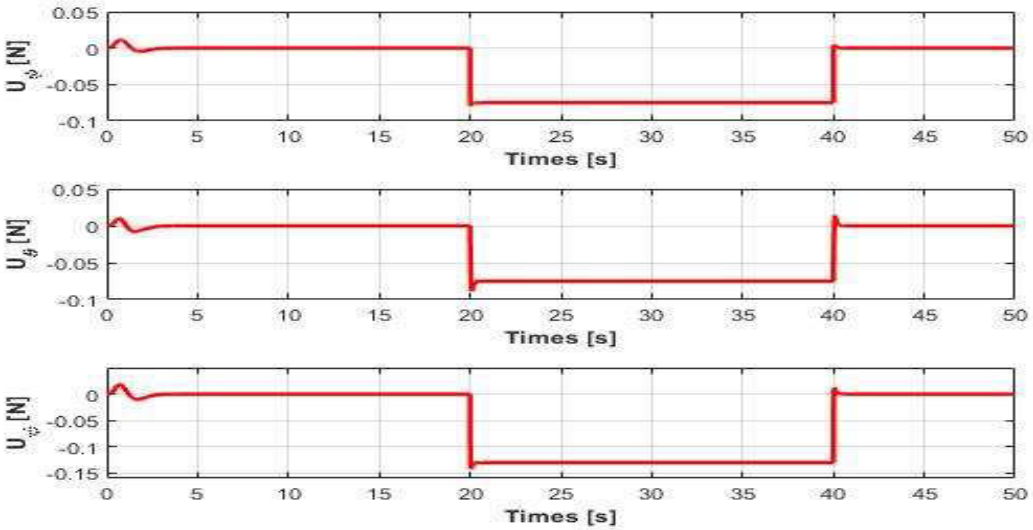

Figure III.2 Control input signals u_ϕ(d), u_θ(e) and u_ψ(f) of AFNN-DBC, (case1).

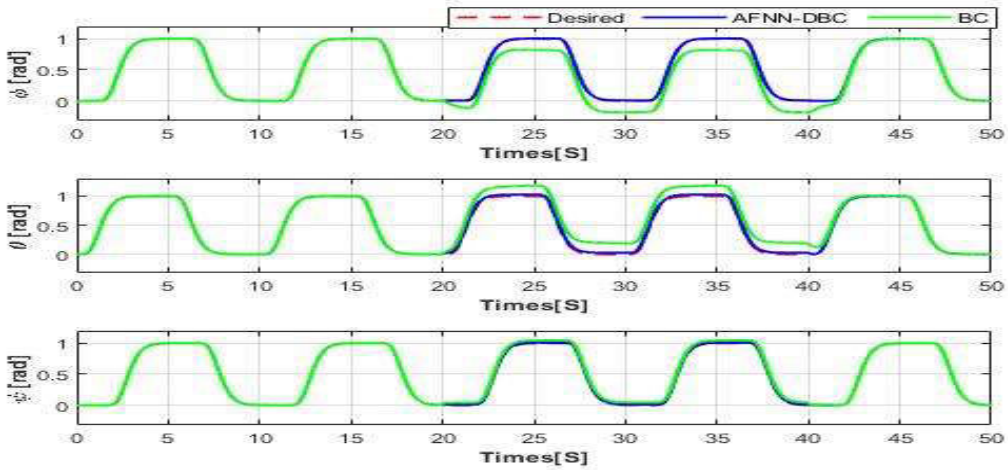

Figure III.3 The attitude responses of quadrotor : roll angle (ϕ), pitch angle (θ) and yaw angle (ψ), (case2).

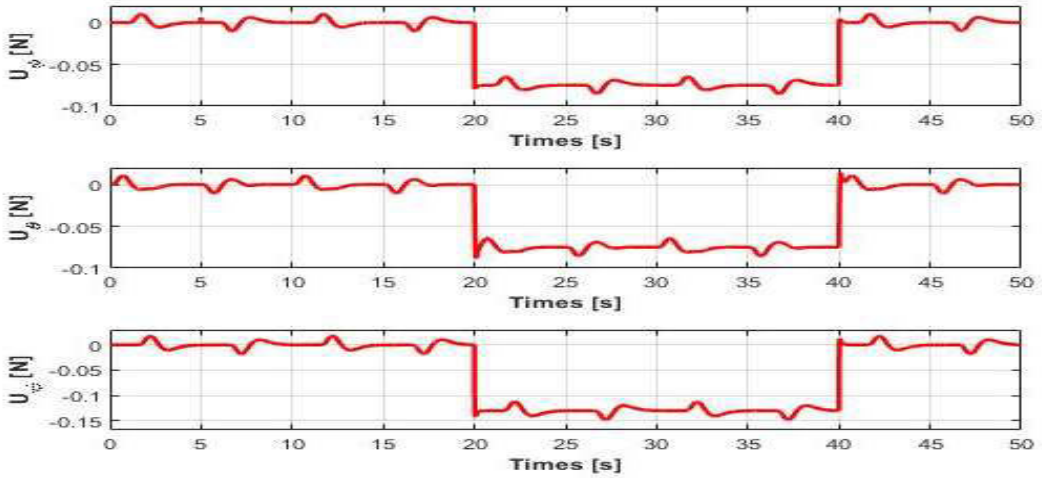

Figure III.4.Control input signals u_ϕ(d), u_θ(e) and u_ψ(f) of AFNN-DBC, (case2)

III.3 Adaptive fuzzy- network-based sliding mode controller

The purpose of this section (2), is to design a controller for quadrotor attitude system. The designed control law combines a continuous second-order sliding mode control (CSOSMC), the Fuzzy-Chebyshev network (FCN) and the adaptive control methodology. The FCN with adaptive parameters is exploited to approximate the nonlinear functions and improve the robustness against parametric uncertainties and external disturbances. Otherwise, the continuous sliding mode aims to completely eliminate the chattering phenomenon. The stability of the quadrotor attitude control system is proven by the Lyapunov stability approach. The simulation results demonstrate the capability and

efficiency of the proposed technique in the presence of uncertainties and external disturbances.

The quadrotor model is considered in this section (2) Same as the section(1). Their dynamics can be described by the following generalized state space equation :

$$\begin{aligned} \dot{x}_{1,i} &= x_{2,i} \\ \dot{x}_{2,i} &= \mathcal{F}_i(\chi) + \mathcal{G}_i u_i + \ p_i,\ i \in \{\phi, \theta, \psi\} \\ \mathrm{y}_i &= x_{1,i} \end{aligned} \tag{III.42}$$

where $\boldsymbol{x_i} = [\boldsymbol{x_{1,i}} \quad \boldsymbol{x_{2,i}}]^{\boldsymbol{T}}$, $\boldsymbol{i} \in \{\boldsymbol{z}, \boldsymbol{\phi}, \boldsymbol{\theta}, \boldsymbol{\psi}\}$ with

$$\begin{aligned} \mathcal{F}_\varphi(x) &= \left[(I_y - I_z)x_{2\theta}x_{2\psi} - J_r\Omega_d x_{2\theta}\right]/I_x \\ \mathcal{F}_\theta(x) &= \left[(I_z - I_x)x_{2\varphi}x_{2\psi} + J_r\Omega_d x_{2\varphi}\right]/I_y \\ \mathcal{F}_\psi(x) &= \left(I_x - I_y\right)x_{2\varphi}x_{2\theta}/I_z \\ \mathcal{G}_\varphi(x) &= l/I_x, \mathcal{G}_\theta(x) = l/I_y,\ \mathcal{G}_\psi(x) = 1/I_z \end{aligned} \tag{III.43}$$

For the quadrotor system (III.42), the objective of the AFCN-CSOSMC is to force the output of the system $\mathbf{y_i}$, to successfully follow a given reference signal $\boldsymbol{y_i^d}$ in the presence of uncertainties such as parametric variations and external disturbances.

III.3.1 Second order sliding mode controllers

In this section, the traditional second order sliding mode (SOSMC) is introduced to control the attitude of quadrotor that is inspired by the sliding mode control (SMC) approach [51]. This technique has been introduced in the literature to solve the chattering problem of classical SMC. One of SOSMC discussed for controlling nonlinear systems those that use a proportional-integral-derivative (PID) sliding surface σ_i as

$$\begin{aligned} \sigma_i &= \dot{s}_i + \beta s_i \\ &= k_d \dot{e}_i(t) + k_p e_i(t) + k_I \int_0^t e_i(v)\, dv \end{aligned} \tag{III.44}$$

where $e_i = \mathrm{y}_i^d - \mathrm{y}_i$ is defined as the tracking error, k_p, k_d and k_I are the proportional, integral and derivative positive gains respectively, β is a strict positive constant that defines the slope of the sliding line $\sigma_i = 0$. For this purpose, the SOSMC law, extensively used in the literatures, is proposed for attitude control which takes for each subsystem the form [51] :

$$u_i = u_{eqi} + u_{swi} \tag{III.45}$$

The above control law is a summation of an equivalent control term u_{eqi} introduced to compensate the nonlinearities of quadrotor system. The second term u_{swi} is a robust switching control term introduced to deal with disturbances and parameters variations. The two components will subsequently be determined using the Lyapunov method.

Step 1: The derivative of sliding surface σ_i in (III.44) is

$$\begin{aligned}\dot{\sigma_i} &= \ddot{s}_\iota + \dot{\beta_\iota}\dot{s}_\iota \\ &= k_{Di}\ddot{e}_i + k_{Pi}\dot{e}_i + k_{Ii}e_i\end{aligned} \tag{III.46}$$

From (III.46), yields

$$\ddot{s}_i = -\beta_i\dot{s}_i + k_{Di}\ddot{e}_i + k_{Pi}\dot{e}_i + k_{Ii}e_i \tag{III.47}$$

Substituting (III.42) into (III.47), it follows that:

$$\ddot{s}_i = -\beta_i\dot{s}_i + k_{Pi}\dot{e}_i + k_{Ii}e_i + k_{Di}\left[\ddot{y}_i^d - \mathcal{F}_i - \mathcal{G}_i u_i - p_i\right] \tag{III.48}$$

In the case where the the system dynamics are well known, and the quadrotor system is not subject at any uncertainties and external disturbances, i.e. $p_i = 0$ and by setting $\ddot{s}_i = 0$ in (III.48), u_{eqi} for each subsystem is obtained as

$$u_{eqi} = \frac{1}{k_D\mathcal{G}_i}\left[-\beta_i\dot{s}_i - k_{Di}\mathcal{F}_i + k_{Di}\ddot{y}_i^d + k_{Pi}\dot{e}_i + k_{Ii}e_i\right] \tag{III.49}$$

To ensure the convergence of sliding variable and guarantee the stability of the closed-loop system when the parametric uncertainties and external disturbances occur, the additional switching control term u_{swi} can be designed using Lyapunov method.

Step 2: Let be the following positive function $V = \sum_{i\in\{\phi,\theta,\psi\}} V_i$, with:

$$V_i = \frac{1}{2}\dot{s}_i{}^2 + \frac{k_{1i}}{2}s_i^2 \tag{III.50}$$

where k_{1i} is a strict positive constant.

Using (III.48), (III.45) and (III.49) the time derivative of V is given as:

$$\begin{aligned}\dot{V}_i &= \dot{s}_i\ddot{s}_i + k_{1i}s_i\,\dot{s}_i \\ &= \{-\beta_i\dot{s}_i + k_{Pi}\dot{e}_i + k_{Ii}e_i + k_{Di}[\ddot{y}_i^d - \mathcal{F}_i - \mathcal{G}_i u_i - p_i]\}\dot{s}_i + k_{1i}s_i\,\dot{s}_i \\ &= k_{Di}[-\mathcal{G}_i u_{swi} - \mathcal{D}_i]\dot{s}_i + k_{1i}s_i\,\dot{s}_i\end{aligned} \tag{III.51}$$

To satisfy the reaching condition, the switching control term designed on the SOSMC algorithm takes the following form

$$u_{swi} = \frac{1}{k_D\mathcal{G}_i}[k_{1i}s_i + k_{2i}sgn(\dot{s}_i)] \tag{III.52}$$

where $k_{2i} > 0$ is the control gain. Substituting (III.52) into (III.51) $\dot{V}$ can be upper bounded as follows :

$$\begin{aligned}\dot{V}_i &= k_{2i}|\dot{s}_i| - k_{Di}p_i\dot{s}_i \\ &\leq -|\dot{s}_i|\{k_{2i} - k_{Di}|p_i|\} \\ &\leq -|\dot{s}_i|\{k_{2i} - k_{Di}\mathcal{L}_i^*\}\end{aligned} \tag{III.53}$$

So, the quadrotor control system is globally stable according to Lyapunov's method with k_{2i} must be selected as $k_{2i} > k_{Di}\mathcal{L}_i^*$.

III.3.2 Fuzzy-chebyshev network approximator

In order to eliminate the dependence of SOSMC control law at dynamic functions and uncertainties of system, an adaptive fuzzy-Chebyshev network is used to estimate the nonlinear functions $\mathcal{F}_i(x)$ in classical controllers. Combining the hybrid network with the continuous SOSMC in equation (III.49) results in developing the proposed AFCN-CSOSMC methodology. The main advantage of this method is that the robust behavior of the quadrotor attitude is guaranteed. The second advantage of the proposed scheme is that the performance of the system in the sense of removing chattering is improved in comparison without using the approximator network.

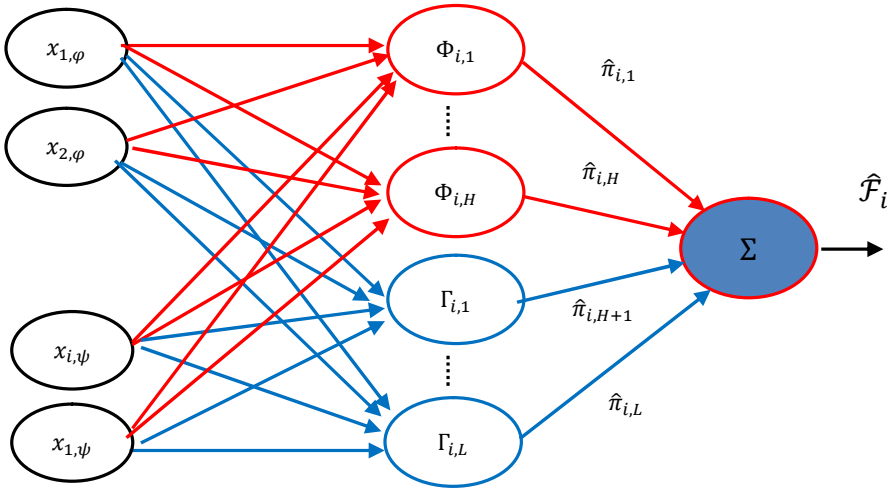

Figure III.5. The structure of the Fuzzy-Chebyshev network (FCN) to estimate $\mathcal{F}_i$.for $i \in \{\phi, \theta, \psi\}$.

The output of the Fuzzy-Chebyshev network to be calculated by:

$$\hat{\mathcal{F}}_i(x, \hat{\pi}_i) = \hat{\pi}_i^T \xi_i(x) \tag{III.54}$$

where $\hat{\pi}_i = [\hat{\pi}_{i,1}, \dots, \hat{\pi}_{i,N}]^T$ is the estimate vector of network parameters and $\xi_i(x)$ is the regressor vector of the proposed hybrid network given as follows (see Fig III.5):

$$\xi_i(x) = [\Phi_{i,1}(x), \dots., \Phi_{i,H}(x), \Gamma_{i,1}(x) \dots. \Gamma_{i,L}(x)]^T \tag{III.55}$$

where $\Phi_{i,j}(x)$ and $\Gamma_{i,l}(x)$ for $j = 1, \dots, H$ and $l = 1, \dots, L$ are the fuzzy basis functions and Chebyshev polynomial functions, respectively calculated according [42]:

$$\Phi_{i,j}(x) = \frac{\mu_{\breve{A}_{1,i}^j}(x_{1,i})\mu_{\breve{A}_{1,i}^j}(x_{2,i})}{\sum_{k=1}^{H} \mu_{\breve{A}_{1,i}^k}(x_{1,i})\mu_{\breve{A}_{2,i}^k}(x_{2,i})}, j = 1, \dots, H \tag{III.56}$$

$$\Gamma_{i,j}(x) = \left[\Gamma_{i,l}^1(x_{1,i}), \Gamma_{i,j}^2(x_{2,i})\right], l = 1, \dots, L \tag{III.57}$$

where $\mu_{A_i^l}(x_{1,i})$are the membership functions which are selected generally as Gaussian membership functions and $\Gamma_{i,j}^1(x_{1,i})$ denotes the Chebyshev polynomials which is produced by the next recursive expression [51]:

$$\Gamma_{i,l+1}^k(x_{1,i}) = 2x_{1,i}\Gamma_{i,l-1}^k(x_{1,i}) - \Gamma_{i,l-1}^k(x), \ \Gamma_{i,0}^1(x) = 1, k = 1,2; \ l = 0, \dots, L. \tag{III.58}$$

According to the universal approximation property, the fuzzy approximations error of (III.54) take the form:

$$\mathcal{F}_i(x) - \hat{\mathcal{F}}_i(x, \hat{\pi}_i) = \tilde{\pi}_i^T \xi_i(x) + \varepsilon_i(x) \quad \text{(III.59)}$$

where $\tilde{\pi}_i = \pi_i^* - \hat{\pi}_i$ denotes the parameter estimation error, $\pi_i^* = [\pi_{i,1}^*, \dots, \pi_{i,N}^*]^T$ is the optimal parameters minimizing the approximation error $\varepsilon_i(x)$ that satisfy $\pi_i^* = \text{argmin}\left[\sup_{x \in \Theta_x} \left|\hat{\mathcal{F}}_i(x|\pi_i) - \mathcal{F}_i(x)\right|\right]$ over a compact set Θ_x.

Based on the above approximations, the control of attitude quadrotor is realized through a decentralized scheme, as shown in figure(III.6), where the local control law (III.45) becomes using (III.49), (III.52) and (III.54) as follows:

$$u_i = \frac{1}{k_D \mathcal{G}_i}\left[-\beta_i \dot{s}_i - k_{Di}\hat{\mathcal{F}}_i + k_{Di}\ddot{y}_i^d + k_{Pi}\dot{e}_i + k_{Ii}e_i + -k_{1i}s_i + \hat{k}_{2i}sgn(\dot{s}_i)\right] \quad \text{(III.60)}$$

Where $\hat{k}_{2i}$ is the estimate of k_{2i} must be positive.

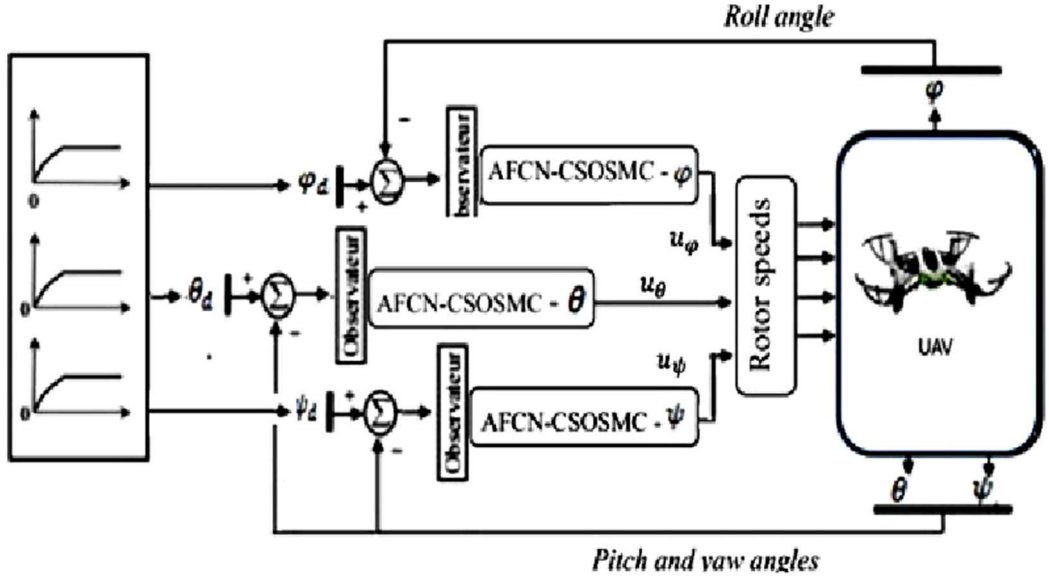

Figure III.6. Constructed of AFCN-CSOSMC for attitude quadrotor.

Theorem: Consider the attitude model of quadrotor system (III.42) with satisfied assumptions (1-4), The proposed (AFCN-CSOSMC) law (III.60) guarantees the boundedness of all signals in the closed-loop system and the asymptotic convergence of the sliding surface σ_i, and the tracking error e_i to zero for $i \in \{\phi, \theta, \psi\}$, if the following adaptation laws hold.

$$\dot{\hat{\pi}}_i = \alpha_i k_{Di} \dot{s}_i \xi_i^T(x) \quad \text{(III.61)}$$

$$\hat{k}_{2i} = \delta_i \int_0^t |\dot{s}_i(\iota)| d\iota \quad \text{(III.62)}$$

Where $\alpha_i > 0$ and $\delta_i > 0$ are design parameters.

Proof. Choose a positive definite function in the form of $V = \sum_{i\in\{\phi,\theta,\psi\}} V_i$, with

$$V_i = \frac{1}{2}\dot{s}_i{}^2 + \frac{k_{1i}}{2}s_i^2 + \frac{1}{2\alpha_i}\tilde{\pi}_i^T\tilde{\pi}_i + \frac{1}{2\delta_i}\tilde{k}_{2i}^2 \tag{III.63}$$

where $\tilde{k}_{2i} = k_{2i} - \hat{k}_{2i}$ are the estimate errors of $\bar{\varepsilon_i}$ for $i \in \{\phi, \theta, \psi\}$.

Taking the time derivative of V which is $\dot{V} = \sum_{i\in\{\phi,\theta,\psi\}} \dot{V}_i$, with

$$\dot{V}_i = \dot{s}_i\ddot{s}_i + k_{1i}s_i\,\dot{s}_i - \frac{1}{\alpha_i}\tilde{\pi}_i^T\dot{\hat{\pi}}_\iota - \frac{1}{\delta_i}\tilde{k}_{2i}\dot{\hat{k}}_{2\iota} \tag{III.64}$$

Substituting (III.58) into (32) one obtains

$$u_i = \frac{1}{k_D\mathcal{G}_i}\left[-\beta_i\dot{s}_i - k_{Di}\hat{\mathcal{F}}_i + k_{Di}\ddot{y}_i^d + k_{Pi}\dot{e}_i + k_{Ii}e_i + -k_{1i}s_i + \hat{k}_{2i}sgn(\dot{s}_i)\right] \tag{III.65}$$

Where $\hat{k}_{2i}$is the estimate of k_{2i} must be positive

$$\begin{aligned}\dot{V}_i &= \left\{-\beta_i\dot{s}_i + k_{Pi}\dot{e}_i + k_{Ii}e_i + k_{Di}\left[\ddot{y}_i^d - \mathcal{F}_i - \mathcal{G}_i u_i - p_i\right]\right\}\dot{s}_i + k_{1i}s_i\,\dot{s}_i \\ &\quad - \frac{1}{\alpha_i}\tilde{\pi}_i^T\dot{\hat{\pi}}_\iota - \frac{1}{\delta_i}\tilde{k}_{2i}\dot{\hat{k}}_{2\iota} \\ &= \left[k_{Di}\left(\hat{\mathcal{F}}_i - \mathcal{F}_i\right) - k_{Di}p_i - \hat{k}_{2i}sgn(\dot{s}_i)\right]\dot{s}_i - \frac{1}{\alpha_i}\tilde{\pi}_i^T\dot{\hat{\pi}}_\iota - \frac{1}{\delta_i}\tilde{k}_{2i}\dot{\hat{k}}_{2\iota}\end{aligned} \tag{III.66}$$

Using (III.59), (III.66) can be expressed as

$$\dot{V}_i = k_{Di}\dot{s}_i\tilde{\pi}_i^T\xi_i(x) - \tfrac{1}{\alpha_i}\tilde{\pi}_i^T\dot{\hat{\pi}}_\iota + \tilde{k}_{2i}|\dot{s}_i| - \tfrac{1}{\delta_i}\tilde{k}_{2i}\dot{\hat{k}}_{2\iota} - [\varepsilon_i(x) + k_{Di}p_i + k_{2i}sgn(\dot{s}_i)]\dot{s}_i \tag{III.67}$$

From (III.66), (III.67), assumption 2,3, the time derivative of Lyapunov equation can be upper bounded as follows:

$$\begin{aligned}\dot{V}_i &= -k_{2i}|\dot{s}_i| - k_{Di}(p_i + \varepsilon_i(x))\dot{s}_\iota \\ &\leq -|\dot{s}_i|\{-k_{2i} - k_{Di}(|p_i| + |\varepsilon_i|)\} \\ &\leq -|\dot{s}_i|\{k_{2i} + k_{Di}(\mathcal{L}_i^* + \bar{\varepsilon_i})\}\end{aligned} \tag{III.68}$$

Hence $V = \sum_{i\in\{\phi,\theta,\psi\}} V_i \in L_\infty$, which implies that the signals e_i, $\dot{e}_i$, s_i, $\dot{s}_i$, σ_i, $\dot{\sigma}_i$, $\tilde{\pi}_i$and $\tilde{k}_{2i}$are bounded. Moreover, by using Barbalat's lemma, we conclude that the tracking errors and its derivatives converge asymptotically to zero.

III.3.3 Simulation results

To validate the feasibility and effectiveness of the presented control algorithm, the AFCN-CSOSMC methodology applied to quadrotor attitude model is tested for two different scenarios in tracking problem. Firstly, the quadrotor system is exposed to the disturbance forces $p_i(t) = 3\sin(6t)$ newton at 20 sec. In the second scenario, the quadrotor system is simulated with parameter uncertainties $\Delta I_x = 0.3I_x$, $\Delta I_y = 0.3I_y$and $\Delta I_z = 0.3I_z$ applied at 30 sec. The reference signals employed in all the simulations consists of a sine waveform with magnitude equal to 1 meter and a frequency of 0.0955Hz. The design parameters of the proposed controllers are set as $\beta_i = 0.1$, $k_{Pi} = 0.1$, $k_{Di} = 0.1$, $k_{Ii} = 3$, , $k_{1i} = 2$, $\delta_i = 2$, $\alpha_i = 2$ for $i\epsilon\{\varphi, \theta, \psi\}$.

The input variables of the hybrid network (III.54) are chosen as $x_i = [x_{1i} \quad x_{2i}]^T$for angles system $i\epsilon\{\phi, \theta, \psi\}$. For every variable five Gaussian membership functions are described by:

$$\mu_{A_i^\iota}(x_i) = exp\left\{\frac{-1}{2}\left(\frac{x_i - \mathbb{C}_i}{\eth_i}\right)^2\right\}, i\epsilon\{\phi, \theta, \psi\}, \iota = 1{:}5$$

where the centers $\mathbb{C}_i$ were selected in $[-3\ ,3]$ and the standard deviations $\eth_i$were chosen equal to 0.034. The results obtained of the proposed control scheme for controlling attitude quadrotor are presented in figures (III.7) and (III.8). It can be seen that the proposed controller presents a good and faster response for reference tracking control in the presence of parameter uncertainties and external disturbance. Figures (III.9) and (III.10) show the control signals obtained from AFCN-CSOSMC. From thoses Figures, it can be observed the substantial chattering reduction in the control signals in comparison with the control signals obtained from the Classical SMC depicted in [53, 54].

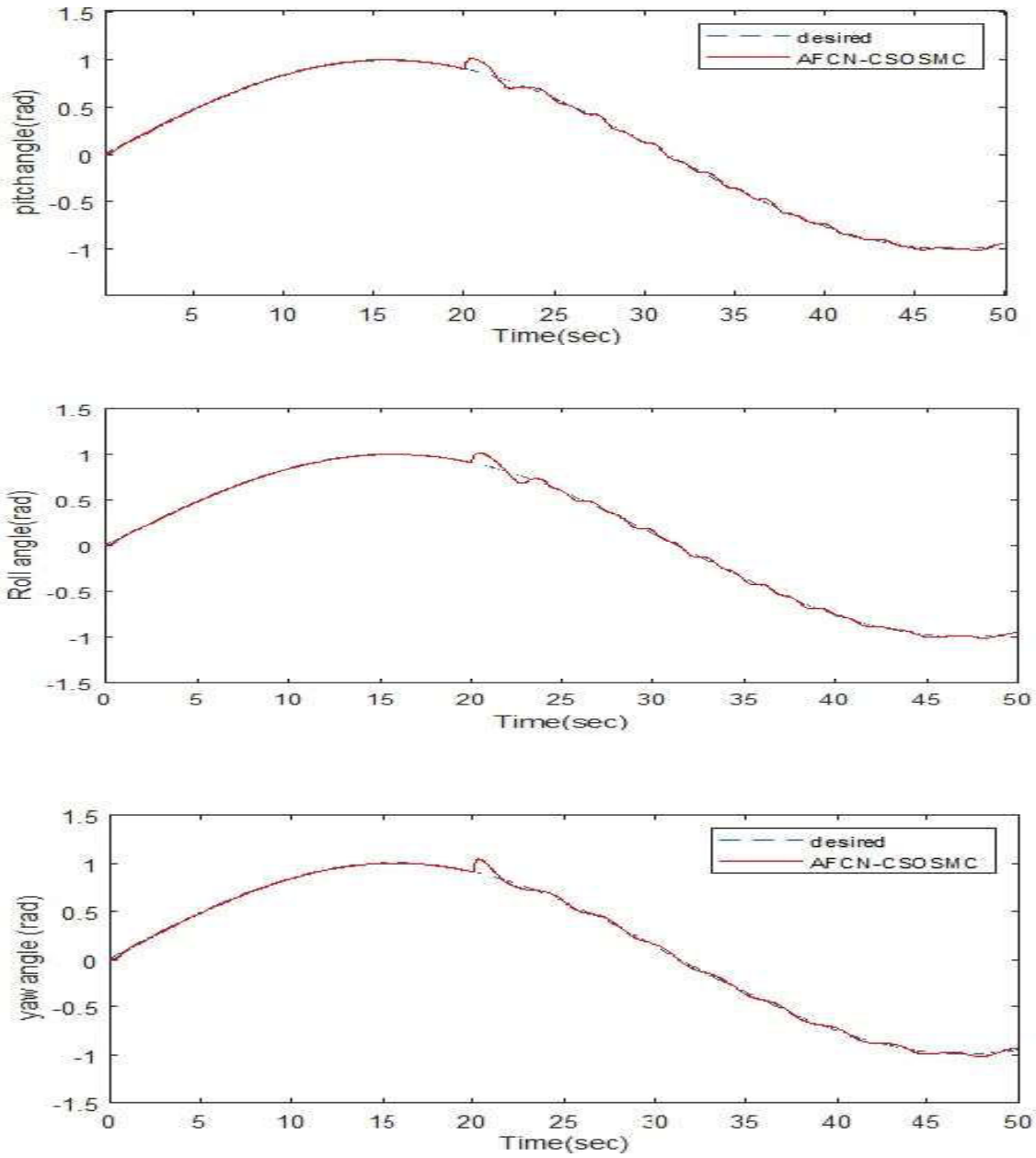

Figure III.7. The attitude responses of quadrotor, roll angle (ϕ), pitch angle (θ), yaw angle (ψ), (first scenario).

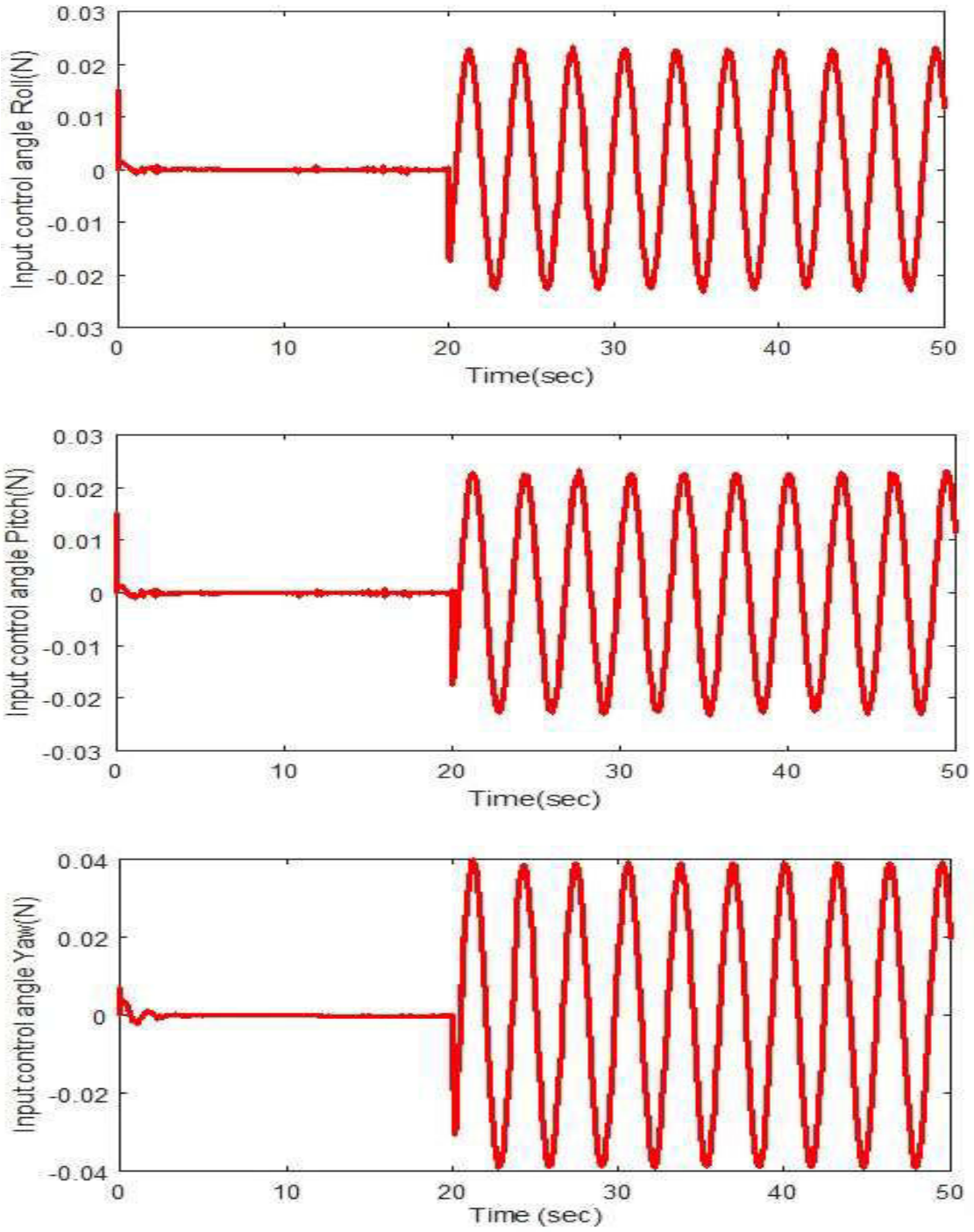

Figure III.8. Control input signals u_{ϕ}(d), u_{θ}(e), u_{ψ}(f) of AFCN-CSOSMC (first scenario).

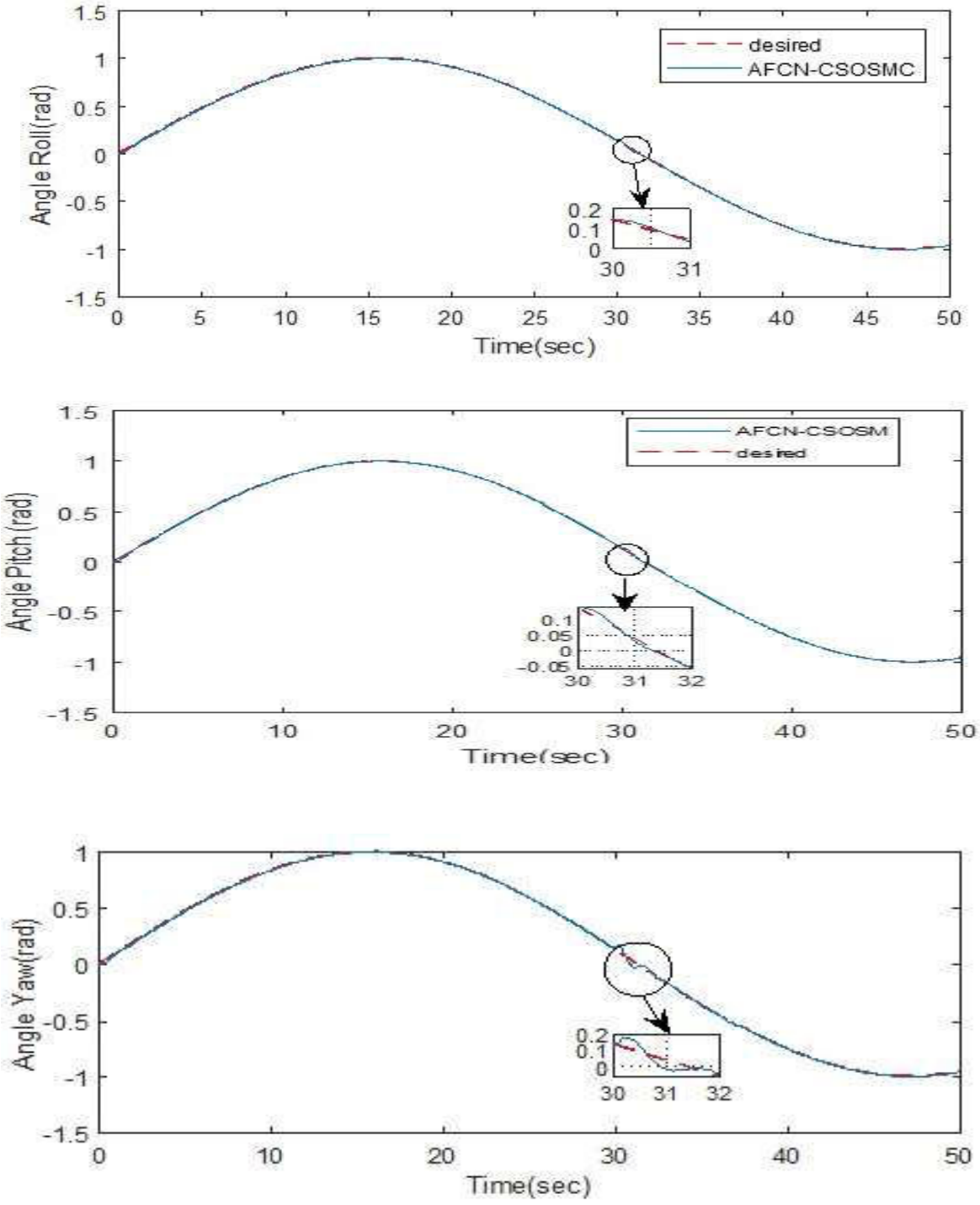

Figure III.9. The attitude responses of quadrotor, roll angle (ϕ), pitch angle (θ), yaw angle (ψ), (second scenario).

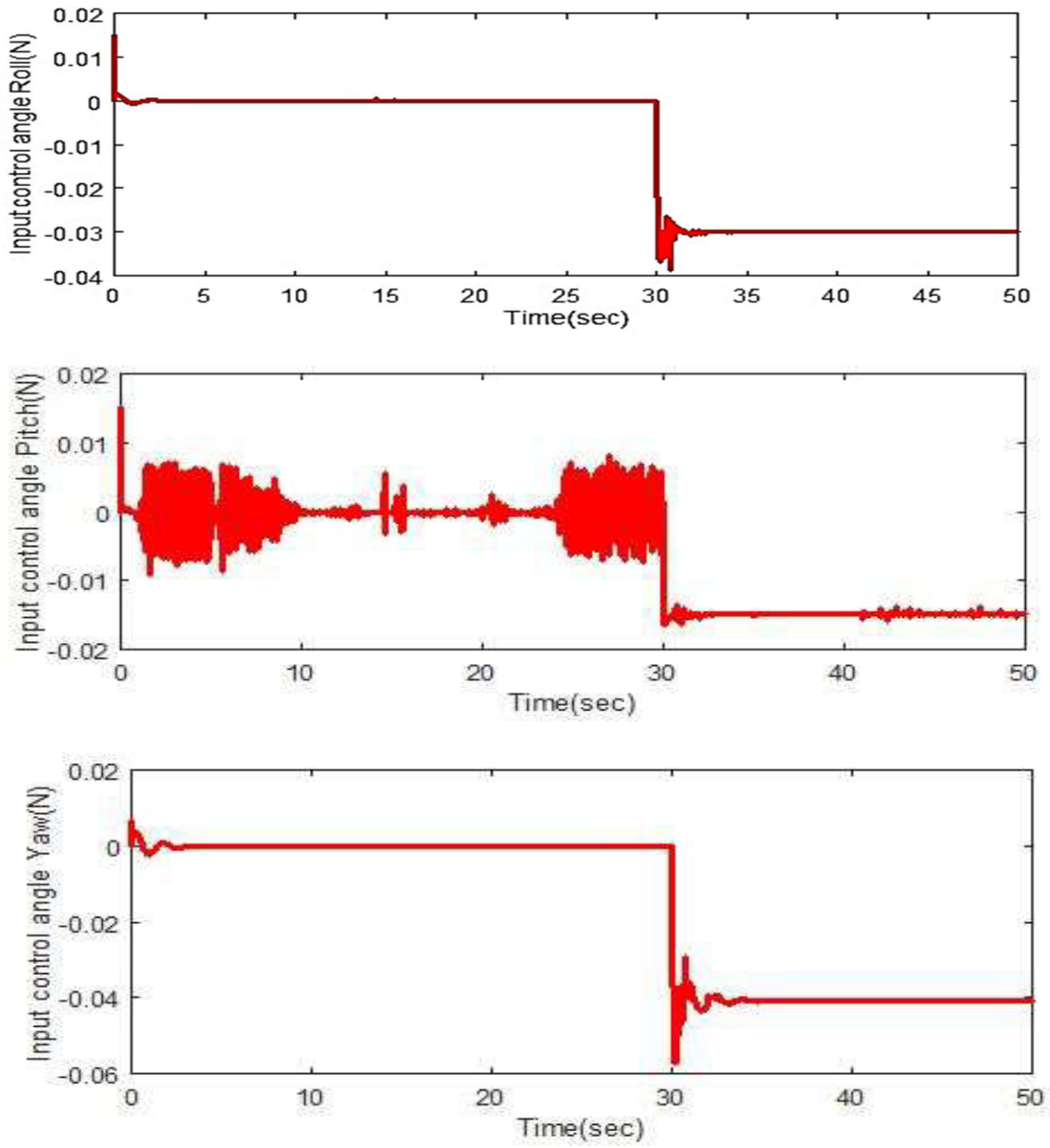

Figure III.10. Control input signals u_ϕ(d), u_θ(e), u_ψ(f) of AFCN-CSOSMC (second scenario).

III.4 Conclusion

In this chapter, two flight control approachs have been developed and studied in two parts :

- In section (1) the application of an adaptive fuzzy neural network (FNN) based backstepping controller for path tracking and stabilization of a quadrotor UAV has been proposed. The attitude quadrotor model is considered as complex

system composed of three simple subsystems, roll, pitch and yaw subsystem, in which the AFNN-DBC is applied within decentralized control scheme. Fuzzy logic system and neural network approach are used to develop a control law to deal with unknown nonlinear dynamics, approximation errors and external disturbances. The stability is guaranteed through the Lyapunov method and the effectiveness of the proposed controller are justified via simulation tests. From the results, the proposed AFNN-DBC improves response tracking and deals with the problems of uncertainties and approximation errors compared to the classical BC.

- In the section (2) the development of a continuous second order sliding mode controller based on an adaptive fuzzy-Chebyshev network estimator (AFCN-CSOSMC) for quadrotor attitude control. In this section, the attitude quadrotor model is considered as a complex system composed of three subsystems, roll, pitch and yaw subsystem, in which the AFCN-CSOSMC is applied within decentralized control scheme. Fuzzy logic systems(FLS's), Chebyshev neural network and second order sliding mode control approach are used to develop a two-term control law to deal with unknown systems dynamics, approximation errors and external disturbances. The stability and robustness of the designed controller are demonstrated using Lyapunov method, and the effectiveness of the proposed control scheme are also justified via simulation tests. From simulation results, the proposed AFCN-CSOSMC improves response tracking and reduces chattering and deals with the problems of uncertainties and approximation errors.

Moreover, the developped controllers able to rapidly and precisely folow the quadrotor path, the asymptotic stability of the closed-loop system is garanteed. The designed control strategy has been shown to assure at least asymptotic stability. Additionally, robustness over disturbances was ensured through the selection of appropriate control parameters. Simulation results obtained in comparison with a number of recent methods illustrate the effectiveness of the developed controllers.

Chapter IV

Control for QUAV Using Fractional-Order Non-linear Control

IV.1 Introduction

The application of fractional order (FO) calculus in control has developed significantly in current years, particularly in robust control. FO control is commonly considered to advance closed-loop system performance by enhancing trajectory following and transient steady-state response, guaranteeing well control performance in integer-order (IO) and FO systems. In this context, a quadrotor is a highly maneuverable unmanned aerial vehicle (UAV) that is sensitive to uncertainties in parameters such as mass, drag coefficient and moment of inertia. The nonlinearities, aerodynamic disturbances, and strong coupling between rotational and translational dynamics of these vehicles make challenges that require robust control systems.

The application of BC on the UAV system has proven the out performances compared to other techniques due to its flexibility and the recursive use of Lyapunov functions [55]. The BC main challenge is the "explosion of terms" by reason of the repetitive derivations of virtual control inputs and the acknowledged of the system dynamics is mandatory. While each variation occurred in the internal system parameters or disturbances could lead to system instability. Hence, in recent years, adaptive and intelligent backstepping control with unknown dynamics, parameter uncertainties and external disturbances has received more consideration [56]. Using a fractional order controller (FO) increases additional degrees of freedom and allows higher performance and improved robustness regarding to integer-order (IO) controllers [57]. The combination of FO with BC results in another approach named FOBC that provides a significant robustness. The major difficulty of the FOBC lies in the requirement to know the mathematical model and the physical parameters of the QUAV. Otherwise, adaptive control strategies using Lyapunov hypothesis have been designed to overcome unknown nonlinear dynamics problem [58], but remain inadequate. Again, to overcome this problem, numerous investigators have employed artificial neural networks (NN) to approximate universal systems but few works for QUAV system [59,60,61]. On the basis of radical basis function adaptive neural networks (RBFNN), by using a neural network, in [59] an adaptive approximation-based tracking control for a family of switched stochastic nonlinear pure-feedback systems is designed without lower triangular structure. The authors in [60], developed a neural network-based adaptive sliding mode controller for QUAV altitude control. On the other hand, in [61] an approach based on the backstepping method and

BFNN was developed to overcome the problem of uncertainty and optimize the design parameters.

In this chapter, we propose a novel neural network-based fractional-order backstepping controller (NNFOBC) for QUAV that comprises the NN and FO design concepts into BC. The aim of this control strategy is to follow a desired path of a 6DOF QUAV position and attitude with unknown nonlinear dynamics, parametric uncertainties and disturbances. It is noted, the QUAV is envisaged as MIMO large-scale system that can be divided into six interconnected single-input–single-output (SISO) subsystems, which define one DOF, i.e., three-angle subsystems with three position subsystems. Next, basing on FOBC and the adaptive RBFNN approximator techniques, a control law is established for all subsystems. Thus, the planned FO control approach offers considerable improvement compared to current works. In comparison with classical backstepping methods [61,62], the proposed FOBC provides further degrees of freedom and having significant effect on decreasing the uncertainties impact on the system and maintains certain features of classical control approaches including simplicity and continuous control signals. Furthermore, the difficulty of controlling MIMO nonlinear systems is solved by modifying it to the simple SISO control synthesis. The authors in [63, 64], developed various control approaches for driving UAVs where the out coming results confirm a remarkable trajectory tracking performance. Nevertheless, the reliability of the controller is not guaranteed because the stability of the system is simply validated locally, which means that the results obtained so far are not enough. Furthermore, in the developed work, the stability analysis and tracking error convergence of the QUAV subsystems as well as the complete closed-loop system are assured using the arguments of the Lyapunov technique in the whole space of working. In contrast in some references as in [65, 66] where, an FO controller is developed by assuming the quadrotor can be modeled by a known local or partial model which considerably limits the range of their applicability in real time. Besides, a successful development of a novel tracking FO control method where any prior knowledge of the dynamic model is not required in this chapter. In [56,57], authors propose intelligent FO backstepping controller (IFOBC) based on intelligent networks to control permanent magnet linear synchronous motor (PMLSM). In order to approximate the uncertainties of PMLSM model induced by unmodeled dynamics, parameters variations and external disturbances, the controllers based on neural networks

and/or fuzzy systems are developed. Whilst, in the present chapter , a simply adaptive estimator to be investigated to deal with the wholly unknown nonlinear functions of QUAV model and the backstepping control technique to design a robust controller and fewer restrictive because it doesn't require mathematical system dynamics information.

In this chapter, we developed an FO controller to allow more flexible control of complex trajectories against parametric uncertainties and disturbances. A modified (NNFOBC) control is designed for quadrotor systems that are based on fractional operators. The improved NNFOBC offers more degrees of freedom (DOF), is more effective at reducing the effects of uncertainty on the system, and retains some properties of traditional control techniques such as backstepping.

IV.2 Preliminaries of FO calculus

In this section, the habitually adopted definitions for general fractional order operator are: Riemann-Liouville (RL) and Caputo [67,68].

Definition 1 The Riemann–Liouville (RL) fractional derivative and integral of q th-order of function $\mathfrak{H}(t)$ respectively, are given by:

$$ {}_{t_0}^{RL}\mathcal{D}_t^{q}\mathfrak{H}(t) = \frac{d^{q}\mathfrak{H}(t)}{dt^{q}} = \frac{1}{\Gamma(\hbar - q)}\frac{d^{\hbar}}{dt^{\hbar}}\int_{t_0}^{t}\frac{\mathfrak{H}(\tau)}{(t-\tau)^{q-\hbar+1}}d\tau \tag{IV.1} $$

and:

$$ {}_{t_0}^{RL}\mathcal{D}_t^{-q}\mathfrak{H}(t) = I_t^{r}\mathfrak{H}(t) = \frac{1}{\Gamma(\nu)}\int_{t_0 0}^{t}\frac{\mathfrak{H}(\tau)}{(t-\tau)^{1-r}}d\tau $$

where $1-\hbar < q < \hbar$, D^{q} and I^{q} indicate the fractional derivative and integral, respectively, and $t0$ is the initial time, $\Gamma(.)$ indicates the Gamma function which given by [69-70]:

$$ \Gamma(q) = \int_0^{\infty} e^{-t}t^{q-1}dt \tag{IV.2} $$

Definition 2 The Caputo fractional derivative of a function $\mathfrak{H}(t)$ is described as:

$$ {}_{t_0}^{Ca}\mathcal{D}_t^{q}\mathfrak{H}(t) = \frac{1}{\Gamma(\hbar-q)}\int_{t_0}^{t}\frac{\mathfrak{H}^{\hbar}(\tau)}{(t-\tau)^{q-\hbar+1}}d\tau, (\hbar-1) < q < \hbar \tag{IV.3} $$

with $\nu \in \mathbb{R}^{+}$,and $\hbar \in \mathbb{N}^{*}$.

Property 1 We can use equation. (IV.3) for the Caputo derivative

$$ {}_{t_0}^{Ca}\mathcal{D}_t^{q-r}\mathfrak{H}(t) = {}_{t_0}^{Ca}\mathcal{D}_t^{q}({}_{t_0}^{Ca}\mathcal{D}_t^{-r}\mathfrak{H}(t)) \quad \text{(IV.4)} $$

Where $q \geq r \geq 0$. It is noted that the FO operator a ${}_{t_0}^{RL}\mathcal{D}_t^{q}$ as $\mathcal{D}$ to simplify the notation.

IV.3 Adaptive RBFNN fractional-order backstepping control

IV.3.1 Fractional-order backstepping control (FOBC)

To enhance the classical BC law described in the chapter III section III.2.1, we have developed a FOBC based on a new FO virtual stabilization function. The FOBC have some advantages such as faster tracking performance and higher control accuracy [71]. FOBC and BC design methodologies are similar. First, we describe the FO virtual stabilization function by:

The design methodology of FOBC is the same as that of the BC

$$ \mathcal{Q}_{\mathcal{F}o,i} = \dot{y}_i^d + \eta_{i,1}\mathcal{D}^{q}\mathrm{e}_{i,1} + \eta_{i,2}\mathcal{D}^{-r}\mathrm{e}_{i,1} + \mathcal{C}_{\mathcal{F}o,i}\mathrm{e}_{i,1}, i \in \{x, y, z, \phi, \theta, \psi\} \quad \text{(IV.5)} $$

Where q and r are the FO derivative and integral orders, respectively $\eta_{1,i,}, \mathcal{C}_{\mathcal{F}o,i}$ and $\eta_{2,i}$are any positive constants. Next, we identify the $\mathrm{e}_{\mathcal{F}o2,i}$virtual tracking error as:

$$ \mathrm{e}_{\mathcal{F}o2,i} = \dot{y}_i - \mathcal{Q}_{\mathcal{F}o,i} = \eta_{1,i}\mathcal{D}^{q}\mathrm{e}_{i,1} + \eta_{2,i}\mathcal{D}^{-r}\mathrm{e}_{i,1} + \mathcal{C}_{\mathcal{F}o,i}\mathrm{e}_{i,1} - \dot{\mathrm{e}}_{i,1} \quad \text{(IV.6)} $$

As seen equation (IV.6), the virtual tracking error $\mathrm{e}_{\mathcal{F}o2,i}$is a lineara sum of the proportional IO derivative, FO derivative, and FO integral of the real tracking error $\mathrm{e}_{i,1}$. Through equation (III.1) and (IV.6), the $\mathrm{e}_{\mathcal{F}o2,\mathrm{i}}$ derivative can be given as:

$$ \begin{aligned} \dot{\mathrm{e}}_{\mathcal{F}o2,\mathrm{i}} &= \mathcal{F}_{\mathrm{i}}(\chi) + \mathcal{G}_{\mathrm{i}}(\chi)\mathcal{U}_{\mathrm{i}} + \mathrm{p}_{\mathrm{i}}(\mathrm{t}) - \dot{\mathcal{Q}}_{\mathcal{F}\mathcal{B},\mathrm{i}} \\ &= -\ddot{\mathrm{e}}_{\mathrm{i},1} + \eta_{i,1}\mathcal{D}^{1+q}\mathrm{e}_{\mathrm{i},1} + \eta_{i,2}\mathcal{D}^{1-r}\mathrm{e}_{\mathrm{i},1} + \mathcal{C}_{\mathcal{F}\mathrm{o},\mathrm{i}}\mathrm{e}_{\mathrm{i},1} \end{aligned} \quad \text{(IV.7)} $$

Theorem 1. *The quadrotor system stability can be guaranteed if the control law of the FOBC system* $\mathcal{U}_{\mathcal{F}OBC,i}$*, described in equation.(* IV.8*), is applied under the condition* $\mathcal{F}_i(\chi)$ *and* $\mathcal{G}_i(\chi)$ *are perfectly known and the system neither subject to any parametric variations and*

external disturbances. In difference to the control law $\mathcal{U}_{BC,i}$ *as expressed in equation (*III.19*), the control law* $\mathcal{U}_{\mathcal{F}OBC,i}$ *with two additional FO parameters* q *and* r *delivers further flexibility and opportunity to perfectly adjust the dynamical properties of the control system.*

$$\mathcal{U}_{\mathcal{F}OBC,i} = \mathcal{G}_i(\chi)^{-1}\big(-\mathcal{F}_i(\chi) + \mathrm{e}_{i,1} - \check{\mathcal{C}}_{\mathcal{F}o,i}\mathrm{e}_{\mathcal{F}o2,i} + \mathrm{e}_{\mathcal{F}02,i}^{-1}\big(\eta_{i,1}\mathrm{e}_{i,1}\mathcal{D}^{q}\mathrm{e}_{i,1} + \eta_{2,i}\mathrm{e}_{i,1}\mathcal{D}^{-r}\mathrm{e}_{i,1}\big) + \dot{\mathcal{Q}}_{\mathcal{F}o,i}\big) \quad (\text{IV.8})$$

Proof. We outline the Lyapunov function candidate as*:*

$$\begin{aligned}\dot{\mathcal{V}}_1 &= \textstyle\sum_{i=\{x,y,z,\phi,\theta,\psi\}} \mathrm{e}_{i,1}\dot{\mathrm{e}}_{i,1} = \sum_{i=\{x,y,z,\phi,\theta,\psi\}} \mathrm{e}_{i,1}(\dot{y}_i^d - \dot{y}_i)\\ &= \textstyle\sum_{i=\{x,y,z,\phi,\theta,\psi\}} \mathrm{e}_{i,1}(\dot{y}_i^d - x_{i,2})\\ &= \textstyle\sum_{i=\{x,y,z,\phi,\theta,\psi\}} \mathrm{e}_{i,1}\,(-\eta_{i,1}\mathcal{D}^{q}\mathrm{e}_{i,1} - \eta_{i,2}\mathcal{D}^{-r}\mathrm{e}_{i,1} - \mathcal{C}_{\mathcal{F}o,i}\mathrm{e}_{i,1})\\ &= \textstyle\sum_{i=\{x,y,z,\phi,\theta,\psi\}}(-\eta_{i,1}\mathrm{e}_{i,1}\mathcal{D}^{q}\mathrm{e}_{i,1} - \eta_{i,2}\mathrm{e}_{i,1}\mathcal{D}^{-r}\mathrm{e}_{i,1} - \mathcal{C}_{\mathcal{F}o,i}\mathrm{e}_{i,1}^2)\end{aligned} \quad (\text{IV.9})$$

For FOBC, we express the second Lyapunov function by:

$$\mathcal{V}_{\mathcal{F}o,i} = \mathcal{V}_1 + \frac{1}{2}\sum_{i=\{x,y,z,\phi,\theta,\psi\}} \mathrm{e}_{\mathcal{F}o2,i}^2 \quad (\text{IV.10})$$

If we differentiate equation.(IV.10) and use equations.(IV.6) and (III.1), we can achieve:

$$\begin{aligned}\dot{\mathcal{V}}_{\mathcal{F}o,i} &= \dot{\mathcal{V}}_1 + \sum_{i=\{x,y,z,\phi,\theta,\psi\}} \mathrm{e}_{i,1}\mathrm{e}_{\mathcal{F}o2,i} + \mathrm{e}_{\mathcal{F}o2,i}\,\dot{\mathrm{e}}_{\mathcal{F}o2,i}\\ &= \sum_{i=\{x,y,z,\phi,\theta,\psi\}}(-\eta_{i,1}\mathrm{e}_{i,1}\mathcal{D}^{q}\mathrm{e}_{i,1} - \eta_{i,2}\mathrm{e}_{i,1}\mathcal{D}^{-r}\mathrm{e}_{i,1} - \mathcal{C}_{\mathcal{F}o,i}\mathrm{e}_{i,1}^2)\\ &+ \sum_{i=\{x,y,z,\phi,\theta,\psi\}} -\mathrm{e}_{i,1}\mathrm{e}_{\mathcal{F}o2,i} + \mathrm{e}_{\mathcal{F}o2,i}\,\big(\mathcal{F}_i(\chi) + \mathcal{G}_i(\chi)\mathcal{U}_i - \dot{\mathcal{Q}}_{\mathcal{F}o,i}\big)\end{aligned} \quad (\text{IV.11})$$

By substituting equation (IV.8) in equation.(IV.11), we obtain:

$$\dot{\mathcal{V}}_{\mathcal{F}o,i} = \textstyle\sum_{i=\{x,y,z,\phi,\theta,\psi\}} -\mathcal{C}_{\mathcal{F}o,i}\mathrm{e}_{i,1}^2 + \sum_{i=\{x,y,z,\phi,\theta,\psi\}} -\check{\mathcal{C}}_{\mathcal{F}o,i}\mathrm{e}_{\mathcal{F}o2,i}^2 \quad (\text{IV.12})$$

$$\begin{aligned}\dot{\mathcal{V}}_{\mathcal{F}o,i} &= -\sum_{i=\{x,y,z,\phi,\theta,\psi\}} \mathcal{C}_{\mathcal{F}o,i}\mathrm{e}_{i,1}^2 - \sum_{i=\{x,y,z,\phi,\theta,\psi\}} \check{\mathcal{C}}_{\mathcal{F}o,i}\mathrm{e}_{\mathcal{F}o2,i}^2\\ &\leq 0\end{aligned} \quad (\text{IV.13})$$

Since $\mathcal{C}_{\mathcal{F}o,i}$, $\check{\mathcal{C}}_{\mathcal{F}o,i}$ are positive constants, the derivative of $\mathcal{V}_{\mathcal{F}o,i}$ is a semi-negative definite function . This involves that the stability of the FOBC closedloop system of QUAV can be ensured and the signals $\mathrm{e}_{i,1}$ and $\mathrm{e}_{\mathcal{F}o2,i}$ go to zero asymptotically. Moreover, we assume that the nonlinear functions $\mathcal{F}_i(\chi)$and $\mathcal{G}_i(\chi)$ are unknown. Hence, it is hard to develop an appropriate control law that makes the system outputs y_i follow quickly and perfectly a definite chosen trajectories y_i^d and ensure the boundedness of every signal in the closed-loop system. Hence, we develop a control strategy based neural network approach to approximate the nonlinearities. Basing on the specified approximations, adaptive controller is intended to succeed the control objective.

Remark 3 *The entire quadrotor, represented by (II.27) as a large-scale system, is stabilized by choosing the virtual control input as (II.28) and the BC law as (III.19). Asymptotic convergence of the outputy_i, position and attitude to the desired trajectory y_i^d is attained by the use of various Lyapunov functions such as (IV.9) and (IV.10) i.e., $\mathcal{V}_1 = \sum_{i=\{x,y,z,\phi,\theta,\psi\}} \mathcal{V}_{i,1}$. This helps ensure the stability of the entire system. This suggestion offers a new solution for constructing candidate Lyapunov functions for control problems in quadrotor and similar application systems. Moreover, the backstepping control technique is applied to the low-dimensional subsystems, thus avoiding the problem of explosion and complexity of the backstepping control technique.*

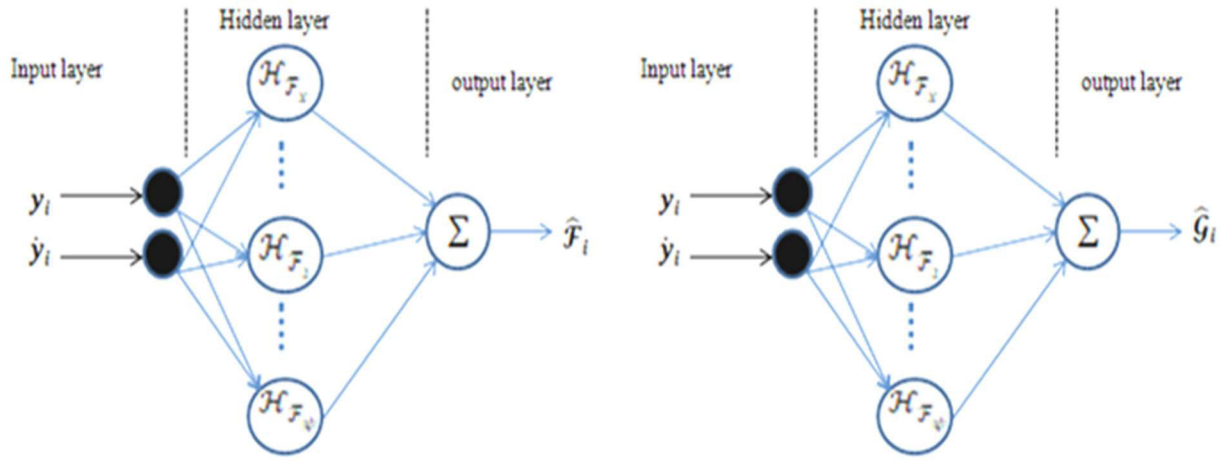

Figure IV.1. Radial basis function neural network (RBFNN) structure.

IV.4 RBF neural network approximator

In this subsection, we designed the NNFOBC which uses a RBFNN to approximate the unknown nonlinear functions $\mathcal{F}_i(\chi)$ and $\mathcal{G}_i(\chi)$ of every subsystem as seen in figure (IV.1). In general, RBFNN can approximate every nonlinear continuous function against a solid set to random accuracy [72].On behalf of the QUAV system, we accept that the nonlinear functions $\mathcal{F}_i(\chi)$ and $\mathcal{G}_i(\chi)$ may be approximated against a compact set $\Omega_\chi \in \mathbb{R}^n$ by the structure of RBFNN as expressed in [72]:

$$\mathcal{F}_i\left(\bar{\bar{\pi}}_{\mathcal{F}_i}, \chi\right) = \pi_{\mathcal{F}_i}^{*T}\mathcal{H}(\chi) + \varepsilon_{\mathcal{F}_i}(\chi) \tag{IV.14}$$

$$\mathcal{G}_i\left(\bar{\bar{\pi}}_{\mathcal{G}_i}, \chi\right) = \pi_{\mathcal{G}_i}^{*T}\mathcal{H}_{\mathcal{G}_i}(\chi) + \varepsilon_{\mathcal{G}_i}(\chi) \tag{IV.15}$$

Assuming $,\chi$ the input of the neural network, $\mathcal{H}_{\mathcal{F}_i}(\chi) = \left[\mathcal{H}_{\mathcal{F}_{1,i}}(\chi), \dots, \mathcal{H}_{\mathcal{F}_{N,i}}(\chi)\right]^T$ and $\mathcal{H}_{\mathcal{G}_i}(\chi) = \left[\mathcal{H}_{\mathcal{G}_{1,i}}(\chi), \dots, \mathcal{H}_{\mathcal{G}_{L,i}}(\chi)\right]^T$ are the RBFNN activate functions of $\mathcal{F}_i(\chi)$ and $\mathcal{G}_i(\chi)$ respective,N and L are their neuron node numbers in hidden layer,$\bar{\bar{\pi}}_{\mathcal{F}_i} = \left[\bar{\bar{\pi}}_{\mathcal{F}_{1,i}}, \dots, \bar{\bar{\pi}}_{\mathcal{F}_{N,i}}\right]^T$ and $\bar{\bar{\pi}}_{\mathcal{G}_i} = \left[\bar{\bar{\pi}}_{\mathcal{G}_{1,i}}, \dots, \bar{\bar{\pi}}_{\mathcal{G}_{L,i}}\right]^T$ are the ideal weight vectors of $\mathcal{F}_i(\chi)$ and $\mathcal{G}_i(\chi)$ minimizing the network approximation errors $\varepsilon_{\mathcal{F}_i}(\chi)$ and $\varepsilon_{\mathcal{G}_i}(\chi)$ respectively. The optimal parameters verify :

$$\bar{\bar{\pi}}_{\mathcal{F}_i} = \arg\min_{\pi_{\mathcal{F}_i}} \left\{\sup_{\chi\in\Omega_\chi} \left|\mathcal{F}_i(\chi) - \hat{\mathcal{F}}_i\left(\pi_{\mathcal{F}_i}, \chi\right)\right|\right\} \tag{IV.16}$$

$$\bar{\bar{\pi}}_{\mathcal{G}_i} = \arg\min_{\pi_{\mathcal{G}_i}} \left\{\sup_{\chi\in\Omega_\chi} \left|\mathcal{G}_i(\chi) - \hat{\mathcal{G}}_i\left(\pi_{\mathcal{G}_i}, \chi\right)\right|\right\} \tag{IV.17}$$

$\hat{\mathcal{F}}_i(\pi_{\mathcal{F}i}, \chi)$ and $\hat{\mathcal{G}}_i\left(\pi_{\mathcal{G}_i}, \chi\right)$ are utilized by RBFNN to approximate equations.(IV.14) and (IV.15) as the ideal weights $\bar{\bar{\pi}}_{\mathcal{F}_i}$and $\bar{\bar{\pi}}_{\mathcal{G}_i}$which usually unknowns are estimated respectively by $\pi_{\mathcal{F}_i}$ and $\pi_{\mathcal{G}_i}$. The mentioned values to be adjusted by a weight learning law that can be specified afterward. Moreover, the RBFNN activation function is considered in this study, one of the common used activation functions is Gaussian function:

$$\mathcal{H}_{\mathcal{F}_{i,j}}(\chi) = \exp\left[-\left(\left\|\chi - c_{\mathcal{F}_{i,j}}\right\|^2\right)/2b_{\mathcal{F}_{i,j}}^2\right] \tag{IV.18}$$

$$\mathcal{H}_{\mathcal{G}_{i,j}}(\chi) = \exp\left[-(\left\|\chi - c_{\mathcal{G}_{i,j}}\right\|^2)/2b_{\mathcal{G}_{i,j}}^2\right] \quad \text{(IV.19)}$$

$c_{\Pi i,j}$is the center of the *j*th neuron node for the χ input signal, and $b_{\Pi i,j}$is the width of the *j*th neuron of the Gaussian function ,where $\Pi = \mathcal{F}, \mathcal{G}$. Trough the above analysis, we conclude:

$$\mathcal{F}_i(\chi) - \hat{\mathcal{F}}_i(\pi_{\mathcal{F}_i}, \chi) = \tilde{\pi}_{\mathcal{F}_i}^T \mathcal{H}_{\mathcal{F}_i}(\chi) + \varepsilon_{\mathcal{F}_i}(\chi) \quad \text{(IV.20)}$$

$$\mathcal{G}_i(\chi) - \hat{\mathcal{G}}_i(\pi_{\mathcal{G}_i}, \chi) = \tilde{\pi}_{\mathcal{G}i}^T \mathcal{H}_{\mathcal{G}_i}(\chi) + \varepsilon_{\mathcal{G}i}(\chi) \quad \text{(IV.21)}$$

$\tilde{\pi}_{\mathcal{F}_i} = \bar{\bar{\pi}}_{\mathcal{F}_i} - \pi_{\mathcal{F}_i}$ and $\tilde{\pi}_{\mathcal{G}_i} = \bar{\bar{\pi}}_{\mathcal{G}_i} - \pi_{\mathcal{G}_i}$represent the parameters estimation errors.

Assumption 5. *From the universal approximation ability, the RBFNN are supposed to ensure the estimate error ultimately converge to a satisfactorily small compact set, i.e. there exists a positive constants* $\varepsilon_{\mathcal{F}_i 0}$*and* $\varepsilon_{\mathcal{G}i0}$ *such as:*

$$\left|\varepsilon_{\mathcal{F}_i}(\chi)\right| \leq \varepsilon_{\mathcal{F}_i 0} \text{ and} \left|\varepsilon_{\mathcal{G}i}(\chi)\right| \leq \varepsilon_{\mathcal{G}i0} \text{for all } \chi \in \Omega_\chi \quad \text{(IV.22)}$$

From the above approximations, the $\mathcal{U}_i$ adaptive control law to be expressed as:

$$\mathcal{U}_i = \mathcal{U}_{NN\mathcal{F}OBC,i} + \mathcal{U}_{robust,i} \quad \text{(IV.23)}$$

The control law described above incorporates the sum of the term adaptive control introduced to handle with nonlinear systems of unknown performance, whilst the second is a robust term dealing with approximation errors and disturbances. The proposed NNFOBC is recapped in figure (IV.2).

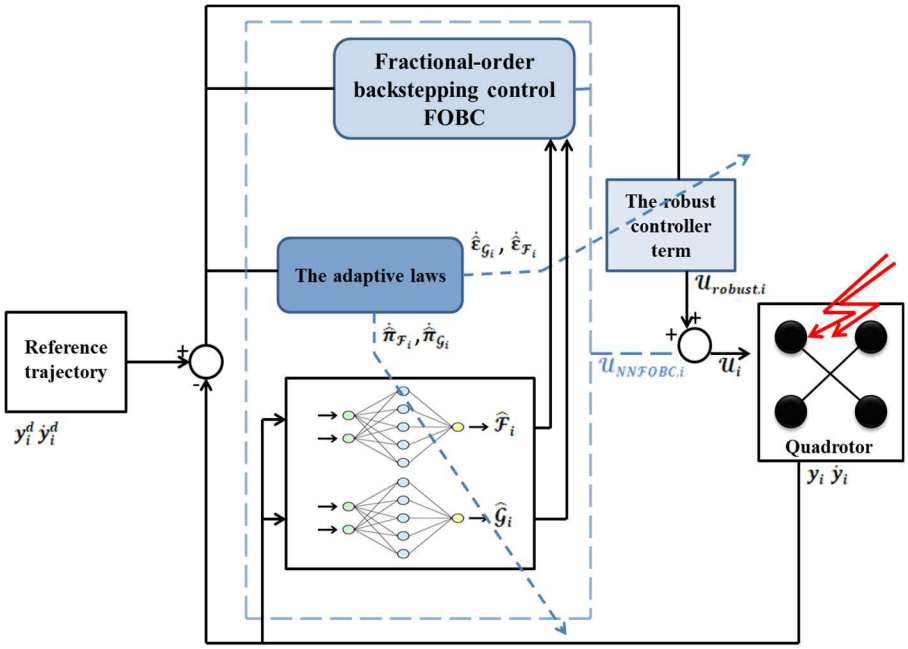

Figure IV.2. Block diagram of quadrotor system based on NNFOBC.

The following form will be taken by the adaptive term:

$$\mathcal{U}_{NN\mathcal{F}OBC,i} = \frac{\hat{\mathcal{G}}_i(\chi)}{\hat{\mathcal{G}}_i(\chi)^2+\propto}\ \Big(-\hat{\mathcal{F}}_i(\chi) + \mathrm{e}_{i,1} - \check{\mathcal{C}}_{\mathcal{F}o,i}\mathrm{e}_{\mathcal{F}o2,i} + \mathrm{e}_{\mathcal{F}02,i}^{-1}\big(\eta_{i,1}\mathrm{e}_{i,1}\mathcal{D}^{q}\mathrm{e}_{i,1} + \eta_{2,i}\mathrm{e}_{i,1}\mathcal{D}^{-r}\mathrm{e}_{i,1}\big) + \dot{\mathcal{Q}}_{\mathcal{F}o,i}\Big) \tag{IV.24}$$

The robust controller term will income the described form below:

$$\mathcal{U}_{robust,i} = \frac{\hat{\mathcal{G}}_i(\chi)}{\hat{\mathcal{G}}_i(\chi)^2+\propto}\ \Big(-\varrho\mathrm{e}_{\mathcal{F}o2,i} - \hat{\varepsilon}_{\mathcal{F}_i}sgn\big(\mathrm{e}_{\mathcal{F}o2,i}\big) - \hat{\varepsilon}_{\mathcal{G}_i}sgn\big(\mathrm{e}_{\mathcal{F}o2,i}\big)\Big) \tag{IV.25}$$

where ϱ is the design positive constant, $\hat{\varepsilon}_{\mathcal{F}_i}$ and $\hat{\varepsilon}_{\mathcal{G}_i}$ are the estimate of $\varepsilon_{\mathcal{F}_{i0}}$ and $\varepsilon_{\mathcal{G}i0}$ respectively.

Remark 4 *From equations (*IV.23*), (*IV.24*) and (*IV.25*),it is obvious that the quadrotor inputs are totally independent since the control values of each subsystem are only calculated through its local measurements, that is,* $\mathcal{U}_i$ *for* $i \in \{x, y, z, \phi, \theta, \psi\}$*are related only to the local tracking errors* $\mathrm{e}_{i,1}$ *and* $\mathrm{e}_{\mathcal{F}o2,i}$*. Thus, no interaction exists between the control of position and attitude subsystems which lead in effect to have a decentralized (decoupled) control structure. Where the decentralized control allowed to manage independently the position and*

orientation dynamic subsystems which makes the control architecture more simple and easy to implement in real time.

We describe the adaptive parameters by:

$$\dot{\tilde{\pi}}_{\mathcal{F}_i} = -\dot{\hat{\pi}}_{\mathcal{F}_i} = \frac{\mathrm{e}_{\mathcal{F}o2,i}\mathcal{H}_{\mathcal{F}_i}(\chi) - \sigma_{\mathcal{F}_i}\hat{\pi}_{\mathcal{F}_i}}{\gamma_{\mathcal{F}_i}^{-1}} \quad \text{(IV.26)}$$

$$\dot{\tilde{\pi}}_{\mathcal{G}_i} = -\dot{\hat{\pi}}_{\mathcal{G}_i} = \frac{\mathrm{e}_{\mathcal{F}o2,i}\mathcal{H}_{\mathcal{G}_i}(\chi)\mathcal{U}_i - \sigma_{\mathcal{G}_i}\hat{\pi}_{\mathcal{G}_i}}{\gamma_{\mathcal{G}_i}^{-1}} \quad \text{(IV.27)}$$

$$\dot{\hat{\varepsilon}}_{\mathcal{F}_i} = \rho_{\mathcal{F}_i}\left|\mathrm{e}_{\mathcal{F}o2,i}\right| \quad \text{(IV.28)}$$

$$\dot{\hat{\varepsilon}}_{\mathcal{G}_i} = \rho_{\mathcal{G}_i}\left|\mathrm{e}_{\mathcal{F}o2,i}\mathcal{U}_i\right| \quad \text{(IV.29)}$$

Where: $\gamma_{\mathcal{F}_i}$, $\sigma_{\mathcal{F}_i}$, $\gamma_{\mathcal{G}_i}$, $\sigma_{\mathcal{G}_i}$, $\rho_{\mathcal{F}_i}$and $\rho_{\mathcal{G}_i}$ are positive designing constants.

Lemma 2 *[72]: For* $\forall(\mathfrak{a},\mathfrak{b}) \in R^2$*, the inequality described below holds:*

$$\mathfrak{a},\mathfrak{b} \leq \frac{\mathfrak{y}^{\mathcal{O}}}{\mathcal{O}}|\mathfrak{a}|^{\mathcal{O}} + \frac{1}{\mathcal{O}}\mathfrak{y}^{\mathcal{S}}|\mathfrak{a}|^{\mathcal{S}\mathcal{O}} \textit{where: } \mathfrak{y} > 0, \mathcal{O} > 1, \mathcal{S} > 1, (\mathcal{O}-1)(\mathcal{S}-1) = 1. \quad \text{(IV.30)}$$

IV.5 Stability analysis

The next theorem reveals the closed-loop system stability to be confirmed via Lyapunov analysis.

Theorem 2 *Considering the quadrotor system model described by equation.*(II.27) *and satisfying assumptions (1-5), The designed NNFOBC shown in equation.*(IV.21), *with the adaptive term equation. (*IV.23*), robust term equation (*IV.23*), and the adaptation laws equations. (*IV.21– IV.28*) guarantees the delimitation of every signals in the closed loop system and the asymptotic convergence of the tracking errors at zero i.e* $\lim_{t\to+\infty} \mathrm{e}_{i,1}(t) = 0$.

Proof : We outline the Lyapunov function candidate as:

$$\begin{aligned}\mathcal{V}_3 = \mathcal{V}_{\mathcal{F}o,i} &+ \sum_{i\in\{x,y,z,\phi,\theta,\psi\}} \frac{1}{2}\left(\frac{\tilde{\pi}_{\mathcal{F}_i}^T\tilde{\pi}_{\mathcal{F}_i}}{\gamma_{\mathcal{F}_i}}\right) + \sum_{i\in\{x,y,z,\phi,\theta,\psi\}} \frac{1}{2}\left(\frac{\tilde{\pi}_{\mathcal{G}_i}^T\tilde{\pi}_{\mathcal{G}_i}}{\gamma_{\mathcal{G}_i}}\right) \\ &+ \sum_{i\in\{x,y,z,\phi,\theta,\psi\}} \frac{1}{2}\left(\frac{\tilde{\varepsilon}_{\mathcal{F}_i}^T\tilde{\varepsilon}_{\mathcal{F}_i}}{\rho_{\mathcal{F}_i}}\right) + \sum_{i\in\{x,y,z,\phi,\theta,\psi\}} \frac{1}{2}\left(\frac{\tilde{\varepsilon}_{\mathcal{G}_i}^T\tilde{\varepsilon}_{\mathcal{G}_i}}{\rho_{\mathcal{G}_i}}\right)\end{aligned} \quad \text{(IV.31)}$$

Where $\tilde{\varepsilon}_{\mathcal{F}_i} = \varepsilon_{\mathcal{F}i0} - \hat{\varepsilon}_{\mathcal{F}_i}$ and $\tilde{\varepsilon}_{\mathcal{G}_i} = \varepsilon_{\mathcal{G}i0} - \hat{\varepsilon}_{\mathcal{G}_i}$ are the parameter estimation errors. So the time derivative of v_3 as follows

$$\dot{\mathcal{V}}_3 = \dot{\mathcal{V}}_{\mathcal{F}o,i} + \sum_{i\in\{x,y,z,\phi,\theta,\psi\}} \left(\frac{\tilde{\pi}_{\mathcal{F}_i}^T \dot{\hat{\pi}}_{\mathcal{F}_i}}{\gamma_{\mathcal{F}_i}}\right) + \sum_{i\in\{x,y,z,\phi,\theta,\psi\}} \left(\frac{\tilde{\pi}_{\mathcal{G}_i}^T \dot{\hat{\pi}}_{\mathcal{G}_i}}{\gamma_{\mathcal{G}_i}}\right) + \sum_{i\in\{x,y,z,\phi,\theta,\psi\}} \left(\frac{\tilde{\varepsilon}_{\mathcal{F}_i}^T \dot{\tilde{\varepsilon}}_{\mathcal{F}_i}}{\rho_{\mathcal{F}_i}}\right) + \sum_{i\in\{x,y,z,\phi,\theta,\psi\}} \left(\frac{\tilde{\varepsilon}_{\mathcal{G}_i}^T \dot{\tilde{\varepsilon}}_{\mathcal{G}_i}}{\rho_{\mathcal{G}_i}}\right) \tag{IV.32}$$

Thus, from equations.(IV.11) and (IV.32), it is shown that of $\dot{\mathcal{V}}_3$satisfies:

$$\begin{aligned}\dot{v}_3 = \sum_{i=\{x,y,z,\phi,\theta,\psi\}} & (-\eta_{i,1}\mathrm{e}_{i,1}\mathcal{D}^{q}\mathrm{e}_{i,1} - \eta_{i,2}\mathrm{e}_{i,1}\mathcal{D}^{-r}\mathrm{e}_{i,1} - \mathcal{C}_{\mathcal{F}o,i}\mathrm{e}_{i,1}^2) \\ & - \sum_{i\in\{x,y,z,\phi,\theta,\psi\}} \mathrm{e}_{i,1}\mathrm{e}_{\mathcal{F}o2,i} - \mathrm{e}_{\mathcal{F}o2,i}\left(\mathcal{F}_i(\chi) + \frac{\hat{\mathcal{G}}_i(\chi)}{\hat{\mathcal{G}}_i(\chi)^2 + \propto}\ \mathcal{U}_i + p_i(t)\right. \\ & \left. - \dot{\mathcal{Q}}_{\mathcal{F}o,i}\right) - \sum_{i\in\{x,y,z,\phi,\theta,\psi\}} \left(\frac{\tilde{\pi}_{\mathcal{F}_i}^T \dot{\hat{\pi}}_{\mathcal{F}_i}}{\gamma_{\mathcal{F}_i}}\right) - \sum_{i\in\{x,y,z,\phi,\theta,\psi\}} \left(\frac{\tilde{\pi}_{\mathcal{G}_i}^T \dot{\hat{\pi}}_{\mathcal{G}_i}}{\gamma_{\mathcal{G}_i}}\right) \\ & - \sum_{i\in\{x,y,z,\phi,\theta,\psi\}} \left(\frac{\tilde{\varepsilon}_{\mathcal{F}_i}^T \dot{\hat{\varepsilon}}_{\mathcal{F}_i}}{\rho_{\mathcal{F}_i}}\right) - \sum_{i\in\{x,y,z,\phi,\theta,\psi\}} \left(\frac{\tilde{\varepsilon}_{\mathcal{G}_i}^T \dot{\hat{\varepsilon}}_{\mathcal{G}_i}}{\rho_{\mathcal{G}_i}}\right)\end{aligned} \tag{IV.33}$$

Substituting equations.(IV.20), (IV.21) and (IV.21) into equation.(IV.33) results in:

$$\begin{aligned}\dot{v}_3 = \sum_{i=\{x,y,z,\phi,\theta,\psi\}} & \mathrm{e}_{\mathcal{F}o2,i}\left[\left(\mathcal{F}_i(\chi) - \hat{\mathcal{F}}_i(\chi)\right) + \left(\mathcal{G}_i(\chi) - \hat{\mathcal{G}}_i(\chi)\right)\mathcal{U}_i\right. \\ & \left. - \hat{\varepsilon}_{\mathcal{F}_i} sgn\left(\mathrm{e}_{\mathcal{F}o2,i}\right) - \hat{\varepsilon}_{\mathcal{G}_i} sgn\left(\mathrm{e}_{\mathcal{F}o2,i}\mathcal{U}_i\right) + p_i(t)\right] - \breve{\mathcal{C}}_{\mathcal{F}o,i}\mathrm{e}_{\mathcal{F}o2,i}^2 \\ & - \varrho\mathrm{e}_{\mathcal{F}o2,i}^2 - \mathcal{C}_{\mathcal{F}o,i}\mathrm{e}_{i,1}^2 - \sum_{i\in\{x,y,z,\phi,\theta,\psi\}} \left(\frac{\tilde{\pi}_{\mathcal{F}_i}^T \dot{\hat{\pi}}_{\mathcal{F}_i}}{\gamma_{\mathcal{F}_i}}\right) \\ & - \sum_{i\in\{x,y,z,\phi,\theta,\psi\}} \left(\frac{\tilde{\pi}_{\mathcal{G}_i}^T \dot{\hat{\pi}}_{\mathcal{G}_i}}{\gamma_{\mathcal{G}_i}}\right) - \sum_{i\in\{x,y,z,\phi,\theta,\psi\}} \left(\frac{\tilde{\varepsilon}_{\mathcal{F}_i}^T \dot{\hat{\varepsilon}}_{\mathcal{F}_i}}{\rho_{\mathcal{F}_i}}\right) \\ & - \sum_{i\in\{x,y,z,\phi,\theta,\psi\}} \left(\frac{\tilde{\varepsilon}_{\mathcal{G}_i}^T \dot{\hat{\varepsilon}}_{\mathcal{G}_i}}{\rho_{\mathcal{G}_i}}\right)\end{aligned} \tag{IV.34}$$

Substituting equations (IV.20) and (IV.21) into equation (IV.34), we achieve:

$$\begin{aligned}\dot{v}_3 = \sum_{i=\{x,y,z,\phi,\theta,\psi\}} & e_{\mathcal{F}o2,i}\left[\mathcal{E}_{\mathcal{F}_i}(t) + \mathcal{E}_{\mathcal{G}_i}(t)\mathcal{U}_i + p_i(t)\right] - \check{\mathcal{C}}_{\mathcal{F}o,i}e_{\mathcal{F}o2,i}^2 - \varrho e_{\mathcal{F}o2,i}^2 \\ & - \mathcal{C}_{\mathcal{F}o,i}e_{i,1}^2 + \sum_{i\in\{x,y,z,\phi,\theta,\psi\}}\left(\sigma_{\mathcal{F}_i}\hat{\pi}_{\mathcal{F}_i}\tilde{\pi}_{\mathcal{F}_i}^T\right) + \sum_{i\in\{x,y,z,\phi,\theta,\psi\}}\sigma_{\mathcal{G}_i}\hat{\pi}_{\mathcal{G}_i}\tilde{\pi}_{\mathcal{G}_i}^T \\ & - \sum_{i\in\{x,y,z,\phi,\theta,\psi\}}\left(\tilde{\varepsilon}_{\mathcal{G}_{io}}^T\left|e_{\mathcal{F}o2,i}\mathcal{U}_i\right| + \tilde{\varepsilon}_{\mathcal{F}_{io}}^T(e_{\mathcal{F}o2,i})\right)\end{aligned} \tag{IV.35}$$

From the adaptive laws equations.(IV.21) – (IV.21), we get:

$$\begin{aligned}\dot{v}_3 = \sum_{i=\{x,y,z,\phi,\theta,\psi\}} & e_{\mathcal{F}o2,i}\left[\mathcal{E}_{\mathcal{F}_i} + \mathcal{E}_{\mathcal{G}_i}\mathcal{U}_i + p_i(t)\right] \\ & - \sum_{i=\{x,y,z,\phi,\theta,\psi\}}\left(\check{\mathcal{C}}_{\mathcal{F}o,i}e_{\mathcal{F}o2,i}^2 + \varrho e_{\mathcal{F}o2,i}^2 + \mathcal{C}_{\mathcal{F}o,i}e_{i,1}^2\right) \\ & - \sum_{i\in\{x,y,z,\phi,\theta,\psi\}}\left(\mathcal{E}_{\mathcal{F}_{i0}}\left|e_{\mathcal{F}o2,i}\right| + \mathcal{E}_{\mathcal{G}_{i0}}\left|e_{\mathcal{F}o2,i}\mathcal{U}_i\right|\right) \\ & + \sum_{i\in\{x,y,z,\phi,\theta,\psi\}}\left(\sigma_{\mathcal{F}_i}\hat{\pi}_{\mathcal{F}_i}\tilde{\pi}_{\mathcal{F}_i}^T\right) + \sum_{i\in\{x,y,z,\phi,\theta,\psi\}}\sigma_{\mathcal{G}_i}\hat{\pi}_{\mathcal{G}_i}\tilde{\pi}_{\mathcal{G}_i}^T\end{aligned} \tag{IV.36}$$

By using the lemma1, yields:

$$\sigma_{\mathcal{F}_i}\tilde{\pi}_{\mathcal{F}_i}^T\hat{\pi}_{\mathcal{F}_i} = \sigma_{\mathcal{F}_i}\tilde{\pi}_{\mathcal{F}_i}^T\left(\bar{\bar{\pi}}_{\mathcal{F}_i} - \tilde{\pi}_{\mathcal{F}_i}\right) \leq \frac{-\sigma_{\mathcal{F}_i}}{2}\left\|\tilde{\pi}_{\mathcal{F}_i}\right\|^2 + \frac{-\sigma_{\mathcal{F}_i}}{2}\left\|\bar{\bar{\pi}}_{\mathcal{F}_i}\right\|^2 \tag{IV.37}$$

$$\sigma_{\mathcal{G}_i}\tilde{\pi}_{\mathcal{G}_i}^T\hat{\pi}_{\mathcal{G}_i} = \sigma_{\mathcal{G}_i}\tilde{\pi}_{\mathcal{G}_i}^T\left(\bar{\bar{\pi}}_{\mathcal{G}_i} - \tilde{\pi}_{\mathcal{G}_i}\right) \leq \frac{-\sigma_{\mathcal{G}_i}}{2}\left\|\tilde{\pi}_{\mathcal{G}_i}\right\|^2 + \frac{-\sigma_{\mathcal{G}_i}}{2}\left\|\bar{\bar{\pi}}_{\mathcal{G}_i}\right\|^2 \tag{IV.38}$$

$$\mathcal{E}_{\mathcal{F}_{i0}}\left|e_{\mathcal{F}o2,i}\right| = \left(\tilde{\varepsilon}_{\mathcal{F}_i}^T + \hat{\varepsilon}_{\mathcal{F}_i}\right)\left|e_{\mathcal{F}o2,i}\right| \leq \frac{\varepsilon_{\mathcal{F}_{io}}^2}{2} + \frac{e_{\mathcal{F}o2,i}^2}{2} \tag{IV.39}$$

$$\mathcal{E}_{\mathcal{G}_{i0}}\left|e_{\mathcal{F}o2,i}\right| = \left(\tilde{\varepsilon}_{\mathcal{G}_i}^T + \hat{\varepsilon}_{\mathcal{G}_i}\right)\left|e_{\mathcal{F}o2,i}\right| \leq \frac{\varepsilon_{\mathcal{G}_{io}}^2}{2} + \frac{e_{\mathcal{F}o2,i}^2}{2} \tag{IV.40}$$

By using hypothesis 3 and 5, and above inequality, equation.(IV.36) can be expressed as:

$$\begin{aligned}\dot{v}_3 \leq & -\sum_{i\in\{x,y,z,\phi,\theta,\psi\}} \mathcal{C}_{\mathcal{F}o,i}\mathrm{e}_{i,1}^2 + \left(\check{\mathcal{C}}_{\mathcal{F}o,i}+\varrho\right)\mathrm{e}_{\mathcal{F}o2,i}^2 \\ & -\sum_{i\in\{x,y,z,\phi,\theta,\psi\}}\left(\frac{\sigma_{\mathcal{F}_i}\tilde{\pi}_{\mathcal{F}_i}^T\tilde{\pi}_{\mathcal{F}_i}}{2}+\frac{\sigma_{\mathcal{G}_i}\tilde{\pi}_{\mathcal{G}_i}\tilde{\pi}_{\mathcal{G}_i}^T}{2}+\frac{\tilde{\varepsilon}_{\mathcal{F}_i}^2}{2}+\frac{\tilde{\varepsilon}_{\mathcal{G}_{io}}^2}{2}\right) \\ & +\sum_{i\in\{x,y,z,\phi,\theta,\psi\}}\left(\frac{\varepsilon_{\mathcal{F}_{io}}^2}{2}+\frac{\varepsilon_{\mathcal{G}_{io}}^2}{2}+\frac{\mathcal{L}_i^{*2}}{2}\right)\end{aligned} \tag{IV.41}$$

Define $\mathfrak{P}_i = min\{2\mathcal{C}_{\mathcal{F}o,i}, 2\left(\check{\mathcal{C}}_{\mathcal{F}o,i}+\varrho\right), \sigma_{\mathcal{F}_i}, \sigma_{\mathcal{G}_i}\}$ and $\mathfrak{D}_i = \left\{\frac{\varepsilon_{\mathcal{F}_{io}}^2}{2}+\frac{\varepsilon_{\mathcal{G}_{io}}^2}{2}+\frac{\mathcal{L}_i^{*2}}{2}\right\}$, results in equation.(IV.41), where $\mathfrak{P} = \sum_{i\in\{x,y,z,\phi,\theta,\psi\}}\mathfrak{P}_i$ and $\mathfrak{D} = \sum_{i\in\{x,y,z,\phi,\theta,\psi\}}\mathfrak{D}_i$.

$$\dot{v}_3 \leq -\mathfrak{P}v_3 + \mathfrak{D} \tag{IV.42}$$

And integrating equation.(IV.42) in $[0, t]$, we can achieve:

$$0 \leq v_3(t) \leq v_3(0)e^{-\mathfrak{P}t} + \frac{\mathfrak{D}}{\mathfrak{P}} \tag{IV.43}$$

From equation.(IV.43), it can be shown that the signals $\mathrm{e}_{i,1}, \mathrm{e}_{\mathcal{F}o2,i}, \hat{\pi}_{\mathcal{F}_i}, \hat{\pi}_{\mathcal{G}_i}, \hat{\varepsilon}_{\mathcal{F}_i}, \hat{\varepsilon}_{\mathcal{G}_i}$ and $\mathcal{U}_{NN\mathcal{F}OBC,i}$ are bounded. Moreover, from equations.(IV.21) and (IV.25) we can write:

$$\left\|\mathrm{e}_{i,1}\right\| \leq \sqrt{2\left(v_3(0)e^{-\mathfrak{P}t}+\frac{\mathfrak{D}}{\mathfrak{P}}\right)} \tag{IV.44}$$

$$\left\|\mathrm{e}_{\mathcal{F}o2,i}\right\| \leq \sqrt{2\left(v_3(0)e^{-\mathfrak{P}t}+\frac{\mathfrak{D}}{\mathfrak{P}}\right)} \tag{IV.45}$$

where $\mathrm{e}_{i,1}, \mathrm{e}_{\mathcal{F}o2,i}$ values can be decreased as near to zero as possible by considering suitably the design parameters $\mathcal{C}_{\mathcal{F}o,i}, \check{\mathcal{C}}_{\mathcal{F}o,i}, \varrho, \sigma_{\mathcal{F}_i}, \sigma_{\mathcal{G}_i}, \gamma_{\mathcal{F}_i}, \gamma_{\mathcal{G}_i}$.

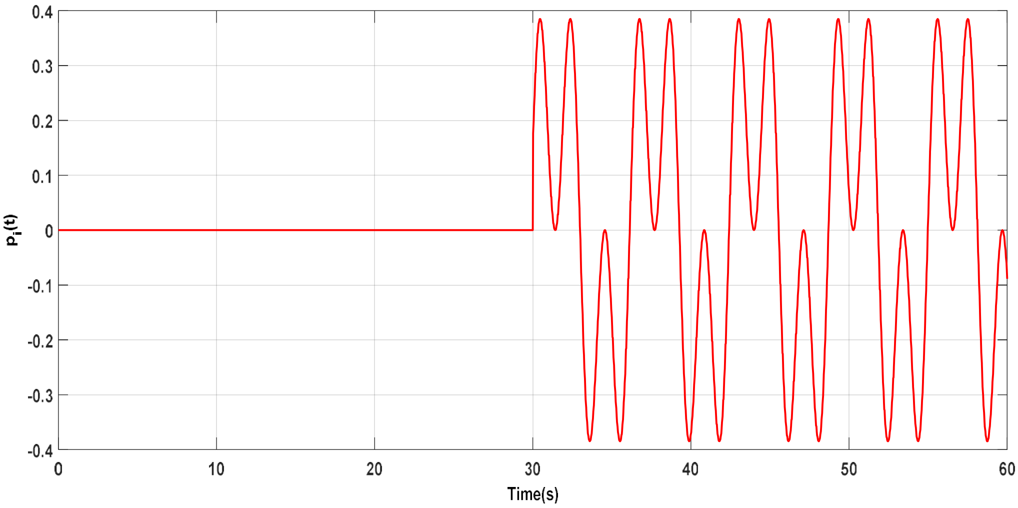

Figure IV.3 External force function.

Table IV.1. Control gains.

Controllers	x, y	z	ϕ, θ	ψ
BC	$c_i = 0.01$ $\check{c}_i = 0.02$	$c_i = 0.01$ $\check{c}_i = 0.02$	$c_i = 0.1$ $\check{c}_i = 0.3$	$c_i = 0.2$ $\check{c}_i = 0.4$
FOBC	$c_{\mathcal{F}o,i} = 1.5$ $\check{c}_{\mathcal{F}o,i} = 4$ $\eta_{1,i} = 4.5$ $\eta_{2,i} = 3.5$	$c_{\mathcal{F}o,i} = 2.5$ $\check{c}_{\mathcal{F}o,i} = 3.5$ $\eta_{1,i} = 4.6$ $\eta_{2,i} = 5.2$	$c_{\mathcal{F}o,i} = 5$ $\check{c}_{\mathcal{F}o,i} = 5.5$ $\eta_{1,i} = 4.7$ $\eta_{2,i} = 4.6$	$c_{\mathcal{F}o,i} = 6$ $\check{c}_{\mathcal{F}o,i} = 5.5$ $\eta_{1,i} = 1.5$ $\eta_{2,i} = 1.5$
NNBC	$c_i = 0.05$ $\check{c}_i = 0.02$	$c_i = 0.01$ $\check{c}_i = 0.09$	$c_i = 0.07$ $\check{c}_i = 0.09$	$c_i = 0.1$ $\check{c}_i = 0.09$
NNFOBC	$c_{\mathcal{F}o,i} = 1.5$ $\check{c}_{\mathcal{F}o,i} = 4$ $\eta_{1,i} = 4.5$ $\eta_{2,i} = 3.5$	$c_{\mathcal{F}o,i} = 1.5$ $\check{c}_{\mathcal{F}o,i} = 4$ $\eta_{1,i} = 4.5$ $\eta_{2,i} = 3.5$	$c_{\mathcal{F}o,i} = 1.5$ $\check{c}_{\mathcal{F}o,i} = 4$ $\eta_{1,i} = 4.5$ $\eta_{2,i} = 3.5$	$c_{\mathcal{F}o,i} = 1.5$ $\check{c}_{\mathcal{F}o,i} = 4$ $\eta_{1,i} = 4.5$ $\eta_{2,i} = 3.5$

IV.6 Numerical results

In this part, using two different cases. To investigate the robustness and effectiveness of the proposed control, the performance of the tracking control problem have been verified, where the developed controller (NNFOBC) is compared with the classical BC and fractional-order backstepping (FOBC). The disturbances and parameter uncertainties have been considered to prove the robustness of the developed control strategy. The disturbances $p(t)$

are shown in Fig. (IV.3), the disturbances used in two cases are the same are applied at t > 30 sec. For the condition of parameter uncertainties, 50% uncertainty are used for moment coefficients I_x, I_y, I_z. The RBFNN employs (2,5,1) neurons at the input, hidden and output layers. Where the $c_{\Pi i,j}$ is spaced uniformly in the interval $[-3\ 3]$ and the width $b_{\Pi i,j} = 1$. Those of FOBC $q = 0.3, r = 0.1$.The proposed NNFOBC parameters and FOBC, BC are listed in Table (IV.1). These parameters were selected by trial-and error processes to realize optimal performances for two different cases. We employed a three-order approximation for the FO procedure. Furthermore, in the experiment, we implemented a three order approximation for the FO operation. In addition, the root-mean-square error (RMSE) criterion can be defined mathematically as : $\mathcal{I}_i = \sqrt{\sum_{j=1}^{N}(y_i^d - y_i)^2/N}$, with N is the sampling time size and $i \in \{x, y, z, \phi, \theta, \psi\}$, where RMSE for the position subsystems is chosen as $\text{RMSE}_{POSITION} = \sum_{i\in\{x,y,z\}} \mathcal{I}_i$, and the RMSE for the rotation subsystems is selected as $\text{RMSE}_{rotation} = \sum_{i\in\{\phi,\theta,\psi\}} \mathcal{I}_i$

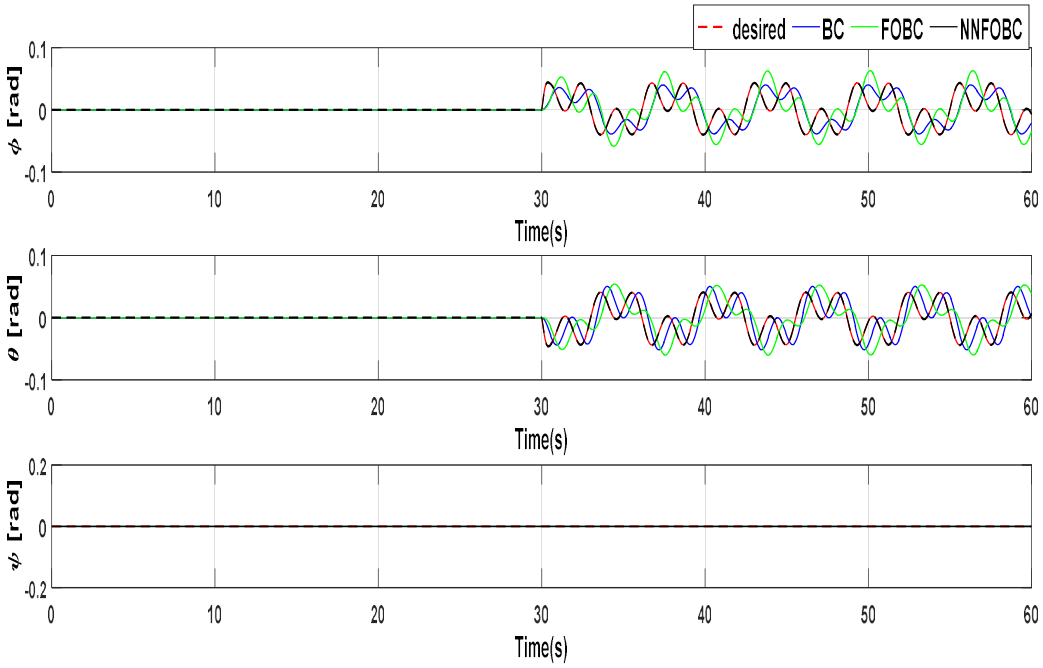

Figure IV.4. Quadrotor attitude response controlled with BC, FOBC and NNFOBC (Case 1).

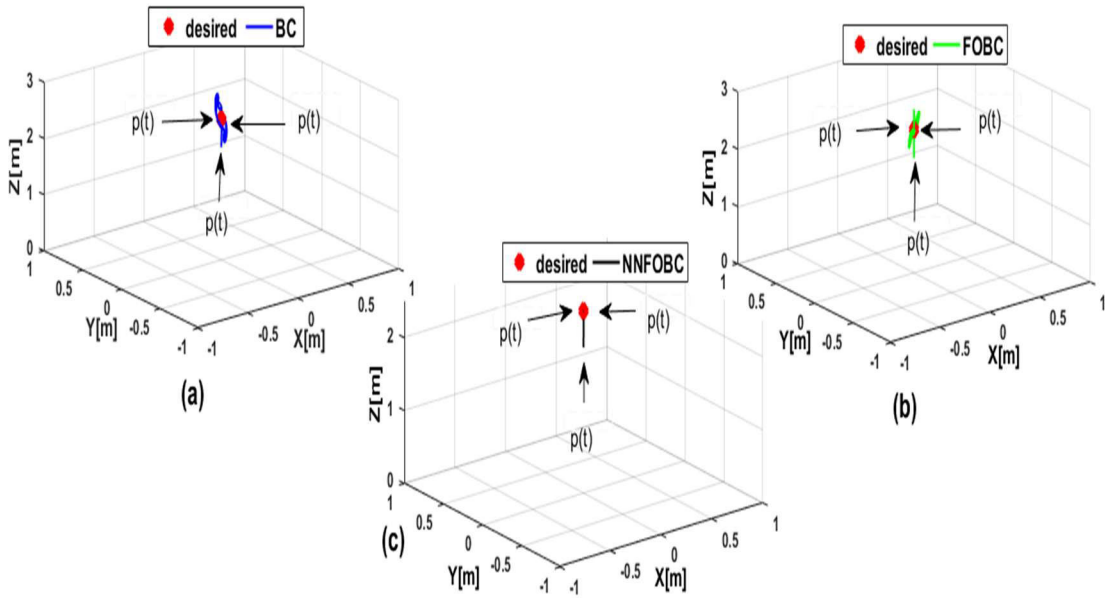

Figure IV.5. 3D space for the quadrotor with BC (a), FOBC (b), NNFOBC (c) against external forces (Case 1).

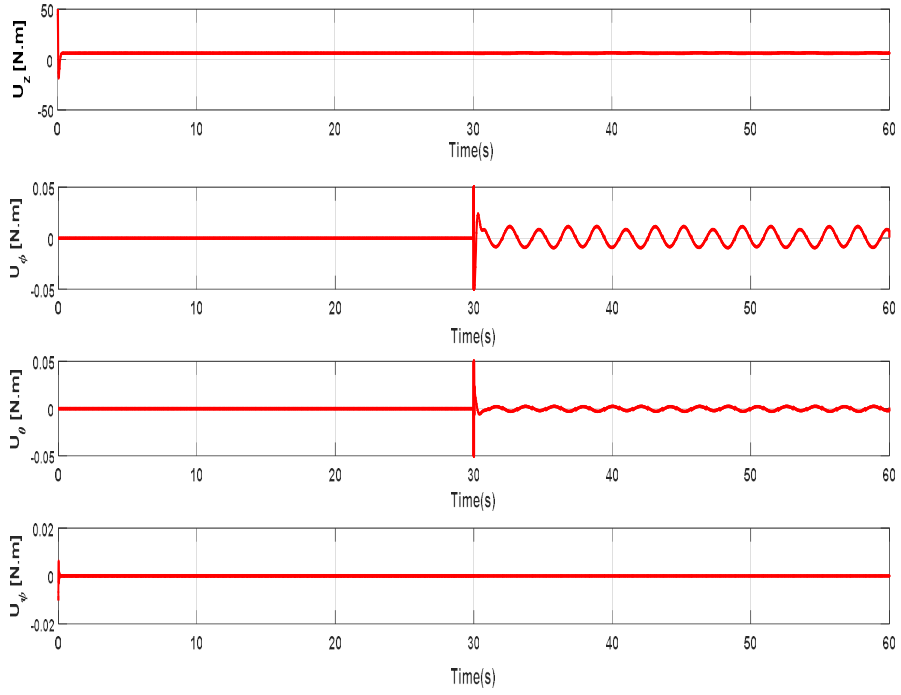

Figure IV.6. Control input of NNFOBC (Case 1).

Case 1: Stability performances under external forces

This case investigates the quadrotor system stability under external disturbances.The wind disturbance is considered in the form of multiplication of three sine waves with different frequencies. The chosen trajectory is outlined.The desired trajectory is defined as: $y_x^d = 0m$,

$y_y^d = 0m$, $y_z^d = 2.5m$, $y_\psi^d = 0rad$. The initial conditions (position,rotation,position velocity,rotation velocity)of the quadrotor is set to be :

$$\begin{cases} x_0 = 0m & y_0 = 0m & z_0 = 2m \\ \phi_0 = 0rad & \theta_0 = 0rad & \psi_0 = 0rad \\ \dot{x}_0 = 0m/s & \dot{y}_0 = 0m/s & \dot{z}_0 = 0m/s \\ \dot{\phi}_0 = 0rad/s & \dot{\theta}_0 = 0rad/s & \dot{\psi}_0 = 0rad/s \end{cases}$$

This case aims stabilizing the quadrotor at a definite chosen attitude, so that the quadrotor be able to fly at a fixed point. The responses of the angles attitude with three controllers BC, FOBC and NNFOBC is presented in figure. **(**IV.4**)**.The numerical outcomes for QUAV stabilization in 3D are showed in Figure **(**IV.6). From figure s **(**IV.6**)** and(IV.5), the BC and FOBC are powerless to stabilize the quadrotor successfully under external forces. Whereas, the proposed controller (NNFOBC) strongly handles external disturbances and maintains flight capability and neglecting tracking errors. Figure. (IV.6) shows the input signals. It is shown that the input signal has a smooth variation.

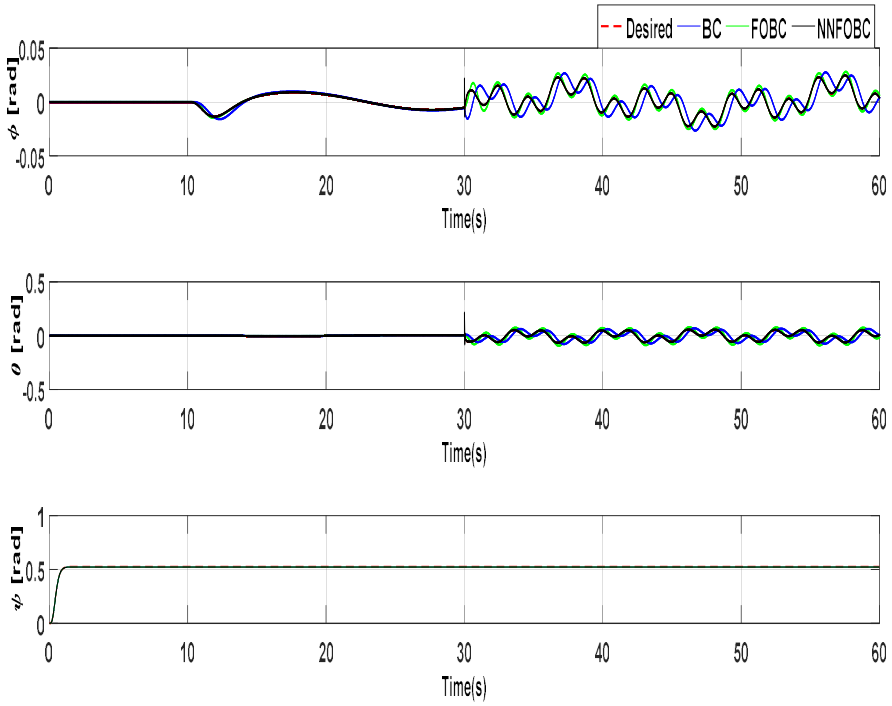

Figure IV.7. Quadrotor attitude response controlled by BC,FOBC and NNFOBC (Case 2).

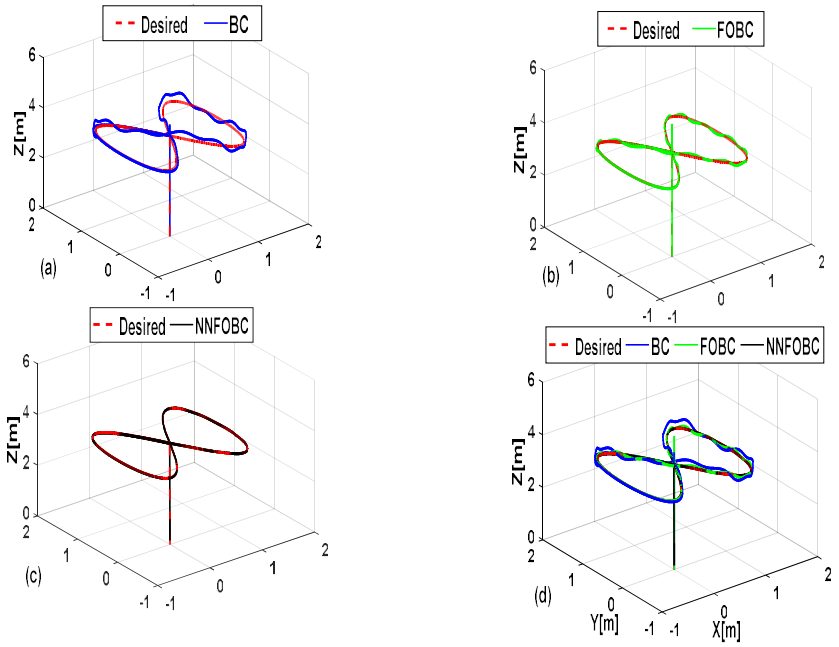

Figure IV.8. **3**D space with BC (a), FOBC (b) and NNFOBC (c) controllers and comparison between them (d) with external forces (Case 2).

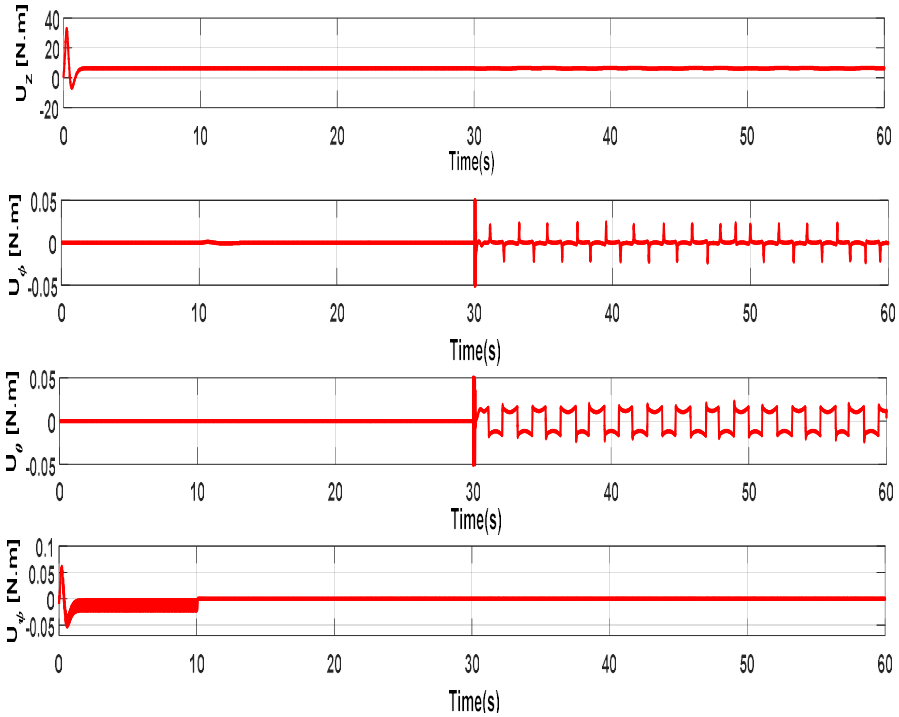

Figure IV.9. Control inputs of NNFOBC (Case 2).

Case2: trajectory tracking performances against external disturbances

This scenario shows the ability of the quadrotor to follow the designed trajectory and its robustness against wind disturbances which are imposed on the quadrotor at $t > 30s$. The desired trajectory 8-shape trajectory with altitude $y_z^d = 4m$, $y_\psi^d = 0.5rad$ is generated using the following command:

$$y_x^d = \begin{cases} 0m, t < 10s \\ \cos\left(\frac{\pi}{20} * t\right) m, 10s \leq t < 60s \end{cases} , \; y_y^d = \begin{cases} 0m, t < 10s \\ -\sin\left(\frac{2\pi}{20} * t\right) m, 10s \leq t < 60s \end{cases}$$

The initial conditions (position,rotation,position velocity,rotation velocity) of the quadrotor

are:
$$\begin{cases} x_0 = 0m & y_0 = 0m & z_0 = 2m \\ \phi_0 = 0rad & \theta_0 = 0rad & \psi_0 = 0rad \\ \dot{x}_0 = 0m/s & \dot{y}_0 = 0m/s & \dot{z}_0 = 0m/s \\ \dot{\phi}_0 = 0rad/s & \dot{\theta}_0 = 0rad/s & \dot{\psi}_0 = 0rad/s \end{cases}$$

Figures (IV.7) and (IV.8**)** present the attitude angles response and The 8-shape trajectory tracking 3D, respectively. It is observed that the proposed NNFOBC control and the comparative BC and FOBC control the attitude angles converge to their references but severe deviations are noticeable under external disturbances with the control BC we observe the most deviation on the reference path than the FOBC control. But the NNFOBC can provide a better performance. It is demonstrated that NNFOBC capable to deal successfully against external disturbances and providing significant tracking performance.

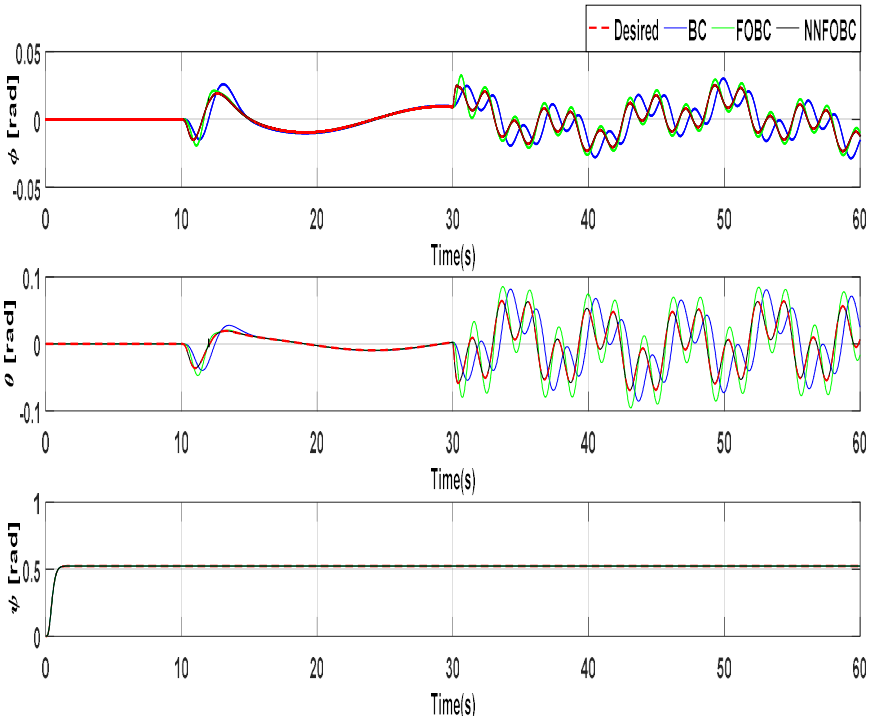

Figure IV.10. Quadrotor attitude response controlled performed by BC, FOBC and NNFOBC (Case3)

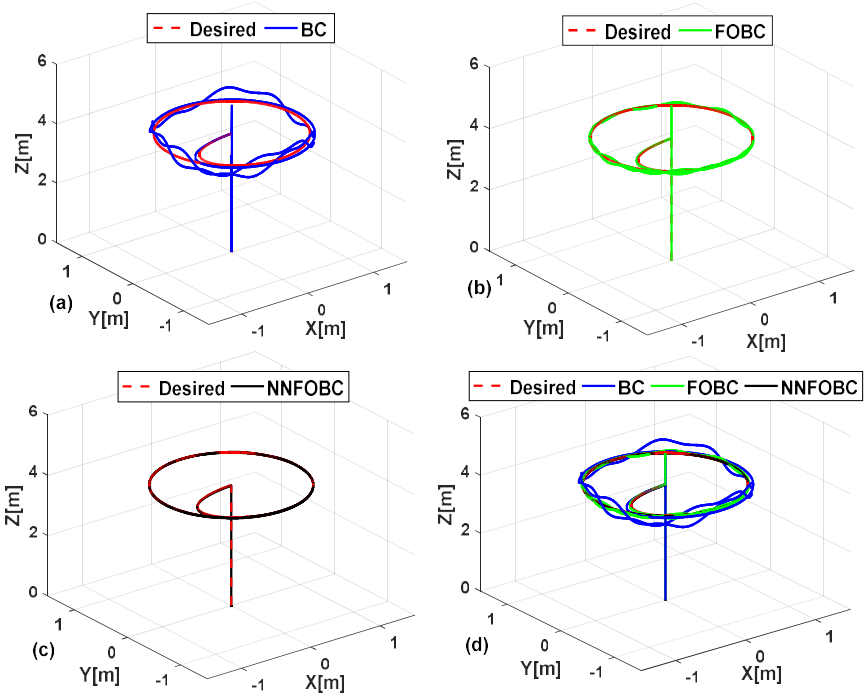

Figure IV.11. 3D space with BC (a) ,FOBC (b) and NNFOBC (c) controllers and comparison between them (d) with external disturbances and uncertainties of the inertia(Case 3).

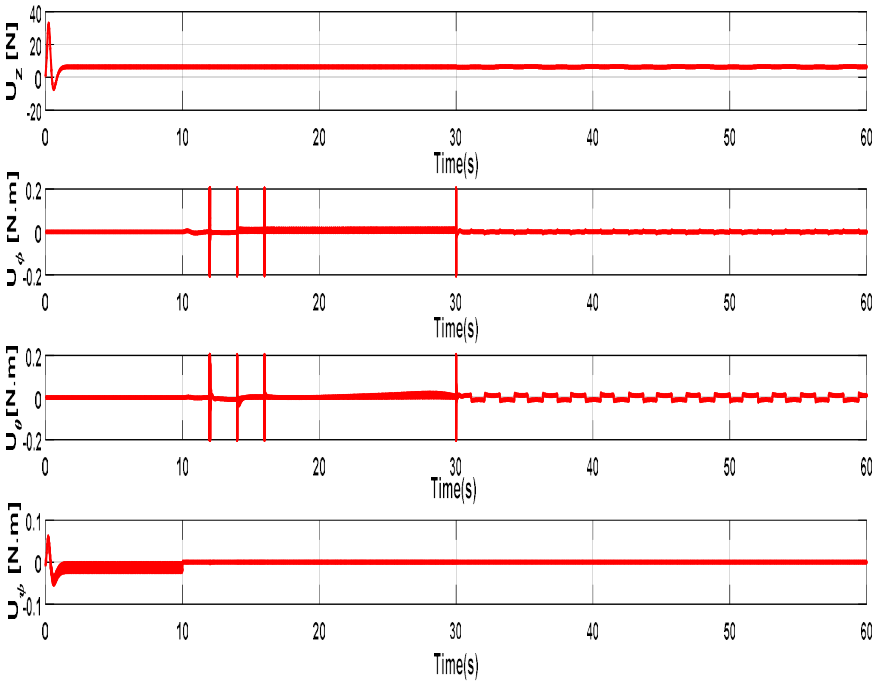

Figure IV.12. Control inputs of NNFBC (Case 3)

Case 3: trajectory tracking performances with external disturbances and uncertainties of the inertia.

The QUAV is supposed in hovering case and tracking space circle trajectory on 3D.The considered space circle trajectory is specified as:

$$y_x^d = \begin{cases} 0m, t < 10s \\ \cos\left(\frac{\pi}{10} * t\right) m, 10s \leq t < 60s \end{cases}, y_y^d = \begin{cases} 0m, t < 10s \\ \sin\left(\frac{\pi}{10} * t\right) m, 10s \leq t < 60s \end{cases}$$

For the studied quadrotor, the positions and angles values initially set to zero. We summarize the inertias uncertainties adopted to confirm the robustness of the designed control approach as $\Delta I_x = 0.5 I_x$, $\Delta I_y = 0.5 I_y$ and $\Delta I_z = 0.5 I_z$ applied at different times at $t \geq 12s$, $t \geq 14s$, $t \geq 16s$ for I_x, I_y, I_z, respectively. The achieved outcomes are represented in figures **(**IV.10), (IV.11**)** and (IV.12).Figure (IV.10) shows the attitude angles response when the parametric variations are introduced. Whereas, we observe that the NNFOBC provided the best converge with the reference trajectories compared to the BC and FOBC techniques. Figure (IV.12) shows the quadrotor position and orientation over its flight in 3D, from which the controller showed a remarkable immunization over parameters change, such as, the closed

loop dynamics stability that proves the designed control approach robustness. From figure IV.12, it is clearly, the inputs signal illustrates a smooth variation.

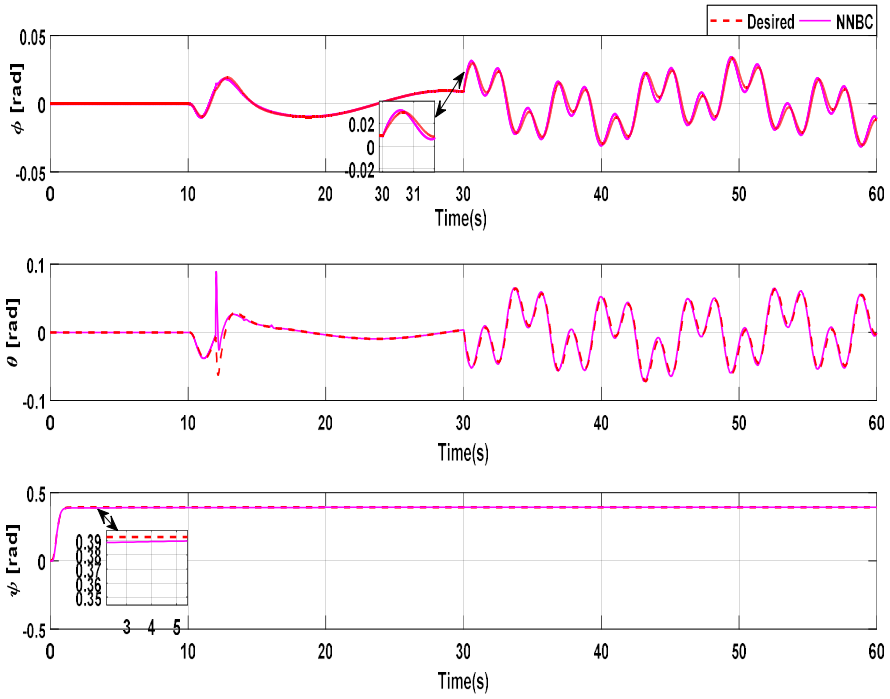

Figure IV.13. Quadrotor attitude response controlled performed by NNFOBC (Case4).

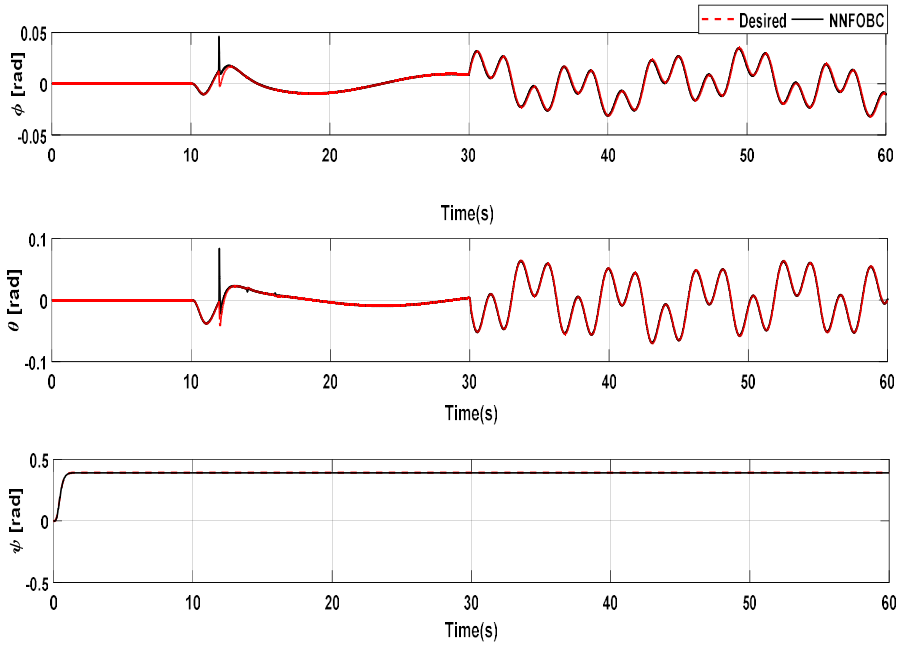

Figure IV.14. Quadrotor attitude response controlled performed by NNFOBC (Case4).

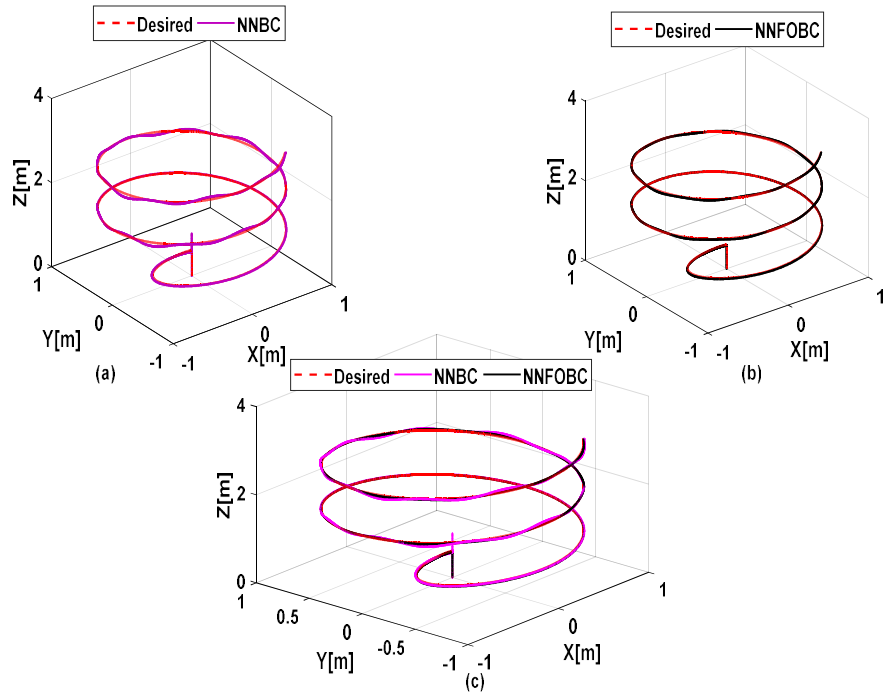

Figure IV.15. 3D space with NNBC (a) , NNFOBC (b) controllers and comparison between them (c) with external disturbances and uncertainties of the inertia (Case 4)

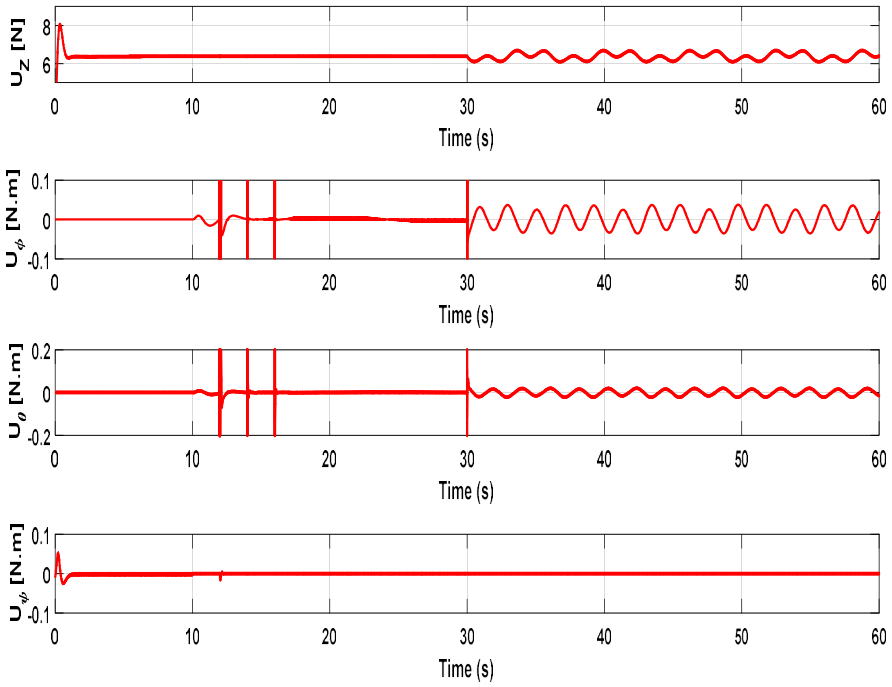

Figure IV.16. Control inputs of NNFOBC (Case 4).

Case 4. Comparison study (NNFOBC-NNBC) with external disturbances and uncertainties of the inertia.

For further verifying the proposed NNFOBC performances, a comparison with the classical adaptive neural network backstepping (NNBC) are conducted. Where, the NNBC combining a (RBFNN) approximator and classical BC. The desired trajectory of the quadrotor is made as: $y_z^d = 0.05(t+2)m$, $y_\psi^d = 0.4rad$

$$y_x^d = \begin{cases} 0m, t < 10s \\ \cos\left(\frac{\pi}{10} * t\right) m, 10s \leq t < 60s \end{cases} \quad y_y^d = \begin{cases} 0m, t < 10s \\ \sin\left(\frac{\pi}{10} * t\right) m, 10s \leq t < 60s \end{cases}$$

The initial position and rotation values of the quadrotor all through this simulation are the same adopted in case 3. Figure (IV.13– IV.16) shows the simulation results for this case. Figures (IV.14) shows how the quadrotor's attitude changes during the simulation. The trajectory tracking performance in 3D space is shown in figure (IV.15), where the position of the quadrotor response is depicted. The transients of the control inputs are shown in figure (IV.16) which illustrates the smooth control signals.

We discover that NNFOBC has the quickest dynamic reaction overall performance and maximum position tracking precision over the disturbances and inertial uncertainties, these last are the same than case 3. Therefore, it is verified that the NNFOBC outperforms the NNBC. Additionally, FO calculations are used to add flexibility in tuning parameters and advance control performance. In short, the application of NNFOBC to quadrotor system is effective and feasible, it possesses the highest position tracking accuracy and the fastest dynamic performance compared with the other three controllers (BC, FOBC, NNBC).

Moreover, it can be further concluded that the introduction of FO calculus can make the performance better. From the preceding figures it is not possible to see the differences between the controllers. For further investigation of the designed controller's performances and get a closer sight on the profound characteristics, RMSE and the maximum absolute values of the tracking errors (MaxAE) were calculated for these cases. Table (IV.2) presents RMS and MaxAE results for BC, FOBC, NNBC and the proposed NNFOBC.

Table IV.2. RMSE and MaxAE values of BC, FOBC, NNBC and the proposed NNFOBC.

Controllers	Subsystem	RMSE				MaxAE			
		case 1	case 2	case 3	case4	case 1	case 2	case 3	case 4
BC	Rotation(rad) Position(m)	0.0520 0.4277	0.006 0.542	0.0192 0.346	/	0.111 0.9036	0.0231 0.855	0.041 0.834	/
FOBC	Rotation(rad) Position(m)	0.0035 0.369	0.0014 0.507	0.20 0.0038	/	0.0092 0.118	0.007 0.638	0.009 0.817	/
NNBC	Rotation (rad) Position(m)	/	/	/	0.018 0.02	/	/	/	0.007 0.615
NNFOBC	Rotation (rad) Position(m)	0.0043 0.081	2.98×10^{-4} 0.0164	1.85×10^{-4} 0.0164	2×10^{-4} 0.024	0.0044 0.0164	0.0114 0.1167	8.65×10^{-4} 0.5094	9×10^{-4} 0.7094

IV.7 Conclusion

In this chapter, we confirmed the efficiency of the developed NNFOBC to surmount the problems in unknown nonlinear dynamics, parametric uncertainty and external disturbances for QUAV model. We considered a classical BC to control the quadrotor then we suggested a FOBC, which based on a FO stabilizing function to produce the suitable control signal, which leads to better response speed and decreases steady-state error. We designed a NNFOBC to deal with unknown system. As a final point, according the Lyapunov stability hypothesis, we derived an adaptive estimation laws for the NNFOBC. The performance evaluation of the proposed NNFOBC illustrated the robustness under parametric uncertainties, unknown system and external disturbances.

Conclusion and Future Work

Conclusion

Because of their exceptional battle capability in distant area even in critical environment, QUAVs have been widely adopted in various fields. Nevertheless, due to the complexity of QUAV structures, modeling error among the adopted perfect model might occur, leading to system uncertainties in QUAV systems. Otherwise, as the flight setting of QUAVs is continuously varying, the consistency of the flight control systems is at risk to external disturbances. System uncertainties and external disturbances will not solely decrease the flight control performance of the QUAV system but could be unstable and unsafe and subsequently dangerous. Besides, backstepping and sliding mode control with their related control techniques are more appropriate designs to control the quadcopter system. Hence, the study of the high order sliding mode control techniques with efficient robustness to uncertainties and external disturbances on the flight QUAV control performances is mandatory to get better the tracking performance that becoming the main issue to be adopted in the investigation of hover control methods for quadrotor system. The uncertainties and external disturbances are considered, and the variation of drag coefficient problems is less taken in the conventional scheme of flight control schemes for QUAV system. As a solution, using the fractional calculus and sliding mode control or backstepping approaches guiding to enhance the rapidity of the response and increase the convergence of states. Thus, a robust fractional order control among the key solutions for investigate on advanced approaches of flight control of QUAV systems, robust fractional-order control is also one of the main solutions to deal with such disturbance but the problem is its difficulty to use in the design of QUAVs control techniques.

In this thesis, external disturbances, QUAV system uncertainties and unknown nonlinear dynamics are taken into account to propose a robust flight control techniques. Below we resume the main contributions an research results:

1. This thesis explores histories and the motivation of QUAVs control, such as the literatures of recent investigations of current control approaches, adaptive control techniques, and the control using fractional-order theories.

2. A model of six degrees of freedom rigid body is considered by the use of the Newton-Euler theory. Next, the key moments and forces performing on QUAVs are adopted. Moreover, the wind effect was investigated and included into the main multi–rotor model. The outcoming equations are nonlinear which complicate the direct application of the synthesis of control and estimation algorithms. To defeat this difficulty, a number of simplifications were used to advance reasonably simple control laws for application purposes. Generally, the QUAV system is expressed in state space outline to demonstrate the controls and wind effects. Considering, this state space version, the control laws and algorithm evaluation are calculated.
3. The advance of an intelligent adaptive control approach which divided into two different parts: the attitude subsystem control. Firstly, the adaptive Fuzzy- neural network (FNN) is considered to approximate unknown dynamic functions for every subsystem that that constitute the system. Secondly, this approximation to be used with a backstepping procedure to carry out the desired. Furthermore, the developed controller can rapidly and perfectly follow the quadrotor path, the asymptotic of the closed-loop system stability is guaranteed. This nonlinear approach ensured the tracking errors convergence.
4. Designing a new controller, a combination of the nonlinear function approximation capability of fuzzy system and Chebyshev network are introduced at the same time in sliding mode continuous controller to design a robust adaptive control scheme.For eliminating the chattering effect of classical SMC technique, second order sliding mode(SOSMC) control is applied as well to deal with the approximation error, parameters uncertainties and external disturbances. Finally, the simulation results demonstrate that the approaches cover an extremely high resistance to perturbations.
5. The tracking control approach named NNFOBC based fractional order (FO) backstepping controller (BC) and neural networks (NNs) for QUAV is proposed . NNFOBC will lead to a strong robustness and high tracking accuracy. FO backstepping controller (FOBC) is employed to decrease uncertainties and disturbances effect. Adaptive RBFNN approximator of unknown dynamics and a local robust control term are incorporated to ensure a robust tracking convergence. NNFOBC be able to successfully improve the control performance

of the classical BC. it doesn't require perfect mathematical system dynamics information.The method is able to maintain best performance of the QUAV even in the presence of unknown dynamics, parametric uncertainties and external disturbance.

6. Lastly, results show proved the efficacy of the proposed approachs in comparison with some robust techniques. Where the method is able to maintain best performance of the QUAV even in the presence of unknown dynamics, parametric uncertainties and external disturbance.

Future research prospect

In this work, the developed flight control of a QUAV has been investigated, by focusing on the control problem of a dynamics model of a QUAV over parametric uncertainties, external disturbances and the unknown dynamics problem, , and various research results have been carried out. Though, because the time and capacity constraints, it is remain a lot to be explored and mastered in the advanced finite time flight control system of quadrotors:

1. Regarding the multirotor model, the formulation of the candidate model to be further enriched with the addition of a number of fundamental ignored terms that are not tested or validated in this study. Otherwise, the four motors that drive the quadcopter have a number of differences due to the manufacturing procedure.
2. Every approaches advanced in this thesis have been confirmed by simulation results. Hence, an experimental confirmation should be carried out to validate the simulation results.
3. In addition, as prospect work, fault diagnosis and fault tolerant control algorithm of multi–rotor systems for quadrotor with actuator fault to be investigated and designed. The idea is when faults happen in the actuator of multi-rotor, a nonlinear observer based on RBFNN or another controller that will be designed to assess the fault information. Once the fault information is achieved, an adaptive controller is considered to control the quadrotor to attain the preferred path.

Bibliography

Bibliography

[1] Bailey, Mark Willis. Unmanned aerial vehicle path planning and image processing for orthoimagery and digital surface model generation. Diss. 2012. https://etd.library.vanderbilt.edu/etd-11302012-151303.

[2] A. Azzam and Xinhua Wang. Quad rotor arial robot dynamic modeling and configuration stabilization. In Informatics in Control, Automation and Robotics (CAR), 2010 2nd International Asia Conference on, volume 1, pages 438–444, 2010. https://doi.org/10.1109/car.2010.5456804.

[3] Schwing, Richard P. Unmanned aerial vehicles-Revolutionary tools in war and peace. ARMY WAR COLL CARLISLE BARRACKS PA, 2007. https://apps.dtic.mil/sti/pdfs/ADA469608.pdf

[4] Wilson, J. R. "UAV worldwide roundup 2009." Aerospace America 47.4 (2009): 3036.

[5] Timothy H Cox, Christopher J Nagy, Mark A Skoog, Ivan A Somers, and R Warner. Civil UAV capability assessment. NASA, Tech. Rep., draft Version, 2004. https://www.nasa.gov/centers/dryden/pdf/111760main_UAV_Assessment_Report_Overview.pdf.

[6] Carrillo, Luis Rodolfo García, et al. Quad rotorcraft control: vision-based hovering and navigation. Springer Science & Business Media, 2012.

[7] Morcego, Bernardo. “Coaxial UAV Helicopter Control Laboratory Design.” 2012 20th Mediterranean Conference on Control & Automation (MED), July 2012. https://doi.org/10.1109/med.2012.6265866.

[8] L. R. G. Carrillo, A. E. D. López, R. Lozano, and C. Pégard, Quad rotorcraft control: vision-based hovering and navigation. Springer Science & Business Media, 2012.

[9] Drouot, Adrien. « Stratégies de commande pour la navigation autonome d'un drone projectile miniature ». Université de Lorraine. 2013. https://theses.hal.science/file/index/docid/921953/filename/These-Adrien-Drouot-2013.pdf

[10] Hou, Hongning, Jian Zhuang, Hu Xia, Guanwei Wang, and Dehong Yu. "A Simple Controller of Minisize Quad-Rotor Vehicle." 2010 IEEE International Conference on Mechatronics and Automation, August 2010. https://doi.org/10.1109/icma.2010.5588802.

[11] S. Bouabdallah, A. Noth, and R. Siegwart. PID vs LQ control techniques applied to an indoor micro quadrotor. In Intelligent Robots and Systems, 2004. (IROS 2004). Proceedings. 2004 IEEE/RSJ International Conference on, volume 3, pages 2451–2456 vol.3, 2004. https://doi.org/10.1109/iros.2004.1389776

[12] V. Mistler, A. Benallegue, and N.K. M'Sirdi. Exact linearization and noninteracting control of a 4 rotors helicopter via dynamic feedback. In Robot and Human Interactive Communication, 2001. Proceedings. 10th IEEE International Workshop on, pages 586–593, 2001. https://doi.org/10.1109/roman.2001.981968.

[13] AHMED, Ahmed Hassan, OUDA, Ahmed Nasr, KAMEL, Ahmed Mohsen, et al. Attitude stabilization and altitude control of quadrotor. In : 2016 12th International Computer Engineering Conference (ICENCO). IEEE, 2016. p. 123-130. https://doi.org/10.1109/icenco.2016.7856456

[14] Jun Li and Yuntang Li. Dynamic analysis and PID control for a quadrotor. In Mechatronics and Automation (ICMA), 2011 International Conference on, pages 573–578, 2011. https://doi.org/10.1109/icma.2011.5985724.

[15] S. Bouabdallah and R. Siegwart. Backstepping and sliding-mode techniques applied to an indoor micro quadrotor. In Robotics and Automation, 2005. ICRA 2005. Proceedings of the 2005 IEEE International Conference on, pages 2247– 2252, 2005. https://doi.org/10.1109/robot.2005.1570447.

[16] Samir Bouabdallah. Design and control of quadrotors with application to autonomous flying. Phd. thesis, Ecole Polytechnique Federale de Lausanne, 2007. https://doi.org/10.5075/epfl-thesis-3727

Bibliography

[17] Kendoul, Farid. "Survey of advances in guidance, navigation, and control of unmanned rotorcraft systems." Journal of Field Robotics 29.2 (2012): 315–378. https://doi.org/10.1002/rob.20414.

[18] Jinpeng Yang, Zhihao Cai, Qing Lin, and Yingxun Wang. Self-tuning pid control design for quadrotor uav based on adaptive pole placement control. In Chinese Automation Congress (CAC), 2013, pages 233–237. IEEE, 2013. https://doi.org/10.1109/cac.2013.6775734.

[19] Raffo, Guilherme V., Manuel G. Ortega, and Francisco R. Rubio. "An integral predictive/nonlinear H^{∞} control structure for a quadrotor helicopter." Automatica 46.1 (2010): 29-39. https://doi.org/10.1016/j.automatica.2009.10.018.

[20] Waslander, S.L., G.M. Hoffmann, Jung Soon Jang, and C.J. Tomlin. “Multi-Agent Quadrotor Testbed Control Design: Integral Sliding Mode vs. Reinforcement Learning.” 2005 IEEE/RSJ International Conference on Intelligent Robots and Systems, 2005. https://doi.org/10.1109/iros.2005.1545025.

[21] Madani, Tarek, and Abdelaziz Benallegue. “Backstepping Control for a Quadrotor Helicopter.” 2006 IEEE/RSJ International Conference on Intelligent Robots and Systems, October 2006. https://doi.org/10.1109/iros.2006.282433.

[22] Fang, Zheng, Weinan Gao, and Lei Zhang. "Robust adaptive integral backstepping control of a 3-DOF helicopter." International Journal of Advanced Robotic Systems, 9(3) (2012): 79. https://doi.org/10.5772/50864.

[23] Lee, Hyeonbeom, Suseong Kim, Tyler Ryan, and H. Jin Kim. “Backstepping Control on SE(3) of a Micro Quadrotor for Stable Trajectory Tracking.” 2013 IEEE International Conference on Systems, Man, and Cybernetics, October 2013. https://doi.org/10.1109/smc.2013.769.

[24] Hongtao Zhen, Xiaohui Qi, and Hairui Dong. An adaptive block backstepping controller for attitude stabilization of a quadrotor helicopter. WSEAS Transactions on Systems & Control, 8(2), 2013. http://www.wseas.us/journal/pdf/control/2013/56-421.pdf.

[25] Ivan Gonzalez, Sergio Salazar, and Rogelio Lozano. Chattering-free sliding mode altitude control for a quad-rotor aircraft: Real-time application. Journal of Intelligent & Robotic Systems, 73(1-4):137–155, 2014. https://doi.org/10.1007/s10846-013-9913-8.

[26] Younes Al Younes et al. “Quadrotor position Control using cascaded adaptive integral backstepping controllers”. In: Applied Mechanics and Materials. Vol. 565. Trans Tech Publ. 2014.https://doi.org/10.4028/www.scientific.net/AMM.565.98

[27] Mostafa Mohammadi and Alireza Mohammad Shahri. “Adaptive nonlinear stabilization control for a quadrotor UAV: Theory, simulation and experimentation”. In: Journal of Intelligent & Robotic Systems 72.1 (2013), https://doi.org/10.1007/s10846-013-9813-y.

[28]Jing-Jing Xiong and En-Hui Zheng. “Position and attitude tracking controlfor a quadrotor UAV”. In: ISA transactions 53.3 (2014), https://doi.org/10.1016/j.isatra.2014.01.004.

[29] ZERARI, Nassira, CHEMACHEMA, Mohamed, et ESSOUNBOULI, Najib. Neural network based adaptive tracking control for a class of pure feedback nonlinear systems with input saturation. IEEE/CAA Journal of Automatica Sinica, 2018, vol. 6, no 1, https://doi.org/ 10.1109/JAS.2018.7511255.

[30] Labbadi, Moussa, Yassine Boukal, and Mohamed Cherkaoui. Advanced Robust Nonlinear Control Approaches for Quadrotor Unmanned Aerial Vehicle: Roadmap to Improve Tracking-Trajectory Performance in the Presence of External Disturbances. Vol. 384. Springer Nature, 2021. https://doi.org/10.1007/978-3-030-81014-6.

[31] Mellinger, Daniel, Nathan Michael, and Vijay Kumar. "Trajectory generation and control for precise aggressive maneuvers with quadrotors." The International Journal of Robotics Research 31.5 (2012): 664–674. https://doi.org/10.1177/0278364911434236.

[32] Prayitno, Agung, Veronica Indrawati, and Gabriel Utomo. "Trajectory tracking of AR. Drone quadrotor using fuzzy logic controller." TELKOMNIKA (Telecommunication Computing Electronics and Control) 12.4 (2014): 819–828. https://doi.org/10.12928/telkomnika.v12i4.368.

[33] Hussein, Amir, and Rayyan Abdallah. "Autopilot Design for a Quadcopter. " Khartoum: University Of Khartoum (2017). https://www.researchgate.net/publication/331298873_Autopilot_Design_for_a_Qu adcopter.

[34] Nagaty, Amr, et al. "Control and navigation framework for quadrotor helicopters." Journal of intelligent & robotic systems 70 (2013): 1–12. https://doi.org/10.1007/s10846-012-9789-z.

[35] Derafa, L., T. Madani, and A. Benallegue. “Dynamic Modelling and Experimental Identification of Four Rotors Helicopter Parameters.” 2006 IEEE International Conference on Industrial Technology, (2006). 1834–1839. https://doi.org/10.1109/icit.2006.372515.

[36] Li, Zhi, Xin Ma, and Yibin Li. " Robust tracking control strategy for a quadrotor using RPD – SMC and RISE." Neurocomputing 331.(2019), 312–322. https://doi.org/10.1016/j.neucom.2018.11.070.

[37] García, R.A., F.R. Rubio, and M.G. Ortega. “Robust PID Control of the Quadrotor Helicopter.” IFAC Proceedings 45(3) (2012): 229–34. https://doi.org/10.3182/20120328-3-it-3014.00039.

[38] Zulu, Andrew, and Samuel John. “A Review of Control Algorithms for Autonomous Quadrotors.” Open Journal of Applied Sciences 04, (14) (2014): 547–56. https://doi.org/10.4236/ojapps.2014.414053.

[39] Glida, Hossam Eddine, et al. "Optimal direct adaptive fuzzy controller based on bat algorithm for UAV quadrotor." 2019 8 th International conference on systems and control (ICSC). IEEE, 2019. https://doi.org/10.1109/icsc47195.2019.8950585.

[40] Glida, Hossam-Eddine, Latifa Abdou, and Abdelghani Chelihi. "Optimal fuzzy adaptive backstepping controller for attitude control of a quadrotor helicopter." 2019 International conference on control, automation and diagnosis (ICCAD). IEEE, 2019. https://doi.org/10.1109/iccad46983.2019.9037915.

[41] Zheng, En-Hui, Jing-Jing Xiong, and Ji-Liang Luo. "Second order sliding mode control for a quadrotor UAV." ISA transactions 53.4 (2014): 1350–1356. https://doi.org/10.1016/j.isatra.2014.03.010.

[42] Jia, Zhenyue, et al. "Integral backstepping sliding mode control for quadrotor helicopter under external uncertain disturbances." Aerospace Science and Technology 68 (2017): 299-307. https://doi.org/10.1016/j.ast.2017.05.022.

[43] Bounemeur, A., Chemachema, M., & Essounbouli, N. Indirect adaptive fuzzy fault-tolerant tracking control for MIMO nonlinear systems with actuator and sensor failures. ISA transactions, 79 (2018) 45–61.https://doi.org/10.1016/j.isatra.2018.04.014.

[44] Qiu, J., Sun, K., Rudas, I. J., & Gao, H. Command filter-based adaptive NN control for MIMO nonlinear systems with full-state constraints and actuator hysteresis. IEEE transactions on cybernetics, 50(7) (2019) 2905–2915.https://doi.org/10.1109/ TCYB.2019.2944761.

[45] Wang, T. H., Zhao, X. M., & Jin, H. Y. (2021). Robust tracking control for permanent magnet linear servo system using intelligent fractional-order backstepping control. Electrical Engineering, 103(3), 1555-1567. https://doi.org/10.1007/s00202-020-01188-z.

[46] Yang, H., & Yin, S. Descriptor observers design for Markov jump systems with simultaneous sensor and actuator faults. IEEE Transactions on Automatic Control, 64(8) (2018) 3370–3377. https://doi.org/10.1109/TAC.2018.2879765.

[47] Delavari, H., & Jokar, R. Intelligent Fractional-Order Active Fault-Tolerant Sliding Mode Controller for a Knee Joint Orthosis. Journal of Intelligent & Robotic Systems, 102 (2) (2021) 1–18. https://doi.org/10.1177/1045389x15577660.

[48] Beyhan, Selami, and Mehmet Itik. "Adaptive fuzzy-Chebyshev network control of a conducting polymer actuator." Journal of Intelligent Material Systems and Structures 27.8 (2016): 1019–1029. https://doi.org/10.1016/j.ast.2019.04.055.

[49] Razmi, Hadi, and Sima Afshinfar. "Neural network-based adaptive sliding mode control design for position and attitude control of a quadrotor UAV." Aerospace Science and technology 91 (2019): 12–27. https://doi.org/10.1016/j.ast.2019.04.055 .

[50] Ba, Desheng, Yuan-Xin Li, and Shaocheng Tong. "Fixed-time adaptive neural tracking control for a class of uncertain nonstrict nonlinear systems." Neurocomputing 363 (2019): 273–280. https://doi.org/10.1016/j.neucom.2019.06.063

[51] Moawad, Nada M., Wael M. Elawady, and Amany M. Sarhan. "Development of an adaptive radial basis function neural network estimator-based continuous sliding mode control for uncertain nonlinear systems." ISA transactions 87 (2019): 200-216. https://doi.org/10.1016/j.isatra.2018.11.021.

[52] Beyhan, Selami, and Mehmet Itik. "Adaptive fuzzy-Chebyshev network control of a conducting polymer actuator." Journal of Intelligent Material Systems and Structures 27.8 (2016): 1019-1029. https://doi.org/10.1177/1045389x15577660.

[53] Fessi, Rabii, et al. "Terminal sliding mode controller design for a quadrotor unmanned aerial vehicle." Applications of sliding mode control in science and engineering (2017): 81-5

[54] Jia, Zhenyue, et al. "Integral backstepping sliding mode control for quadrotor helicopter under external uncertain disturbances." Aerospace Science and Technology 68 (2017): 299-307. https://doi.org/10.1016/j.ast.2017.05.022.

[55] Nikdel, N., Badamchizadeh, M., Azimirad, V., & Nazari, M. A. Fractional-order adaptive backstepping control of robotic manipulators in the presence of model uncertainties and external disturbances. IEEE Transactions on Industrial Electronics, 63(10) (2016) 6249–6256. https://doi.org/10.1109/TIE.2016.2577624.

[56] Wang, T. H., Zhao, X. M., & Jin, H. Y. (2021). Robust tracking control for permanent magnet linear servo system using intelligent fractional-order backstepping control. Electrical Engineering, 103(3), 1555-1567. https://doi.org/10.1007/s00202-020-01188-z

[57] Chen, S. Y., Li, T. H., & Chang, C. H. Intelligent fractional-order backstepping control for an ironless linear synchronous motor with uncertain nonlinear dynamics. ISA transactions, 89 (2019) 218–232. https://doi.org/10.1016/j.isatra.2018.12.036.

[58] Ejaz, F., Hamayun, M. T., Hussain, S., Ijaz, S., Yang, S., Shehzad, N., & Rashid, A. An adaptive sliding mode actuator fault tolerant control scheme for octorotor system. International Journal of Advanced Robotic Systems, 16(2) (2019) 1729881419832435. https://doi.org/10.1177/1729881419832435.

[59] Niu, Ben, et al. "Adaptive neural tracking control scheme of switched stochastic nonlinear pure-feedback nonlower triangular systems." IEEE Transactions on Systems, Man, and Cybernetics: Systems 51.2 (2019): 975-986.https://doi.org/10.1109/TSMC.2019.2894745.

[60] Razmi, H. Adaptive neural network based sliding mode altitude control for a quadrotor UAV. Journal of Central South University, 25(11) (2018) 2654–2663. https://doi.org/10.1007/s11771-018-3943-0.

[61] Mohd Basri, M. A. Trajectory tracking control of autonomous quadrotor helicopter using robust neural adaptive backstepping approach. Journal of Aerospace Engineering, 31(2) (2018) 04017091. https://doi.org/10.1061/(ASCE)AS.1943-5525.0000804.

[62] Liu, Peng, et al. "Full backstepping control in dynamic systems with air disturbances optimal estimation of a quadrotor." IEEE Access 9 (2021): 34206–34220. https://doi.org/ 10.1109/ACCESS.2021.3061598

[63] Kucherov, Dmytro, et al. "Stabilizing the spatial position of a quadrotor by the backstepping procedure." Indonesian Journal of Electrical Engineering and Computer Science 23.2 (2021): 1188-1199. https://doi.org/ 10.11591/ijeecs.v23.i2.pp1188-1199.

[64] Zeghlache, Samir, et al. "Actuator fault tolerant control using adaptive RBFNN fuzzy sliding mode controller for coaxial octorotor UAV." ISA transactions 80 (2018): 267–278. https://doi.org/10.1016/j.isatra.2018.06.003

[65]Hasseni, S.E.I., Abdou, L.: Decentralized pid control by using GA optimization applied to a quadrotor. J. Autom. Mobile Robot. Intell. Syst. 12, 33–44 (2018). https://doi.org/10.14313/JAMRIS_2-2018/9.

[66] Labbadi, Moussa, and Mohamed Cherkaoui. "Adaptive fractional-order nonsingular fast terminal sliding mode based robust tracking control of quadrotor UAV with Gaussian random disturbances and uncertainties." IEEE Transactions on Aerospace and Electronic Systems 57.4 (2021): 2265-2277. https://doi.org/10.1109/TAES.2021.3053109.

[67] Labbadi, Moussa, Yassine Boukal, and Mohamed Cherkaoui. "Path following control of quadrotor UAV with continuous fractional-order super twisting sliding mode." Journal of Intelligent & Robotic Systems 100 (2020): 1429-1451. https://doi.org/10.1007/s10846-020-01256-3.

[68] Ahmed, Saim, Haoping Wang, and Yang Tian. "Robust adaptive fractional-order terminal sliding mode control for lower-limb exoskeleton." Asian Journal of Control 21.1 (2019): 473-482. https://doi.org/10.1002/asjc.1964

Bibliography

[69] Z. L. Liu, B. Chen, and C. Lin, “Adaptive neural backstepping for a class of switched nonlinear system without strict-feedback form,” IEEE Trans. Syst., Man, Cybern., Syst., vol. 47, no. 7, pp. 1315–1320, Jul. 2017. https://doi.org/10.1109/tsmc.2016.2585664

[70] Huang, S., Wang, J., Huang, C., Zhou, L., Xiong, L., Liu, J., & Li, P.. A fixed-time fractional-order sliding mode control strategy for power quality enhancement of PMSG wind turbine. International Journal of Electrical Power & Energy Systems, 134 (2022) 107354. https://doi.org/10.1016/j.ijepes.2021.107354.

[71] Chen, S. Y., Li, T. H., & Chang, C. H. Intelligent fractional-order backstepping control for an ironless linear synchronous motor with uncertain nonlinear dynamics. ISA transactions, 89 (2019) 218–232. https://doi.org/10.1016/j.isatra.2018.12.036.

[72] Li, S., Wang, Y., Tan, J., & Zheng, Y. Adaptive RBFNNs/integral sliding mode control for a quadrotor aircraft. Neurocomputing, 216 (2016) 126–134. https://doi.org/10.1016/j.neucom.2016.07.033.

[73] Polycarpou MM, Ioannou PA. A robust adaptive nonlinear control design. American Control Conference. IEEE, (1993) 1365–1369. https://doi.org/10.23919/acc.1993.4793094